

USE OF DYNAMIC CONE PENETROMETER IN SUBGRADE AND BASE ACCEPTANCE



Shin Wu and Shad Sargand

Prepared in cooperation with the
Ohio Department of Transportation
Office of Research and Development

and the
United States Department of Transportation
Federal Highway Administration

State Job Number 14817(0)

April 2007



OHIO
UNIVERSITY

Russ College of Engineering
and Technology

Ohio Research Institute for
Transportation and the Environment



1. Report No. FHWA/ODOT-2007/01	2. Government Accession No.	3. Recipient's Catalog No.	
4. Title and Subtitle Use of Dynamic Cone Penetrometer in Subgrade and Base Acceptance		5. Report Date April 2007	
7. Author(s) Shin Wu, Shad Sargand		6. Performing Organization Code	
		8. Performing Organization Report No.	
9. Performing Organization Name and Address Ohio Research Institute for Transportation and the Environment (ORITE) 141 Stocker Center Ohio University Athens OH 45701-2979		10. Work Unit No. (TRAIS)	
		11. Contract or Grant No. State Job Number 14817(0)	
12. Sponsoring Agency Name and Address Ohio Department of Transportation Office of Research and Development 1980 West Broad St. Columbus OH 43223		13. Type of Report and Period Covered Final Technical Report	
		14. Sponsoring Agency Code	
15. Supplementary Notes			
16. Abstract <p>The Dynamic Cone Penetrometer (DCP) is a simple device for measuring the stiffness of unbound materials. The DCP works by driving a steel rod into bases and soil with a preset amount of energy; the stiffness of unbound materials at different depths can be measured by continuously monitoring the rate of penetration, yielding a stiffness profile. With its ability to collect and analyze data quickly and easily, the DCP compares favorably with other devices used to evaluate an in-situ base and subgrade during construction. The DCP is also the only device available today that can evaluate subgrade quality in all three dimensions.</p> <p>Most highway agencies accept unbound materials in base and subgrade based on density tests. But density is not a measurement of the strength (stiffness) of these materials. Field data collected in this study indicated that accepting the subgrade based on density tests did not guarantee the strength met design requirements. Accepting the base and subgrade based on density is thus one of the weak links in the process of designing and constructing pavement.</p> <p>During the 2003 and 2004 construction seasons, the Ohio Research Institute for Transportation and the Environment (ORITE) collected DCP data from 10 road projects in Ohio. Experience from this study proves that the DCP is a viable alternative device to evaluate in-situ base and subgrade materials during construction. Data collected shows that engineers can use the DCP to quantify the construction quality of the as-built materials. Based on this study, ORITE concludes that adopting DCP testing in unbound material acceptance specifications can greatly improve the monitoring of final product quality and thus enhance pavement performance.</p> <p>This report describes the ORITE study. The report also provides a construction site DCP testing procedure and proposes a set of DCP unbound material acceptance criteria and standards.</p>			
17. Key Words Dynamic Cone Penetrometer (DCP), pavement performance, subgrade testing, acceptance specification, subgrade stiffness		18. Distribution Statement	
19. Security Classif. (of this report) Unclassified	20. Security Classif. (of this page) Unclassified	21. No. of Pages 120	22. Price

SI* (MODERN METRIC) CONVERSION FACTORS

APPROXIMATE CONVERSIONS TO SI UNITS

Symbol	When You Know	Multiply By	To Find	Symbol
LENGTH				
in	inches	25.4	millimetres	mm
ft	feet	0.305	metres	m
yd	yards	0.914	metres	m
mi	miles	1.61	kilometres	km
AREA				
in ²	square inches	645.2	millimetres squared	mm ²
ft ²	square feet	0.093	metres squared	m ²
yd ²	square yards	0.836	metres squared	m ²
ac	acres	0.405	hectares	ha
mi ²	square miles	2.59	kilometres squared	km ²
VOLUME				
fl oz	fluid ounces	29.57	millilitres	mL
gal	gallons	3.785	litres	L
ft ³	cubic feet	0.028	metres cubed	m ³
yd ³	cubic yards	0.765	metres cubed	m ³

NOTE: Volumes greater than 1000 L shall be shown in m³.

MASS

oz	ounces	28.35	grams	g
lb	pounds	0.454	kilograms	kg
T	short tons (2000 lb)	0.907	megagrams	Mg

TEMPERATURE (exact)

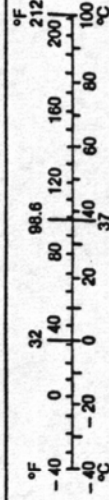
°F	Fahrenheit temperature	5(F-32)/9	Celsius temperature	°C
----	------------------------	-----------	---------------------	----

APPROXIMATE CONVERSIONS FROM SI UNITS

Symbol	When You Know	Multiply By	To Find	Symbol
LENGTH				
mm	millimetres	0.039	inches	in
m	metres	3.28	feet	ft
m	metres	1.09	yards	yd
km	kilometres	0.621	miles	mi
AREA				
mm ²	millimetres squared	0.0016	square inches	in ²
m ²	metres squared	10.764	square feet	ft ²
ha	hectares	2.47	acres	ac
km ²	kilometres squared	0.386	square miles	mi ²
VOLUME				
mL	millilitres	0.034	fluid ounces	fl oz
L	litres	0.264	gallons	gal
m ³	metres cubed	35.315	cubic feet	ft ³
m ³	metres cubed	1.308	cubic yards	yd ³
MASS				
g	grams	0.035	ounces	oz
kg	kilograms	2.205	pounds	lb
Mg	megagrams	1.102	short tons (2000 lb)	T

TEMPERATURE (exact)

°C	Celsius temperature	1.8C + 32	Fahrenheit temperature	°F
----	---------------------	-----------	------------------------	----



* SI is the symbol for the International System of Measurement

(Revised April 1989)

**USE OF DYNAMIC CONE PENETROMETER
IN
SUBGRADE AND BASE ACCEPTANCE**

**Ohio University
Ohio Research Institute for Transportation and the Environment
Stocker Center 141
Athens, Ohio 45701-2979**

Principal Investigators:

Shin Wu
Ohio University - Stocker Center 141
Athens, Ohio 45701-2979
740-593-1467
shinwu@bellsouth.net

Shad Sargand
Russ Professor of Civil Engineering
Ohio University - Stocker Center 141
Athens, Ohio 45701-2979
740-593-1467
ssargand@bobcat.ent.ohiou.edu

The contents of this report reflect the views of the authors who are responsible for the facts and the accuracy of the data presented herein. The contents do not necessarily reflect the official views or policies of the Ohio Department of Transportation or the Federal Highway Administration. This report does not constitute a standard, specification or regulation.

Final Report

April 2007

Acknowledgements

The authors would like to acknowledge the support and of the Ohio Department of Transportation (ODOT) technical liaisons, Roger Green and Aric Morse, as well as Monique Evans of the ODOT Research and Development Office. Issam Khoury of ORITE spent countless hours collecting DCP data. Without his tireless effort, there would not be enough data to reach a reasonable conclusion.

Table of Contents

1	INTRODUCTION	1
2	OBJECTIVES OF THIS STUDY	3
3	LITERATURE REVIEW	4
3.1	The Dynamic Cone Penetrometer.....	4
3.2	Terminology.....	4
3.3	Early Development of DCP Testing.....	6
3.4	Developing Correlations Between DCP Readings and CBR Values	7
3.5	Relating DCP Readings to Other Common Indexes	9
3.6	Applications of DCP Testing.....	12
4	DATA COLLECTION FOR THIS STUDY.....	14
4.1	Sample Projects	14
4.2	Testing and Data Collection Procedure	15
4.3	DCP Operation.....	16
4.3.1	Manual DCP Operation	16
4.3.2	Automated DCP Operation	17
5	DATA ANALYSIS.....	18
5.1	DCP Data Processing.....	18
5.1.1	Noise Reduction for Automated DCP Results.....	18
5.1.2	Identification of Uniform Layers.....	20
5.2	AC Surface Course.....	23
5.3	Treated Soil.....	24
5.4	Granular Base	29
5.5	Natural Soil.....	32
5.6	Relationship Between Resilient Modulus and PR	35
6	SUBGRADE ACCEPTANCE CRITERIA.....	37
6.1	The Subgrade Strength Requirement	37
6.2	Establishing a PR Requirement for Subgrade Soil.....	37
6.2.1	Selecting a Pavement Design Model	38
6.2.2	Designing the Pavement Structure.....	38
6.2.2.1	Conversion Equations Used in This Study.....	38
6.2.2.2	Experimental Design and Analysis	39
6.2.3	Calculating Sustainable Stress Values	41
6.2.3.1	Calculating Stress Values for Single-Layer Soil.....	41
6.2.3.2	Calculating Stress Values for Multiple-Layer Soil	43
6.2.3.3	Variable Pavement Strength, Single-Layer Soil.....	45
6.3	Application Example.....	49
7	FINDINGS.....	52
8	CONCLUSIONS AND RECOMMENDATIONS.....	53
9	IMPLEMENTATION PLAN	55
9.1	Phase 1.....	55
9.2	Phase 2.....	55
10	REFERENCES.....	56
	APPENDIX: PLOTS OF PENETRATION RATE DATA COLLECTED FOR THIS STUDY	59

List of Tables

Table 1. Summary of Tested Projects	15
Table 2. Summary of Treated Soil PR	25
Table 3. Student t Independent Samples Test Results	25
Table 4. Summary of Stabilized Soil Data.....	28
Table 5. Statistical Summary of US 50 Test Results	31
Table 6. Resilient Modulus Test Results	35
Table 7. Pavement Structure Design Layer Thicknesses	40
Table 8. Asphalt Material Properties	41
Table 9. Sustainable Stresses at Different PR and Traffic Loading.....	41
Table 10. PR-Stress Regression Results	42
Table 11. Vertical Stresses At Different Depths	44
Table 12. Vertical Stresses under SPS1 Designs	46
Table 13. Soil Stresses and Maximum Allowable PRs for AC Pavements of Given Thicknesses Handling Selected Traffic Loads	48
Table 14. Summary of Stresses in Application Example.....	50

List of Figures

Figure 1. Foundation Balance Graph (from Kleytn) (1 in = 25.4 mm).....	5
Figure 2. Strength-Balance Curve (from Kleytn) (1 in = 25.4 mm)	6
Figure 3. Comparing Different CBR-Modulus Relationships	11
Figure 4. Raw DCP Field Data	19
Figure 5. Phase One Noise Reduction	19
Figure 6. Phase Two Noise Reduction.....	20
Figure 7. Pavement Response Value (arbitrary units)	20
Figure 8. Cumulative Area and Cumulative Average Area (arbitrary units).....	21
Figure 9. Z Values (arbitrary units)	22
Figure 10. Plot of Z Values.....	22
Figure 11. Field Data with Statistically Uniform Sections represented by the flat segmented line.....	23
Figure 12. Penetration Rate of the AC Surface and the Cement Treated Soil	23
Figure 13. Plot of Stiffness of CT Versus AC Surface	24
Figure 14. Example of Stabilized Soil Layer 300 mm (11.8 in) Thick.....	25
Figure 15. Example of a 150 mm (5.9 in) Effective Layer of Stabilized Soil	26
Figure 16. Example of Stabilized Soil on Top of Stiff Soil.....	26
Figure 17. Stabilized Soil is Weaker than Soil Underneath.....	27
Figure 18. Distribution of Penetration Rate	28
Figure 19. Distribution of Effective Thicknesses	29
Figure 20. New Jersey Open Graded Granular Base on Top of Ohio Dense Graded Granular Base	29
Figure 21. A Weak Layer (NJ OGGB) Near the Top of the Base on U.S. Route 50 in Athens County.....	30
Figure 22. Iowa Open Graded Granular Base on Top of Ohio Dense-Graded Granular Base	30
Figure 23. Difference Between DCP PR Distributions for New Jersey and Iowa Open Graded Granular Bases	31
Figure 24. PR Distribution for the Ohio 304 Dense Graded Granular Base.....	32
Figure 25. Example of a Good Quality Subgrade Layer.....	33
Figure 26. Example of a Weak Upper Subgrade Layer	33
Figure 27. Example of a Weak Lower Subgrade Layer.....	34
Figure 28. Example of a Subgrade Layer Weaker Than the Foundation.....	34
Figure 29. Example of a Possible Compaction Problem.....	35
Figure 30. Resilient Modulus versus PR. Left in English units, right in metric units.	36
Figure 31. Sustainable Stress at Different ESAL.....	42
Figure 32. Vertical Stress When Subgrade Strength Increases with Depth	45
Figure 33. Vertical Stress When Subgrade Strength Decreases with Depth.....	45
Figure 34. Sustainable Stress vs. Required PR under Different Traffic Loadings (in kESAL).....	49
Figure 35. Required PR and Test Results	50
Figure 36. A Questionable Subgrade Stiffness	51

1 Introduction

Pavement structure design is based on three factors: loading (projected traffic), paving material properties (strength, aging, environmental effects, etc.), and subgrade support. But many uncertainties exist in pavement design. Even after a road is opened to traffic, the engineer cannot verify the accuracy of the traffic projection until the project has been through its design life. During the design stage, the engineer selects a subgrade support value based on a few samples taken from the project site and some engineering assumptions. The engineer controls paving material properties through quality assurance/quality control (QA/QC) programs during construction. Most states use density of the in-place subgrade and unbound base for construction quality control. However, density is not a load-bearing indicator. Also, in most cases, thickness of the unbound base layer is not monitored closely.

Experience shows that it is very costly to repair a failed pavement caused by poor base or subgrade quality. Therefore it is very important and beneficial to verify and improve, if needed, the quality of the base and subgrade prior to paving operations and to provide engineers an opportunity to reevaluate and modify pavement structure design during paving operations.

Pavement performance depends greatly upon the quality and uniformity of materials incorporated into the pavement structure. Careful monitoring of material quality and the dimensions of pavement layers during construction improves overall compliance with specifications as well as in-service performance of the pavement. Proof rolling is one of the techniques used by the Ohio Department of Transportation (ODOT) to verify the quality of unbound material. However, proof rolling does not accurately measure stiffness and cannot define the stiffness profile throughout the depth of base and subgrade. Moreover, proof rolling is time consuming.

Nuclear density gauges are also used to measure the density and moisture of base and soil for acceptance. But density is not the only factor affecting stiffness. Stiffness is a function of soil moisture, density, and type, as well as the magnitude of the stress level. Moreover, nuclear density gauges can only measure to shallow depths. Such measurements are inadequate for assessing the performance-related properties of the unbound materials. Mechanistic, empirically based design and rehabilitation procedures require knowing the stiffness of unbound material to predict the structural capacity of a pavement system. To ensure the long-term performance of a pavement, it is essential to know the stiffness of the base and subgrade during design and construction.

The Dynamic Cone Penetrometer (DCP) provides a quick and simple field test method for evaluating the in-situ stiffness of base and subgrade layers, and DCP testing has been used in many countries and some states for subgrade evaluation. The greatest advantage offered by the DCP is its ability to penetrate underlying layers and accurately locate zones of weakness within the pavement system. This quick and dirty method can measure soil properties to a depth of 3 ft (0.91 m).

On a construction project, between grading and paving operations, engineers can use the DCP to collect in-situ subgrade data to evaluate the stiffness and uniformity of the subgrade and unbound

base. The engineers can correct or modify soil as needed to meet minimum requirements prior to paving operations, or modify the pavement structure design to accommodate field conditions.

With the DCP, engineers can check unbound base material uniformity and layer thickness to ensure improved structural and functional performance of the pavement and prevent premature failure. Better performance and fewer premature failures save money, because less maintenance work is required. Finally, the ability of a DCP to evaluate soil stiffness at depth allows engineers to more accurately estimate undercut quantities, which reduces change orders during construction.

In the United States, the DCP is gaining acceptance as a tool for determining the stiffness of pavement unbound layers. There is therefore a great need to develop a procedure for implementing DCP testing to characterize subgrade and base materials during construction for QA/QC and to determine undercut limits and depths.

2 Objectives of This Study

In 2002, ODOT established a research project to be performed by the Ohio Research Institute for Transportation and the Environment (ORITE) to investigate the use of the DCP to gather data needed for construction acceptance. The primary objectives of this research project are as follows:

1. Develop and implement a procedure for using the DCP as an acceptance criterion for subgrade and unbound base material.
2. Develop a threshold, based on DCP readings, for unsuitable material.
3. Establish stiffness parameters, based on DCP readings, for pavement design and rehabilitation.
4. Develop QA/QC procedures for subgrade acceptance based on stiffness.

3 Literature Review

3.1 The Dynamic Cone Penetrometer

The DCP was developed in South Africa for evaluation of in-situ pavement strength or stiffness in the 1960s. Dr. D. J. van Vuuren designed the original DCP with a 30° cone (van Vuuren, 1969). The Transvaal Roads Department in South Africa began using the DCP to investigate road pavement in 1973 (Kleyn, 1975). Kleyn reported the relative results obtained using a 30° cone and a 60° cone. In 1982, Kleyn described another DCP design, which used a 60° cone tip, 8 kg (17.6 lb) hammer, and 575 mm (22.6 in) free fall (Kleyn, 1982). This design was then gradually adopted by countries around the globe. In 2004, the ASTM D6951-03 Standard Test Method for Use of the Dynamic Cone Penetrometer in Shallow Pavement Applications described using a DCP with this latest design (ASTM, 2004).

DCP testing consists of using the DCP's free-falling hammer to strike the cone, causing the cone to penetrate the base or subgrade soil, and then measuring the penetration per blow, also called the penetration rate (PR), in mm/blow. This measurement denotes the stiffness of the tested material, with a smaller PR number indicating a stiffer material. In other words, the PR is a measurement of the penetrability of the subgrade soil.

3.2 Terminology

During the early stages of DCP development, many indexes were derived from DCP sounding data to present DCP results. The following paragraphs discuss the resulting terminology.

Kleyn et al. defined the DCP Structure Number (DSN) as the number of blows required to penetrate a layer of material (Kleyn, Maree, and Savage, 1982).

They further defined the DSN of the i^{th} layer, DSN_i , as the number of blows required to penetrate the layer thickness h_i in mm (or in) at an average PR of DN_i mm (or in) per blow.

$$DSN_i = \frac{h_i}{DN_i}$$

The pavement DSN was defined as the number of blows required to penetrate the whole pavement structure:

$$DSN = \sum DSN_i$$

The pavement strength balance N_{DCP} was defined as the number of blows required to penetrate 10 cm (3.9 in).

DCP readings have been represented in the following chart formats (Kleyn, 1975):

- The Foundation Balance Graph: a plot of depth over PR with both axes in log scale (see Figure 1)

- The DCP Factor: the area enclosed by the foundation balance graph

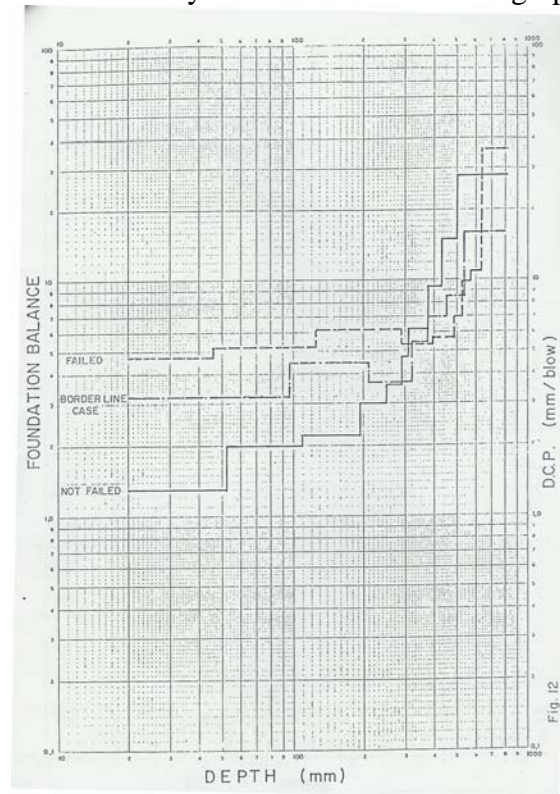


Figure 1. Foundation Balance Graph (from Kleyn) (1 in = 25.4 mm)

DCP readings have also been represented in these formats (Kleyn, Maree, and Savage, 1982):

- The Strength-Balance Curve (see Figure 2)
- The Layer Strength Diagram: the depth in natural numbers and the PR in log scale
- The DCP Curve: the number of blows needed to reach a certain depth

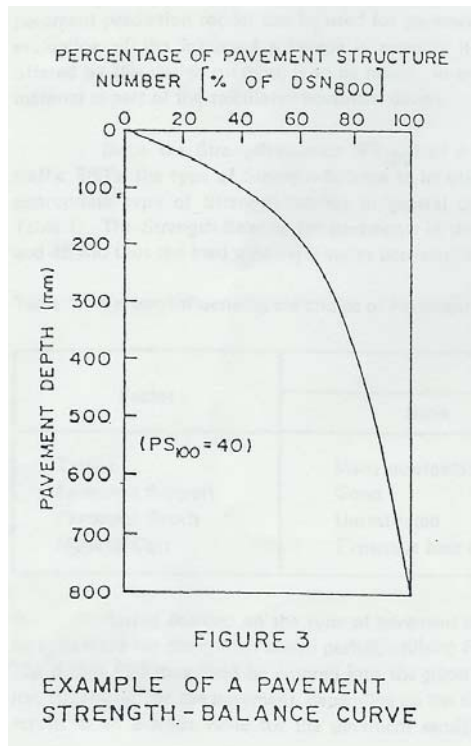


Figure 2. Strength-Balance Curve (from Kleyn) (1 in = 25.4 mm)

As explained earlier, the DCP reading is a measure of the amount of penetration per blow. Over the years, different agencies have used various terms for this measurement. The following are some of the most common names for DCP readings, which measure the depth of penetration per blow:

- Penetration Rate (PR)
- DCP Number (DN) (Kleyn, 1975)
- DCP Index (DI or DCPI) (Harison, 1989)
- Blow Number (BN)

Consulting Webster's Third New International Dictionary to help determine the best term for our use yielded the following definitions:

- Index: "...a ratio or other number derived from a series of observations and used as an indicator or measure..."
- Rate: "...quantity, amount, or degree of something measured per unit of something else..."
- Number: "...the enumerative aspect of things existing in countable units..."

The DCP reading is an actual measurement rather than a countable natural number or ratio. Rate is a more appropriate and self-explanatory term. Therefore this report uses PR, which is expressed in millimeters per blow.

3.3 Early Development of DCP Testing

In 1969, van Vuuren (van Vuuren, 1969) reported the results of comparing a DCP reading with the California Bearing Ratio (CBR).

The Transvaal Roads Department of South Africa started using the DCP in 1973 to evaluate the pavement structure of existing roads, as reported by Kleyn (Kleyn 1975). Based on lab testing results, Kleyn found that when a DCP reading is plotted against a CBR on a log-log chart, the relationship is linear. Kleyn devoted much effort to finding a way to use the DCP curve as an indicator of pavement condition, but he found no pattern that would provide such an indicator. Yet when comparing sound pavement sections with failed pavement sections, he noticed there appeared to be a minimum strength or suitability for the base course. From this study, he concluded that DCP testing is highly repeatable and sensitive enough for use in practice. He further suggested that DCP testing can be used to assess earthwork construction quality, evaluation of pavements, and design of pavements.

3.4 Developing Correlations Between DCP Readings and CBR Values

Base, subgrade soil, and paving material strength values derived from cone penetration resistance can be converted into CBR, Limestone Bearing Ratio (LBR), subgrade modulus k , resilient modulus E , and Soil Support Value (SSV). The most common conversion is expressed in the form of equations for CBR as a function of PR (in mm/blow). The following are some of the empirical correlations developed by various agencies.

The Australian Road Research Board (ARRB) (Smith and Pratt, 1983) developed an empirical correlation between PR and CBR, which is:

$$\text{Log } (CBR) = 2.56 - 1.15 \text{ Log } (PR)$$

The North Carolina Department of Transportation (NCDOT) (Wu, 1987) developed the following DCP and CBR relationship, based on the field CBR and the average of three DCP readings taken within an area with a radius of less than 1 ft (0.3 m) around the CBR test location:

$$\text{Log } (CBR) = 2.64 - 1.08 \text{ Log } (PR) \quad \text{or} \quad CBR = \frac{435}{PR^{1.08}} \quad (R^2 = 0.79) \quad (1)$$

Livneh presented the following relationship during the Southeast Asian Geotechnical Conference in Bangkok, Thailand in 1987:

$$\text{Log } (CBR) = 2.20 - 0.7 [\text{Log } (PR)]^{1.5}$$

Harison (Harison, 1989) of ARRB developed another equation:

$$\text{Log } (CBR) = 2.81 - 1.32 \text{ Log } (PR)$$

The U.S. Army Corps of Engineers (USACE) (Webster, Grau and Williams, 1992) developed another equation representing the relationship between the CBR and the DCP reading, used by many state departments of transportation (DOTs) and federal agencies:

$$\text{Log } (CBR) = 2.465 - 1.12 \text{ Log } (PR) \quad \text{or} \quad CBR = \frac{292}{(DCPI)^{1.12}} \quad (2)$$

The USACE study was based on lab CBR values, while the NCDOT study was based on field CBR values. It is known that a field CBR value is generally twice as large as a lab CBR value. Considering this characteristic, the results of these two independent studies actually match very well.

In 1994, Webster (Webster, Brown and Porter, 1994) further refined this equation to fit specific soil types:

$$CBR = \frac{1}{(0.002871DCPI)} \quad \text{for high plasticity clay soil (CH)}$$

$$CBR = \frac{1}{(0.017019DCPI)^2} \quad \text{for low plasticity clay soil (CL)}$$

Kleyn developed a similar equation in 1992:

$$\text{Log } (CBR) = 2.62 - 1.27 \text{ Log } (PR)$$

Livneh et al. (Livneh, Ishai, and Livneh, 1992) used automated DCP readings to develop the following equation:

$$\text{Log } (CBR) = 2.20 - 0.71 \text{ Log } (PR)$$

Where

$$CBR = 0.84 CBR_A$$

and

CBR_A is the CBR derived from the automated DCP reading

Ese (Ese, Myre, Noss, and Vaernes, 1994) presented the following equation during the Fourth International Conference on the Bearing Capacity of Roads and Airfields:

$$\text{Log } (CBR) = 2.669 - 1.065 \text{ Log } (PR)$$

Ese, of the Norwegian Road Research Laboratory, then correlated field DCP readings with lab CBR values. The result is:

$$\text{Log } CBR_{lab} = 2.438 - 1.65 \text{ Log } PR_{field}$$

Where

CBR_{lab} is the CBR value obtained in the lab

and

PR_{field} is the DCP reading obtained in the field

In 1999, Coonse presented the following correlation (Coonse, 1999):

$$\text{Log} (CBR_{field}) = 2.53 - 1.14 \text{Log} (PR_{field})$$

In the work leading to Equation 2 earlier in this section, Webster, Grau, and Williams (1992) compared many DCP-to-CBR correlations developed by agencies and researchers around the world. It is evident that general agreement was reached among the various sources of information. On the basis of these results, Equation 2 was selected as the best correlation and has been adopted by many researchers and practitioners (Livneh 1995; Webster, Grau, and Williams, 1992; Siekmeier et al, 2000).

3.5 Relating DCP Readings to Other Common Indexes

The Louisiana Transportation Research Center also used the last correlation in the preceding section for their evaluation of trench backfill at a highway cross-drain pipe (in 2003 and 2004), as follows:

$$N_{DCP} = \frac{10}{\frac{\sum_{i=1}^n PR_i}{n}} = \frac{10 * n}{\sum_{i=1}^n PR_i} \quad (\text{blows}/10 \text{ cm}) \quad (3)$$

Where

N_{DCP} = the average blow counts over a 5 cm (2 in) soil layer in units of blows/10 cm (blows/3.9 in)

and

$$PR = \frac{DCP}{10} \quad (\text{mm}/10 \text{ blows})$$

and

n = the number of PR readings in a 5 cm (2 in) thick soil layer

If $n = 0$ in Equation 2, then

$$N_{DCP} = \frac{10}{PR_{adjacent}} \quad (\text{blows}/10 \text{ cm})$$

Here, $PR_{adjacent}$ is the penetration rate of the top 5 cm (2 in) soil layer.

Several researchers have concluded that changes in moisture content and dry density do not affect the CBR-to-DCP test value relationship. The Minnesota DOT (Kremer, 2004) developed a specification stating that the CBR value should be at least 6 to minimize rutting damage to the finished grade (before paving) and to provide adequate subgrade support for proper compaction of the base and subgrade layers. Soils with CBR values less than 8 may need remedial procedures. Based on their experience with the DCP, Chen et al. of the Kansas DOT (KDOT) (Chen, Hossain, and LaTorella, 1999) suggested that existing relationships between DCP readings and CBR values are unreliable for relatively high CBR values or low DCP readings. To improve the accuracy of DCP results, KDOT developed a relationship between DCP values and falling weight deflectometer (FWD) back-calculated subgrade moduli.

The modulus is one of the most common parameters in pavement design. The American Association of State Highway and Transportation Officials (AASHTO) Design Guide suggests the use of the following equation, which was developed by Shell, to convert a CBR value to a Young's modulus value E in English units (psi) or metric units (MPa):

$$E(\text{psi}) = 1,500 * CBR \quad \text{or} \quad E(\text{MPa}) = 10.34 * CBR \quad (4)$$

Other common conversion equations follow:

From the U.S. Army Corps of Engineers Research and Development Center Waterways Experiment Station:

$$E(\text{psi}) = 5409 * CBR^{0.711} \quad \text{or} \quad E(\text{MPa}) = 37.3 * CBR^{0.711} \quad (5)$$

From the Transport & Road Research Laboratory (TRRL) in the United Kingdom:

$$E(\text{psi}) = 2550 * CBR^{0.64} \quad \text{or} \quad E(\text{MPa}) = 17.6 * CBR^{0.64} \quad (6)$$

From the Danish Road Laboratory:

$$E(\text{psi}) = 1500 * CBR^{0.73} \quad \text{or} \quad E(\text{MPa}) = 10 * CBR^{0.73} \quad (7)$$

Once the CBR value is determined from Equation 2 and is input into one of Equations 4 through 7, a modulus is calculated. Results from these equations are quite different. Figure 3 illustrates the differences among these equations. As one can see from the variety of conversion equations, groups tend to develop their own equations suited for local conditions.

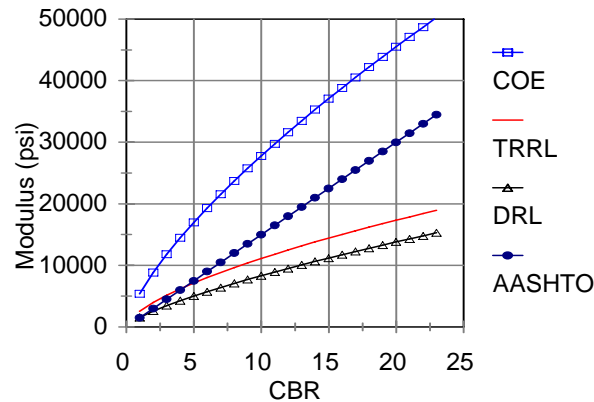


Figure 3. Comparing Different CBR-Modulus Relationships

The variety among the local soils tested by the groups is a likely factor contributing to the differences among equations 4-7. The AASHTO equation (equation 4) reflects a middle-of-the-road number. The U.S. Army Engineer Research and Development Center Waterways Experiment Station is in Vicksburg, Mississippi, and the equation (equation 5) developed there likely reflects soils in that region. The TRRL is in the United Kingdom, and the Danish Road Lab is in Denmark.

ORITE conducted a federally funded experiment on U.S. Route 35 to compare the stiffness determined by DCP testing, the stiffness gauge, German plate, FWD, Dynaflect, and laboratory data. The experiment was conducted during construction. The first series of nondestructive tests were performed when the subgrade was finished, and the second series of tests were performed when the base was completed. The project was successfully concluded and the report was provided to the Federal Highway Administration (FHWA) and ODOT. Currently, ORITE is preparing a technical note from that report.

De Villiers (1980) developed an equation representing the relationship between DCP readings and unconfined compressive strength (UCS) and found reasonably good correlation.

Kleyn and Savage (1982) suggested that analyzing to a depth of 800 mm (31.5 in) beneath the surface is sufficient for pavement structure investigation. Therefore, DSN800 is considered the pavement structural number. Based on heavy vehicle simulator results (rut criteria), equations expressing the relationship between sustainable axle load and DSN800 were developed.

Chen et al. (Chen, Lin, Liau, and Bilyeu, 2005) tried to estimate modulus based on DCP testing results. After eliminating outlier data, they developed a correlation equation as follows:

$$E(\text{ksi})=78.05*PR^{-0.6645} \text{ or } E(\text{MPa})=537.76*PR^{-0.6645} \quad (R^2=0.855)$$

where E is Young's modulus and PR is the penetration rate of the DCP in mm/blow.

To assess in-situ test methods, Abu-Farsakh et al. (Abu-Farsakh, Alshibli, Nazzal, and Seyman, 2004) developed equations showing the correlations between the DCP (PR) data and Static Plate Load (SPL) test, Falling Weight Deflectometer (FWD) test, and CBR test data collected in the field. The correlations between the PR and both the initial modulus and the reloading stiffness of the SPL test are as follows:

For initial modulus,

$$E_i \text{ (MPa)} = \frac{17421.2}{PR^{2.05} + 62.53} - 5.71 \quad \text{or} \quad E_i \text{ (ksi)} = \frac{2526.7}{PR^{2.05} + 62.53} - 0.828 \quad (R^2 = 0.94),$$

and for reloading modulus,

$$E_R \text{ (MPa)} = \frac{5142.61}{PR^{1.57} - 14.8} - 3.49 \quad \text{or} \quad E_R \text{ (ksi)} = \frac{745.873}{PR^{1.57} - 14.8} - 0.506 \quad (R^2 = 0.95)$$

The correlation between the PR and back-calculated modulus from a FWD test is:

$$\ln(M_{FWD}) = 2.35 + \frac{5.21}{\ln(PR)} \quad (R^2 = 0.91),$$

and the correlation between the PR and CBR is:

$$CBR = \frac{5.1}{PR^{0.2} - 1.41} \quad (R^2 = 0.93)$$

Abu-Farsakh et al. concluded that the values calculated using DCP results are more consistent and correct than values calculated based on data from either a Geogauge or a Light Falling Weight Deflectometer (LFW). The DCP is an effective tool for identifying layers and can take deeper measurements than the other devices. In particular, this study showed that the DCP readings correlate better with CBR values than data gathered using the other two devices. Therefore, DCP test results can be used to profile in-situ CBR values or the modulus of the base and subgrade.

Good correlations between PR and other common soil property parameters indicate that DCP testing is a reliable means of measuring base and subgrade stiffness. DCP testing should therefore be accepted as an alternative means of doing so, and the engineer should be able to present the in-situ stiffness of base and subgrade directly in terms of PR.

3.6 Applications of DCP Testing

After using a DCP to evaluate the in situ strength of many pavement projects, Kleyn, Maree, and Savage (1982) found that DCP testing can be applied to construction projects to evaluate the following:

- Potentially collapsible soils
- Construction control

- Efficiency of compaction
- Stabilized layers
- Subgrade moisture content

They also suggested that an engineer can monitor pavement structural strength using a layer-strength diagram.

The Wisconsin DOT (Crovetti & Schabelski, 2001) applied DCP and rolling wheel deflectometer testing for construction acceptance and found that both are viable tools for identifying poor areas of in-situ subgrade.

Kleyn and Savage (June 1982) developed a pavement design procedure based on the concept of pavement strength-balance, which is derived from DCP data. Their procedure was developed using performance data collected using a Heavy Vehicle Simulator (HVS) as well as performance data collected from in-service, thin-surfaced, unbound gravel pavement.

Kleyn et al. (1983) presented a practical pavement design procedure based on in situ DCP sounding.

After comparing results obtained from LFWD, Geogauge, and DCP testing, Murad et al. (Murad, Abu-Farsakh, Alshibli, Nazzal, and Seyman, 2004) found that the DCP is an excellent and reliable device to use in evaluating the strength (stiffness) of tested materials. It is inexpensive, easy to use, and records a continuous profile of the stiffness of the material throughout the depth tested. Moreover, the DCP can test to a greater depth. Therefore, the DCP is an excellent tool for assessing unbound base and subgrade stiffness.

In 1997, the Minnesota DOT adopted a DCP specification for QA/QC testing on aggregate base material (Kremer and Dai, 2004). They found that the in-situ moisture has a considerable effect on aggregate base strength or stiffness and suggested that a proper evaluation should include measuring the in-situ moisture content when doing the in-situ DCP testing.

Searching for a replacement for the time-consuming nuclear density gauge, which is the standard quality control device, Chen, et al. (1999) compared several in-situ soil testing devices and found that the DCP is a good candidate.

4 Data Collection for This Study

ORITE at Ohio University (OU) has used the DCP for characterizing subgrade and base materials for years. Initially ORITE used a manually operated DCP, which required two people. There are two problems with manual operation of the DCP: (1) in some cases, it is very difficult to retract the cone from the ground, and (2) if the rod penetrates the subsurface at an angle and creates side friction, the stiffness will be overestimated. In 1998, ORITE acquired an automated DCP that requires only one person to operate and only takes one-fifth of the time required for manual testing. The automated DCP also guarantees vertical penetration, minimizing the chance of measurement error.

The automated DCP was used in this study. Field DCP data were collected during the 2003 and 2004 construction seasons on ODOT projects.

4.1 Sample Projects

For this study, ODOT gave ORITE a list of scheduled construction projects expected to have exposed subgrade for testing during the 2003 and 2004 construction seasons. Then ORITE contacted the construction engineers to learn the actual time window available for DCP testing. Due to weather or other construction restrictions, many projects in the list were not available for testing in 2003 and 2004, and some projects did not have subgrade exposed long enough for ORITE to do the testing. With all the coordination effort, sections actually tested were fewer than originally planned in the proposal.

During the two-year period of this study, ORITE tested ten projects using the DCP. The number of samples taken depended on the length of finished subgrade available for testing when the DCP testing team was on site. Of these ten projects, five were tested after the asphalt concrete (AC) layers were in place. In four of these, DCP tests were performed on the subgrade through core holes; in the fifth, DCP tests were performed on and through the thin AC surface. Some of the tested projects have more than one pavement structure design represented in the test sections. Table 1 summarizes the projects ORITE tested. The “Chestnut” project was a road built in the Chestnut Woods Subdivision of Independence; it is the one road that was not an ODOT project it was included as an example of a low-traffic road.

Table 1. Summary of Tested Projects

Project	Sample ID	Core	Tested on	No of Samples
Chestnut	1 to 23		2 in (50.8 mm) AC on 12 in (304.8 mm) CT	23
Chestnut	24 to 26		natural soil	3
DEL23	1 to 6		12 in (304.8 mm) CT	6
DEL23CT	1 to 33	core hole	12 in (304.8 mm) CT	31
ERI02	A1 to A6	core hole	12 in (304.8 mm) CT	6
ERI02	B1 to B6	core hole	natural soil	5
ERI02	C1 to C6	core hole	12 in (304.8 mm) LCT	4
HAM126	1b to 6b	core hole	natural soil	6
Livingston	1 to 6		12 in (304.8 mm) LT	6
LOG33	A1 to A6	core hole	12 in (304.8 mm) CT	6
US35	1654 to 1698		natural soil	10
US30	1 to 21		natural soil	18
US50	E1 to E17		4 in (101.6 mm) NJ and 6 in (152.4 mm) Ohio 304 aggregate base	17
US50	W1 to W17		4 in (101.6 mm) Iowa and 6 in (152.4 mm) Ohio 304 aggregate base	17

Notes:

The project labeled “Chestnut” is a subdivision road in Chestnut Woods Subdivision, in Independence, Ohio. This was not an ODOT project and may have been built to different standards.

The project labeled “US35” in this table and in the appendix is a stretch of U.S. Route 35 in Ross County, Ohio.

One project was tested on top of a 2 in (50.8 mm) AC surface.

There were five cement-treated (CT) soil test sections, one lime-treated (LT) soil section, one lime/cement-treated (LCT) soil section, and five natural soil (untreated) test sections.

The two sections on U.S. Route 50 were tested through a granular base.

4.2 Testing and Data Collection Procedure

After grading operations were completed and the subgrade was finished, DCP tests were performed at every station (100 ft (30.48 m) intervals, at +00). The test point could be anywhere transversely within the future lanes. Testing could be stopped when penetration depth reached 1 m (3.3 ft) or upon refusal. For each project with an unbound base or a subgrade stabilized by lime or cement, testing was performed on top of the finished base or the stabilized soil. Four of the ten projects tested were tested through core holes, which cut through asphalt layers.

The original plan included collecting undisturbed soil samples to establish the DCP/M_R relationship. It was proposed that at each location where DCP readings were uniform for a layer at least 6 in (152.4 mm) deep, two more DCP tests would be performed at an 18 in (457.2 mm) distance to form an equilateral triangle. The depth of the uniform layer would be recorded and a

Shelby tube sample would be taken at the center of the triangle. The undisturbed soil sample within the uniform layer was to be tested in the lab to determine the resilient modulus M_R . Due to schedule problems, this part of the proposed testing was not done.

4.3 DCP Operation

There are two types of DCP available for field data collection. Although only the automated DCP was used in this study, this report describes operation procedures for both manual and automated DCPs in the following sections.

4.3.1 Manual DCP Operation

A two-person team is needed to operate a manual DCP. One serves as the operator and the other is the recorder. In addition to the DCP, the team must also have a hammer on hand. After locating a test point, the operator follows these steps.

1. Gently place the DCP tip at the test point.
2. Use one hand to hold the handle (that is, the rod above the upper stopper). Keep the DCP vertical (with the help of the recorder if needed). Picking a fixed reference object around you is a good way to keep the DCP plumb.
3. Record the initial height of the bottom of the lower stop (the marker) with a marking stick (the stick).
4. With one hand holding the DCP, use the other hand to raise the weight to the bottom of the upper stop (be careful not to hit the upper stop), then let the weight fall freely to hit the top of the lower stop.
5. Mark the new position of the marker on the stick.
6. Repeat steps 4 and 5 until the maximum depth of penetration is reached.
Attention: Keep the DCP vertical all the time and take care to avoid hitting your thumb!
7. Extract the DCP from the testing hole by hitting the upper stop with a hammer.

Stop DCP testing when one of the following conditions is satisfied:

1. Penetration depth reaches 1 m (39 in)
2. Penetration depth is greater than 0.6 m (24 in) and at least 10 consecutive blows return a PR of less than 1 mm/blow (0.04 in/blow)

To record your results for reporting, measure the marks on the stick and record the results in a DCP Record Form. Here are a few suggestions to make field data recording easy.

- Cover a 4 ft (1.22 m) survey stick with masking tape. Use it to mark the height of the marker and blow number. Up to eight tests can be marked on one stick. Penetration depth can be measured and recorded in the office, and the stick is reusable after being covered with new tape.
- When the penetration rate is less than 2.5 mm (0.1 in) per blow, do not mark every blow.

Marking every 5 or 10 blows is sufficient.

- Use project numbers and stations to identify data points. If two or more tests are performed at one station, add A, B, etc., at the end of the station number. For surcharge testing add “S” to the end of the identifier.

Caution: The DCP hammer is very heavy. To avoid harming yourself or your coworker, take precautions and keep safety in mind at all times.

- Make sure all the connections are tightly secured.
- Always hold the hammer when moving the DCP.
- Watch where you place your fingers while operating the DCP.
- Construction sites are very dangerous. Follow construction safety rules at all times.

4.3.2 Automated DCP Operation

Operating an automated DCP is like operating a manual DCP, except the DCP penetration and extraction are done using machine power and the computer records the data. One person can operate an automated DCP. The time needed to complete a test is much shorter with an automated DCP than with a manual DCP.

Following are the steps to perform when using an automated DCP.

1. Before testing a project, input the information necessary to set up the header for the data record and files.
2. Establish a file naming convention.
3. Locate the trailer so the DCP tip is aimed precisely at the test point.
4. Ensure the DCP rod is perfectly vertical.
5. Lower the DCP tip to the ground surface and start data collection. The computer records the penetration depth after every blow.
6. When data collection at this test point is done and the DCP is extracted from the ground, move the DCP trailer to the next location.
7. At the end of the day’s testing, be sure to save the data file to a disk. Name the file using the naming convention.

5 Data Analysis

In the early stages of DCP development, researchers tended to concentrate their efforts on correlating DCP readings to commonly accepted strength or stiffness parameters, such as CBR, resilient modulus, or UCS values. The purpose of such correlation was to prove the validity of the DCP as a soil stiffness measurement device. Converting DCP data to a commonly accepted parameter also enabled the incorporation of DCP data into an established pavement design procedure. Such conversion, which helped users understand and accept DCP, does have historical value. As seen in this report's Literature Review section, DCP readings correlate well with CBR, resilient modulus, and UCS values. The study results cited demonstrate that the DCP is a viable tool for measuring the stiffness of unbound materials. Development of the relationship between DSN800 and pavement performance by Kleyn (Kleyn and Savage, 1982) pioneered the application of DCP measurement to pavement design. It is now time to accept DCP into the mainstream.

It is important to understand that no matter how sound the correlation, estimation errors are unavoidable. If we agree to accept the use of the DCP to measure the stiffness of unbound material (and in some cases, bound material such as a thin AC layer), then it is logical to accept the use of DCP readings, that is, PR (in mm/blow), in practical application. This approach makes field operation and implementation much easier. Therefore in this study the researchers used PR values gathered using DCP sounding and developed acceptance criteria in terms of DCP measurements instead of older measures.

5.1 DCP Data Processing

While processing DCP raw data, the researcher must keep in mind that subgrade soil is not homogeneous in terms of material, moisture content, or level of compaction (density). Thus as the DCP penetrates the subgrade, it is expected to register a different PR for almost every blow. However, the pavement engineer is interested in evaluating the subgrade as uniform layers, not as material shown to be different with every blow. The raw data must be reduced to a form the engineer can reasonably use. To achieve this, raw DCP data must go through a two-step data reduction process:

1. Noise reduction
2. Determination of uniform layers

5.1.1 Noise Reduction for Automated DCP Results

The automated DCP recorded the penetration depth at every blow. Due to the nonhomogenous nature of subgrade soil, especially when small rocks were present, several very small penetration rates were recorded. In some cases, a negative penetration was recorded (that is, a bounce of the DCP). These very small and negative readings are "noise" and can be seen in the PR plot. Figure 4, the raw data plot of Hamilton 5B data, is a nice example of a PR plot with noise.

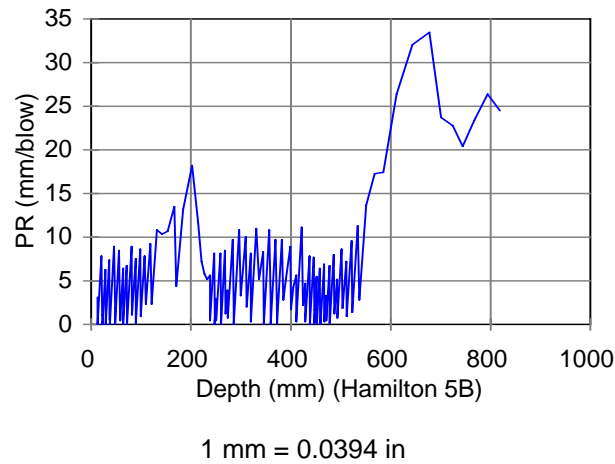


Figure 4. Raw DCP Field Data

Recall that the pavement engineer wants to know the stiffness of the soil stratum, not the micro-level variations. In noise reduction, these micro measurements are combined to form a larger picture. For demonstration purposes, two phases of noise reduction are presented. The first phase is to recalculate the PR using

$$PR = \text{Depth of Penetration} / \text{Adjusted Number of Blows},$$

Where the adjusted number of blows disregards those blows where the change in depth was less than 1 mm (0.04 in), including all negative values. Figure 5 is a plot of the data from Figure 4 after this phase of noise reduction.

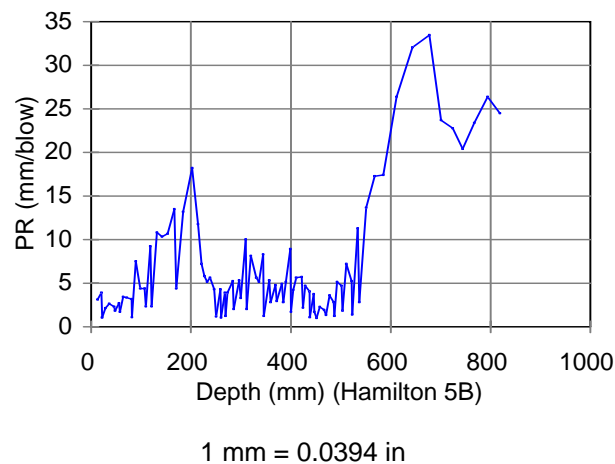


Figure 5. Phase One Noise Reduction

The second phase reduces the noise shown as the oscillating PR readings. This is done by deleting each data line that has a PR value that is less than one-fourth of the two adjacent PR values and then recalculating the PR. The result of applying this second noise-reduction phase to the data

shown in Figure 5 is presented in Figure 6. For graphical presentation of DCP results, this last version is definitely easier to read and makes more sense to highway engineers.

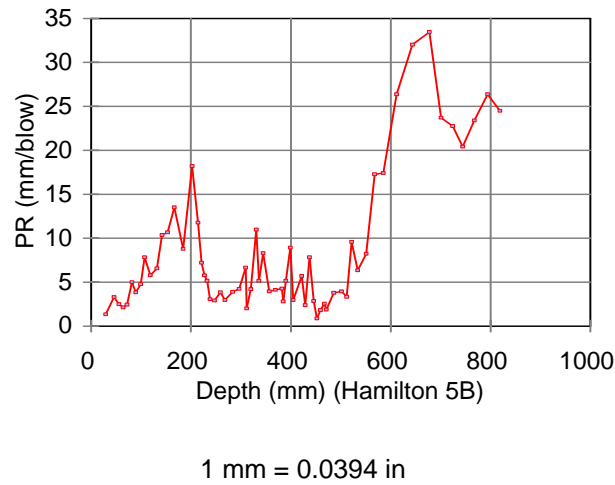


Figure 6. Phase Two Noise Reduction

5.1.2 Identification of Uniform Layers

The AASHTO pavement design guide (AASHTO, 1986, Appendix J) describes a method of determining the boundaries of uniform units. The procedure is referred to as *delineating statistically homogeneous units by Cumulative Differences Method*. This method can be used to determine the boundaries of uniform sections for linear-spatial measurement. The design guide uses the following approach to explain this procedure.

Figure 7 is a pavement test response values-to-distance plot along one highway section showing three distinct, uniform responses.

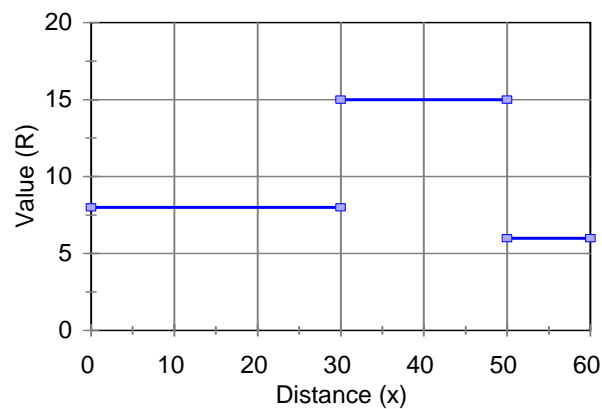


Figure 7. Pavement Response Value (arbitrary units)

Figure 8 shows the cumulative area and the cumulative average area. The cumulative area $A(x)$, which is the accumulated area below the response curve

$$A(x) = \int_0^x R dx$$

is shown as a solid line in Figure 8. The average response R_a is

$$R_a = \frac{\int_0^a R dx}{a}$$

where a is the end of the study section.

The cumulative average area A_a at location x is

$$A_a(x) = R_a * x$$

which is shown as a dashed line in Figure 8.

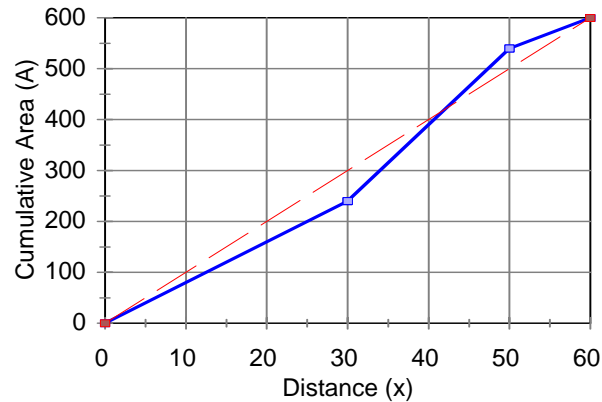


Figure 8. Cumulative Area and Cumulative Average Area (arbitrary units)

The difference $Z(x)$ between the cumulative area and cumulative average area is

$$Z(x) = A(x) - A_a(x).$$

Figure 9 shows that the location of the unit boundary coincides with the location where the slope of the $Z(x)$ function changes algebraic signs, that is, from negative to positive or vice versa.

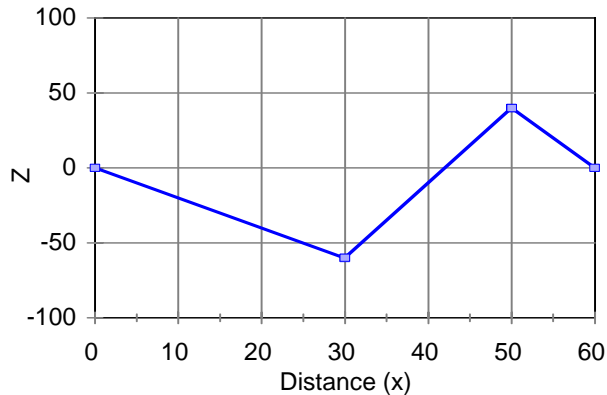


Figure 9. Z Values (arbitrary units)

DCP data are linear-spatial (in depth). Therefore, the AASHTO Cumulative Differences Method can be applied to DCP data to divide the subgrade soil into statistically uniform layers. The penetration depth is the distance, and the corresponding PR is the response. The statistically uniform layers can be identified by calculating the Z values. Each point at which Z reverses direction (where the slope changes from positive to negative or vice versa) indicates a border between uniform layers.

Figure 10 is a plot of the Z values calculated from the Hamilton 5B data set. The locations where the Z curve changes slope direction are labeled A, B, and C, at approximately 100 mm (3.9 in), 225 mm (8.9 in), and 510 mm (20.0 in), respectively.

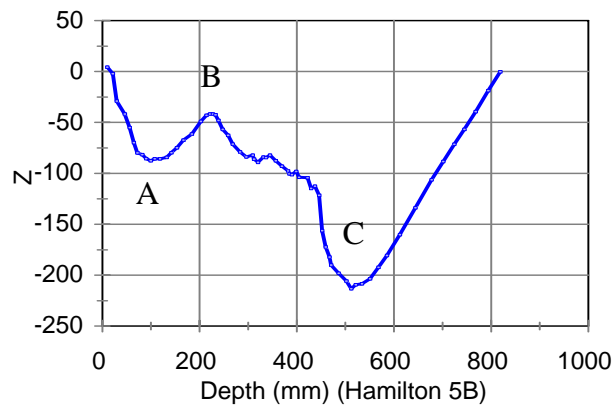
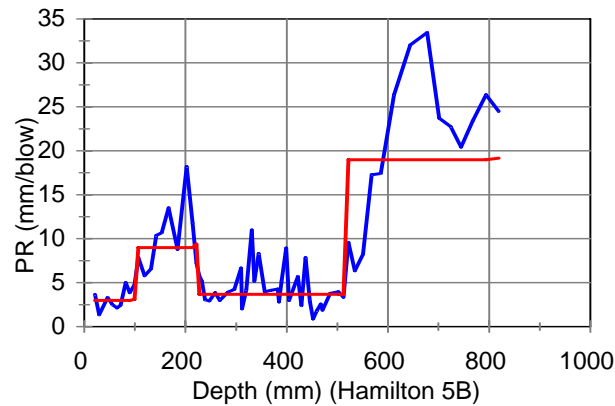


Figure 10. Plot of Z Values

1 mm = 0.0394 in

Figure 11 is a plot of the Hamilton 5B data showing the four statistically uniform layers divided at the points that were labeled A, B, and C in Figure 10.



1 mm = 0.0394 in

Figure 11. Field Data with Statistically Uniform Sections represented by the flat segmented line

5.2 AC Surface Course

Part of the Chestnut project was constructed with a 50 mm (2 in) AC surface on 300 mm (11.8 in) cement-stabilized soil. The rest was constructed on untreated natural soil. In this pavement section, DCP tests were performed on top of the AC surface layer. Test results indicated that the PR of the AC surface ranged from 14.4 to 2.1 mm/blow (0.56 to 0.08 in/blow) with the average PR equal to 5.2 mm/blow (0.2 in/blow) and a standard deviation of 2.9 mm/blow (0.11 in/blow). Figure 12 is a bar chart comparing the PRs of the surface course with those of the cement-treated (CT) soil layer.

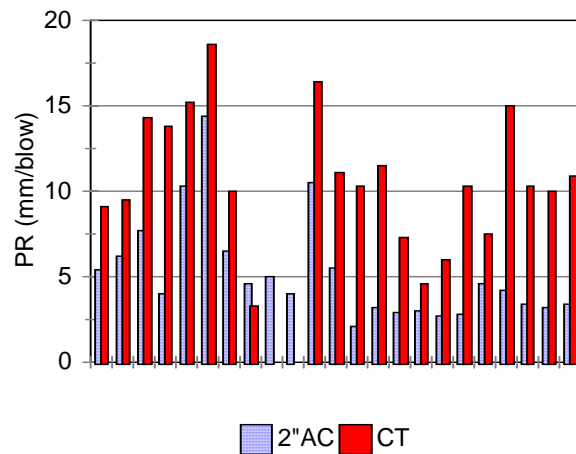


Figure 12. Penetration Rate of the AC Surface and the Cement Treated Soil

Figure 13 is a scatter plot of the stiffness of the surface course versus that of the CT soil. It is interesting to point out that for the less-stiff subgrade (with a PR less than 14 mm/blow [0.55 in/blow]), the PR of the AC surface is directly proportional to the PR of the CT soil, perhaps

because the softer subgrade did not provide enough support to enable proper compaction of the AC surface. The design thickness of the AC layer is 51 mm (2 in) and the measured thickness ranges from 105 to 35 mm (4.1 to 1.4 in). Field coring data substantiate that this wide range of thickness variation is not uncommon.

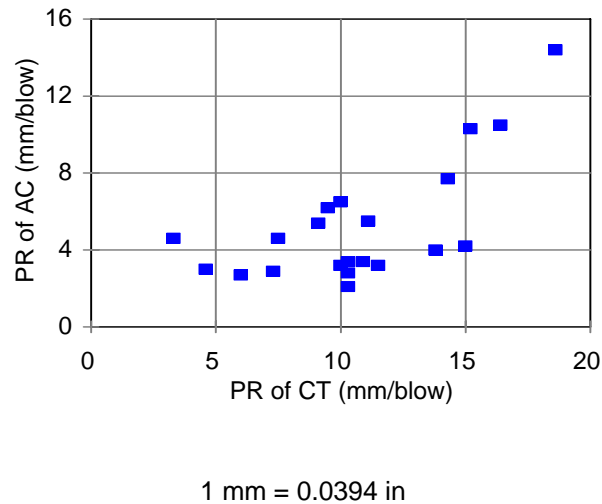


Figure 13. Plot of Stiffness of CT Versus AC Surface

Based on these results, the PR of a properly compacted AC surface is expected to be from 2 to 7 mm/blow (0.08 to 0.28 in/blow). When the PR is greater than 12 mm/blow (0.47 in/blow), proper compaction of the AC is questionable.

5.3 Treated Soil

Projects tested during this study included three types of soil treatment, namely, cement-treated (CT) (Chestnut, DEL23, DEL23CT, ERI02, and LOG33), lime-treated (LT) (Livingston) and lime/cement-treated (LCT) (ERI02). For all the treated layers, the designed thickness is 305 mm (12 in).

Table 2 is the statistical summary of test results from all the treated soil projects. Results indicate that the average PRs are quite close, with the exception of the Chestnut project. Student's t-test independent samples testing was used to test the null hypothesis that the difference of the two means is zero. The results showed that PRs from the Chestnut project are significantly different from PRs from all other projects. For the rest of the project pairs, including all the ODOT projects, the LCT data is significantly different from only one set of CT data. The student's t-test results indicated that data sets from the different treatment methods are not significantly different at the 10 percent level (see Table 3). In other words, despite the different material used to stabilize soils in these projects (cement or lime or a combination of the two), DCP test results taken from these projects can be considered to have been taken from the same population; that is, the data sets can be pooled into one. The average PR for the pooled data is 4.01 mm/blow (0.16 in/blow), and the standard deviation is 2.42 mm/blow (0.09 in/blow). As a result, in this study the type of stabilization is not considered.

Table 2. Summary of Treated Soil PR

		(mm/blow)						
Project	Chestnut	DEL23	DEL23CT	ERI02A	ERI02C	Livingston	LOG33	
Average	10.95	5.28	3.56	2.38	3.15	5.23	5.43	
Standard Deviation	3.71	1.25	2.63	1.45	0.23	3.00	0.77	
COV	0.34	0.24	0.74	0.61	0.07	0.57	0.14	

		(in/blow)						
Project	Chestnut	DEL23	DEL23CT	ERI02A	ERI02C	Livingston	LOG33	
Average	0.43	0.21	0.14	0.09	0.12	0.21	0.21	
Standard Deviation	0.15	0.05	0.10	0.06	0.01	0.12	0.03	
COV	0.01	0.01	0.03	0.02	0.00	0.02	0.01	

COV = Coefficient of variance

Table 3. Student t Independent Samples Test Results

(degrees of freedom in parenthesis)

	DEL23 (CT)	DEL23CT (CT)	ERI02A (CT)	LOG33 (CT)	ERI02C (LCT)	Livingston (LT)
Chestnut	3.5 (24) *	7.8 (45) *	4.9 (23) *	3.5 (24) *	4.0 (22) *	3.3 (24) *
DEL23		1.5 (31)	3.2 (9) *	0.2 (10)	3.0 (8)	0.3 (10)
DEL23CT			0.9 (30)	1.7 (31)	0.3 (29)	1.3 (31)
ERI02A				4.0 (9) *	0.9 (7)	1.8 (9)
LOG33					5.2 (8) *	0.1 (10)
ERI02C						1.2 (8)

* Significant at the 10% confidence level

Samples from some of the test locations showed a homogeneously low-PR (stiff) layer approximately 300 mm (11.8 in) thick. Figure 14 is an example of this good construction quality measured at the Livingston project.

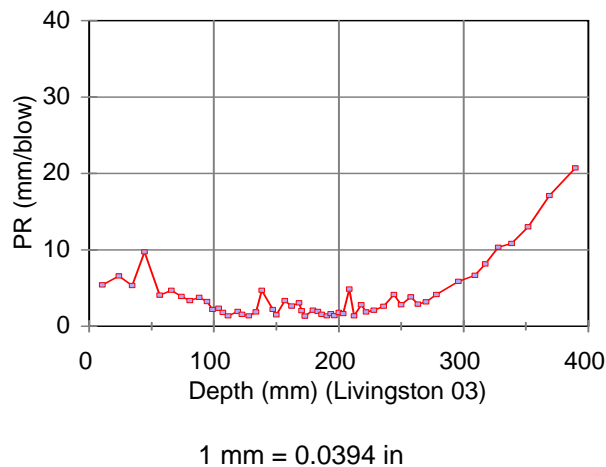


Figure 14. Example of Stabilized Soil Layer 300 mm (11.8 in) Thick

Many other samples showed a stiff layer much less than 300 mm (11.8 in) thick followed by a gradually increasing PR up to 300 mm (11.8 in). Figure 15 is a plot typical of these cases, from LOG33. This plot shows a good quality stabilized layer to a depth of 150 mm (5.9 in) followed by a gradually increasing PR layer to a depth of 300 mm (11.8 in), which indicates a poorer quality stabilized subgrade.

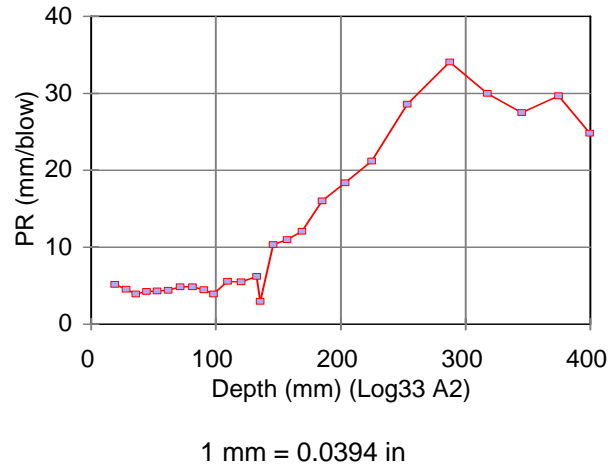


Figure 15. Example of a 150 mm (5.9 in) Effective Layer of Stabilized Soil

The greater stiffness of the top layer of soil indicates that this soil is effectively stabilized by cement or lime; this layer is called the effective layer. The thickness of the effective layer is referred to as the effective thickness. The effective thickness of the stabilized layer ranges from 430 to 95 mm (16.9 to 3.7 in).

Figure 16 is an example of a stiff layer that is thicker than the 300 mm (11.8 in) stabilized layer. This case can be described as comprising 300 mm (11.8 in) of stabilized soil with 100 mm (3.9 in) of good natural soil below the treated layer.

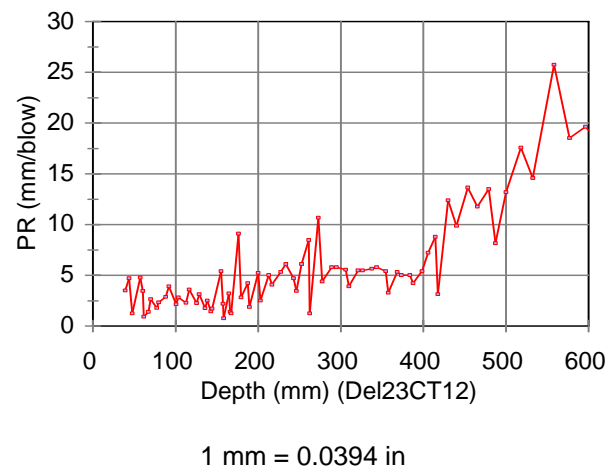


Figure 16. Example of Stabilized Soil on Top of Stiff Soil

In very few cases, the top portion of the treated soil is less stiff than the portion below. Figure 17 is an example of such a case.

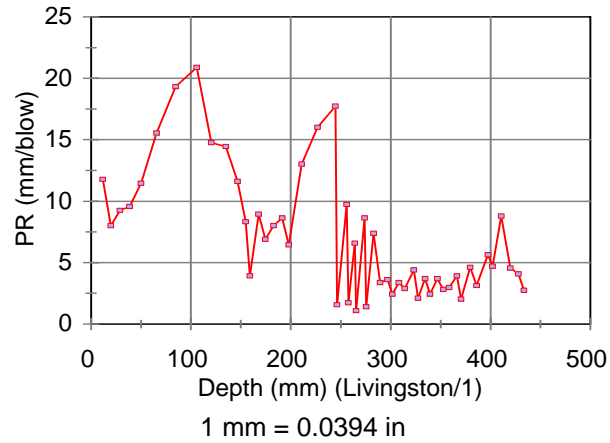


Figure 17. Stabilized Soil is Weaker than Soil Underneath

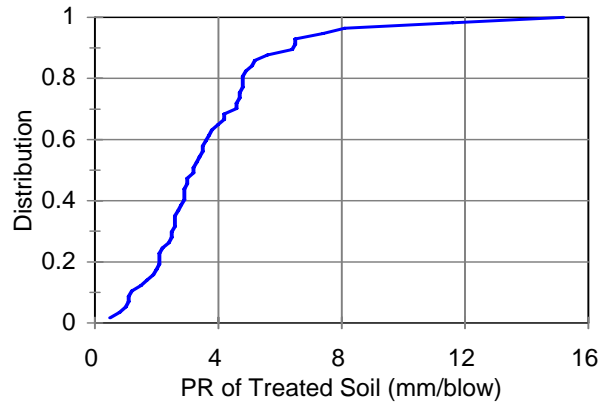
Table 4 summarizes the stabilized soil data from all projects tested. This table shows that the data from the Chestnut project are different than the data from the rest of the projects and also shows that there is not much difference between CT and LT soil. This summary reinforces the decision to pool the data from all the treated-soil projects, except Chestnut, into one set for further analysis.

Table 4. Summary of Stabilized Soil Data

	PR (mm/blow)		Effective Thickness (mm)	
	CT	LT	CT	LT
Average	3.4	4.8	254	240.9
Standard Deviation	2.5	2.12	62.16	106.27
COV	0.74	0.44	0.24	0.44
	PR (in/blow)		Effective Thickness (in)	
	CT	LT	CT	LT
Average	0.13	0.19	10.01	9.49
Standard Deviation	0.1	0.08	2.45	4.19
COV	0.74	0.44	0.24	0.44

COV = Coefficient of variance

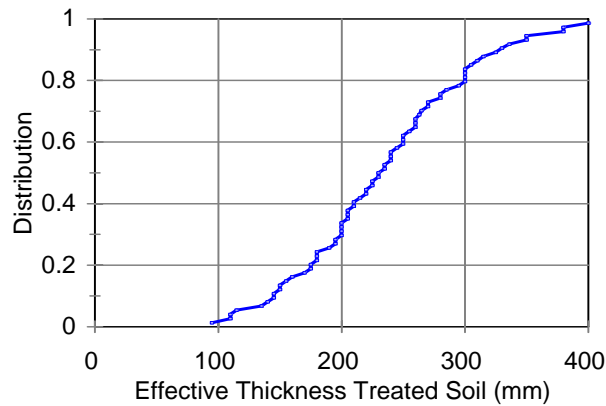
The average PR of the pooled treated soil from the ODOT projects is 3.8 mm/blow (0.15 in/blow), and a standard deviation of 2.5 mm/blow (0.1 in/blow) results in a high coefficient of variation (66 percent). It is clear from Figure 18 that the 95th percentile is 8 mm/blow (0.31 in/blow).



1 mm = 0.0394 in

Figure 18. Distribution of Penetration Rate

When the treated layer at a test site did not maintain its maximum stiffness to the full depth tested, only the depth from the surface down to the point at which the stiffness started to decline (where the PR increased) was considered to be the effective treated layer. Figure 19 is a plot of the distribution of the effective treated layer thicknesses. From this figure it is clear that 80 percent of the projects sampled did not achieve the designed effective depth, which is 300 mm (11.8 in).

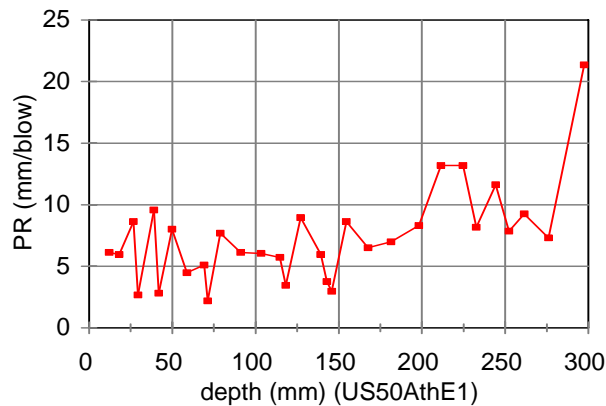


1 mm = 0.0394 in

Figure 19. Distribution of Effective Thicknesses

5.4 Granular Base

The eastbound lane of U.S. Route 50 in Athens County was constructed with a 100 mm (3.9 in) New Jersey open-graded granular base (NJ OGGB) on a 150 mm (5.9 in) Ohio dense-graded granular base (OH DGGB). For this study, DCP tests were performed on top of the NJ OGGB. Figure 20 is a typical plot of results obtained showing an approximately 250 mm (9.8 in) thick stiff layer.



1 mm = 0.0394 in

Figure 20. New Jersey Open Graded Granular Base on Top of Ohio Dense Graded Granular Base

Results obtained at one-third of the eastbound U.S. Route 50 test sites (5 out of 17 samples) show an obviously weaker layer near the top (the open graded layer). Figure 21 is an example of this situation.

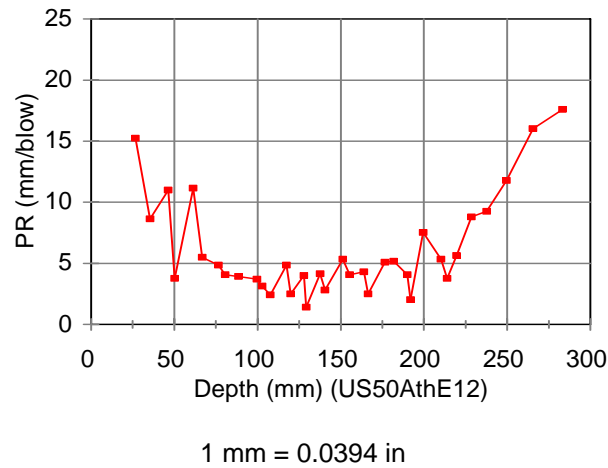


Figure 21. A Weak Layer (NJ OGGB) Near the Top of the Base on U.S. Route 50 in Athens County

The westbound lane of U.S. Route 50 was constructed with a 100 mm (3.9 in) Iowa open graded granular base (IA OGGB) on top of a 150 mm (5.9 in) OH DGGB. All test results at this site showed a weak layer of 100 mm (3.9 in) followed by a stiffer layer (see Figure 22).

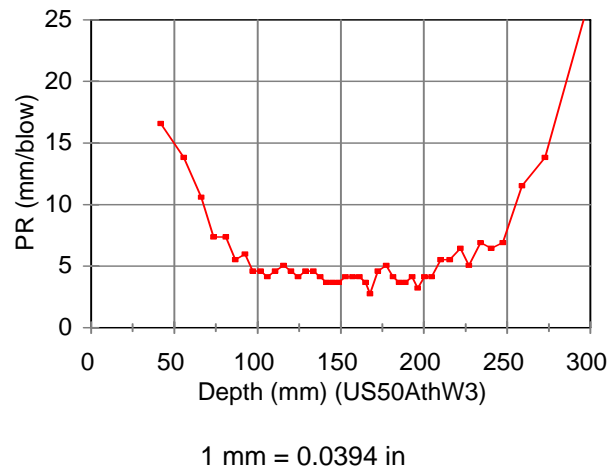
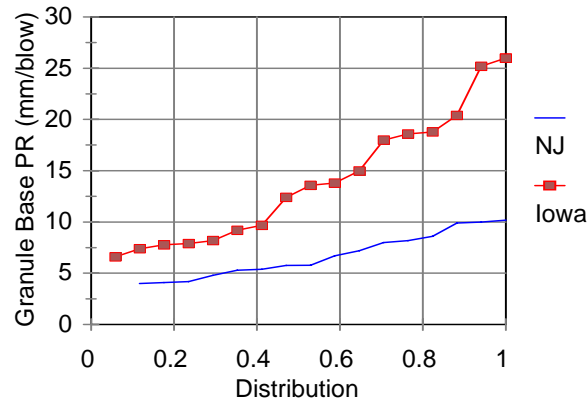


Figure 22. Iowa Open Graded Granular Base on Top of Ohio Dense-Graded Granular Base

Pavement design is based on the assumption that structural layers are laid down as homogeneous layers, especially those layers constructed with manufactured or modified material. However, test results indicate that, in many cases, the in situ OGGB is far from homogeneous. Figure 23 shows that the distributions of a NJ OGGB and an IA OGGB are very different.



1 mm = 0.0394 in

Figure 23. Difference Between DCP PR Distributions for New Jersey and Iowa Open Graded Granular Bases

Table 5 summarizes the average and standard deviation of the eastbound and westbound data from U.S. Route 50. Student’s t-test results show, with 99 percent confidence, that these two base types are significantly different ($t = 4.43$, $df = 32$).

Table 5. Statistical Summary of US 50 Test Results

	PR (mm/blow)		PR (mm/blow)	
	Open Graded Base		Ohio 304 Base	
	NJ	Iowa	East	West
Average	7.01	14.04	4.76	5.94
Standard Deviation	2.27	6.06	1.64	1.68
	PR (in/blow)		PR (in/blow)	
	Open Graded Base		Ohio 304 Base	
	NJ	Iowa	East	West
Average	0.28	0.55	0.19	0.23
Standard Deviation	0.09	0.24	0.06	0.07

To corroborate the U.S. Route 50 data, DCP test data for the eastbound and westbound Ohio 304 DGGB were compared using the Student’s t-test. This comparison showed that these two groups of data are not significantly different at the 95 percent confidence level ($t = -2.0$, $df = 32$). Figure 24 is a plot of the PR distribution for the Ohio 304 base. The 95th percentile PR is 8 mm/blow (0.31 in/blow).

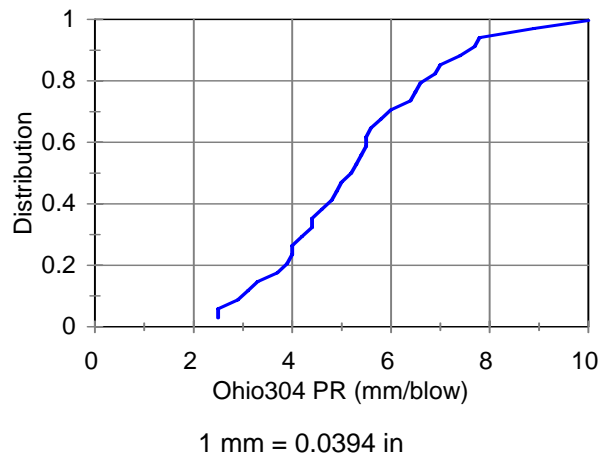


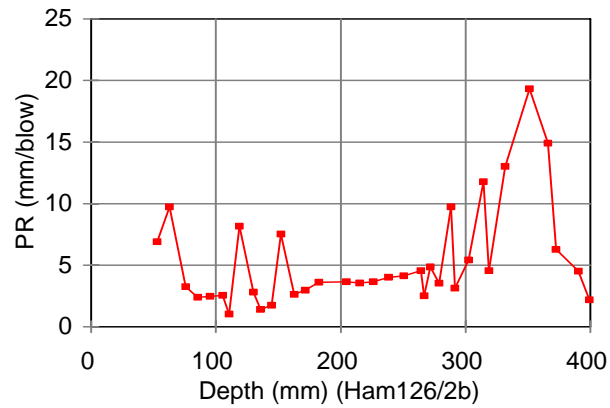
Figure 24. PR Distribution for the Ohio 304 Dense Graded Granular Base

5.5 Natural Soil

The ODOT construction specification considers the soil layer from the top of the subgrade to a depth of 300 mm (11.8 in) to be the subgrade. This report uses the term “subgrade layer” for this layer, distinguishing it from the soil below the subgrade layer (that is, lying deeper than 300 mm (11.8 in) below the top of the subgrade), which this report calls the “foundation.” In the ODOT specification, requirements for subgrade layer construction, such as material and quality of compaction, are different from requirements for the foundation (Ohio DOT, 2002). Requirements governing material used for subgrade layer construction are more stringent, as are the subgrade layer compaction requirements.

DCP tests were performed on five projects in which the subgrade layer was constructed with natural soil. Most of these test results show a clear layer interface at around 300 mm (11.8 in) below the subgrade surface. This is exactly the interface of the subgrade layer and the foundation.

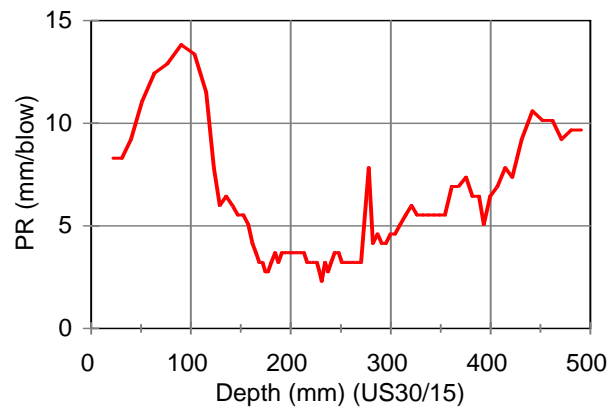
Data from most test sites at the Hamilton project show a good uniform subgrade layer approximately 300 mm (11.8 in) thick (see Figure 25). These results indicate that subgrade layer construction achieved the goal of the specification.



1 mm = 0.0394 in

Figure 25. Example of a Good Quality Subgrade Layer

Most of the data from the U.S. Route 30 project show that the bottom half of the subgrade layer is stiffer than the upper half (see Figure 26).



1 mm = 0.0394 in

Figure 26. Example of a Weak Upper Subgrade Layer

Figure 24 shows a case in which the stiff subgrade layer did not reach the design depth of 300 mm (11.8 in), but instead weakened at about 225 mm (8.9 in).

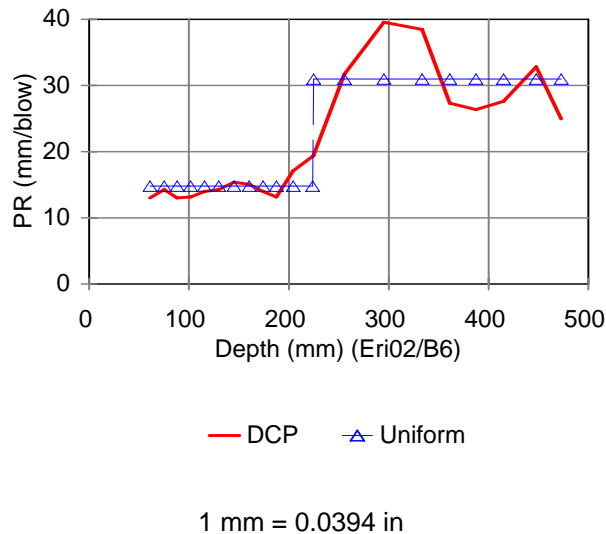


Figure 27. Example of a Weak Lower Subgrade Layer

As seen in the last three figures, some DCP test results show that the subgrade layer is of better quality than the foundation. However, despite the ODOT specification's extra requirements for subgrade layer construction, some results show that the subgrade layer is less stiff than the foundation, such as the results shown in Figure 28.

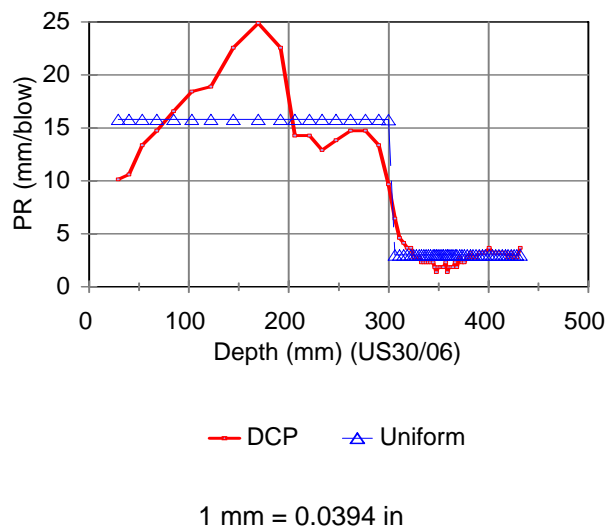


Figure 28. Example of a Subgrade Layer Weaker Than the Foundation

Figure 29 is a good example of a case in which the compaction quality of the subgrade layer is questionable.

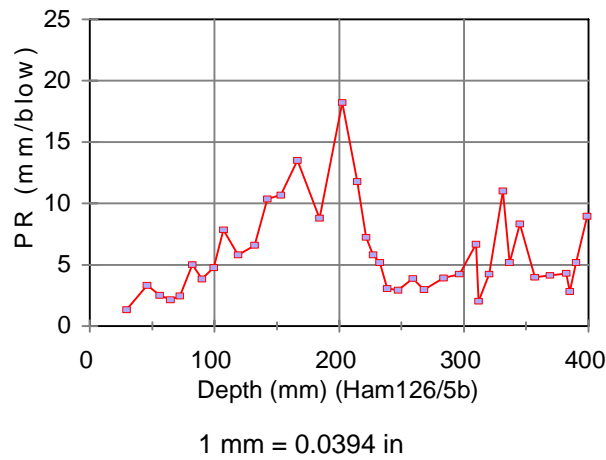


Figure 29. Example of a Possible Compaction Problem

In summary, the DCP test results show that the subgrade layer is far from homogeneous, and the inconsistent results point to potential problems. All the subgrade sections tested for this study , except the non-ODOT Chestnut project, had passed ODOT inspection and were accepted. The extra ODOT requirements for subgrade layer construction did not achieve the goal of ensuring a better quality layer right beneath the pavement structure. Therefore the current Ohio construction specification and acceptance criteria do not guarantee a better quality subgrade layer (one that is stiffer and more uniform).

PR plots of all data collected for this study are presented in the appendix.

5.6 Relationship Between Resilient Modulus and PR

Soil samples were collected from US30 and DEL23 projects for resilient modulus testing. DCP tests were performed in the vicinity where soil samples were taken. Samples were recompacted in the laboratory, making these disturbed soil samples. Results are summarized in Table 6.

Table 6. Resilient Modulus Test Results

Project	Sample	PR		Mr		Soil Type
		(mm/blow)	(in/blow)	(Mpa)	(ksi)	
DEL23	107	12.7	0.500	122.04	17.7	A-7-6
DEL23	110	17.1	0.673	62.74	9.1	A-4
US30	W885	11.9	0.469	26.20	3.8	A-4
US30	E663	2.41	0.095	35.85	5.2	A-4
US30	E876	2.63	0.104	86.87	12.6	A-4
US30	W876	4.98	0.196	63.43	9.2	A-4

Since the resilient moduli were measured on disturbed samples, the density and moisture content

of the each tested specimen will be different from that of the soil in the field. Figure 30 is a plot of Mr against PR. Due to the limited time window for field data collection, field personnel were unable to collect undisturbed soil samples near the DCP test points. Thus the scattering of data points in the figure is not a proof of poor correlation between Mr and PR.

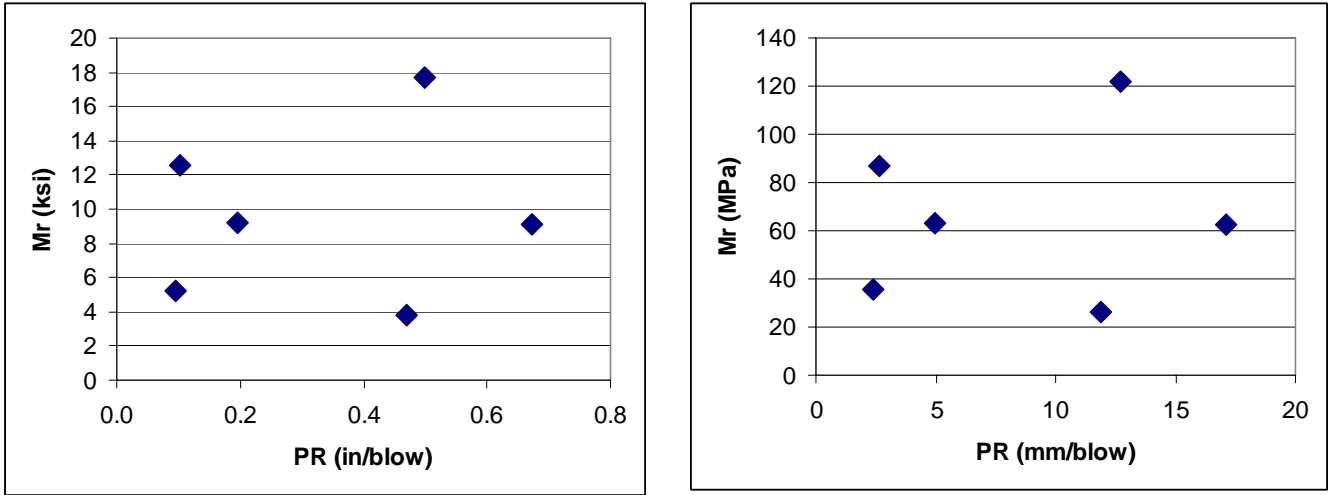


Figure 30. Resilient Modulus versus PR. Left in English units, right in metric units.

6 Subgrade Acceptance Criteria

A pavement system consists of layers of manufactured material placed on top of natural soil. The soil layer is an integral part of the pavement system and affects pavement performance. Most of the highway agencies accept subgrade and earthwork construction based on density testing. But density is not a measurement of soil strength. Hence, fulfilling density requirements doesn't guarantee this layer will perform as designed. One of the reasons for using density testing for quality control is that it can be performed easily in the field. To assure better quality subgrade and earthwork construction, agencies are in need of a reliable, simple method for testing soil strength to replace the current testing and acceptance specification.

6.1 The Subgrade Strength Requirement

The fundamental goals of pavement structure design are:

1. To develop a pavement structure that will sustain repeated loading without structural failure
2. To ensure the pavement layers are stiff enough to spread the repeated loading to the subgrade (selected soil or natural soil) in such a way that the vertical compression stress on the soil will not cause significant permanent deformation

Surface loading induces vertical stress on the subgrade. Thanks to stress distribution, the load is spread down through the soil, and the vertical compression stress at any depth is inversely proportional to the square of the depth. Therefore the soil stiffness (strength) required to sustain a given surface load decreases as depth increases.

DCP testing has been adopted by many highway agencies as a means to evaluate subgrade soil stiffness (strength) to a particular depth. The DCP measures subgrade soil stiffness in terms of PR (mm per blow). Because PR is inversely proportional to soil stiffness, the maximum PR allowed while still sustaining the surface load increases as depth increases.

With PR being a measure of stiffness, it is possible to identify the PR values required at different depths in the subgrade to sustain the designed loading. When these PR values have been identified, DCP testing can then determine whether a subgrade meets stiffness requirements stated in PR values.

6.2 Establishing a PR Requirement for Subgrade Soil

Analysis of pavement stress, strain, and deflection based on elastic theory assumes that the material beneath the pavement structure, the subgrade, is a homogenous layer of infinite depth. In the real world, due to material variation, moisture content, subgrade treatment, and compaction effort, the assumed homogenous condition never exists. One question is how the nonhomogenous nature of the subgrade layer affects the performance of the pavement and what the acceptable strength level is.

Another question is the depth to which soil stiffness must remain within a certain range to manage the vertical stress induced by the design load. Theoretically, at the depth where the induced

vertical stress becomes irrelevant, that is, will not cause significant permanent deformation, the surface loading influence on subgrade soil also becomes negligible. This depth defines the lower boundary of the influence region (Livneh & Ishai, 1987). Beyond this depth, subgrade strength has negligible or no effect on pavement performance. Thus it is not necessary to investigate soil strength beyond the influence region. Kleyn suggested that investigation to a depth of 800 mm (31.5 in) from the pavement surface is enough for pavement structure evaluation (Kleyn & Savage, 1982).

When a pavement structure is designed using a design model, on a given subgrade and under a given traffic loading, the vertical stress on top of the subgrade induced by an axle load is the sustainable stress of the given subgrade for that traffic loading.

Once the sustainable stress of a soil with a given PR is established, it is possible to establish the required PR for a given traffic loading value. The proposed methodology to establish the required PR is as follows:

1. First, choose a pavement design model.
2. Then design a pavement structure for a given soil stiffness (PR) and traffic loading.
3. Finally, apply a mechanistic model to this pavement system to calculate the vertical stress on the subgrade under a standard wheel load. The calculated stress is the sustainable vertical stress for the given soil stiffness (PR) under the given traffic loading (number of equivalent standard axle loads [ESALs]).

6.2.1 Selecting a Pavement Design Model

Over the years, many flexible pavement performance models have been proposed and used in the practical design of pavement. Of these, the AASHTO model and the Asphalt Institute model are the most widely adopted and the second most widely adopted models in the United States. Since the AASHTO design model is the most widely adopted design model in the US, the 1993 AASHTO model was used in this study to establish the influence depth and the required PR.

6.2.2 Designing the Pavement Structure

6.2.2.1 Conversion Equations Used in This Study

The USACE Waterways Experiment Station developed the following PR and lab California Bearing Ratio (CBR) relationship (Webster, Grau and Williams, 1992).

$$CBR = \frac{292}{(DCP)^{1.12}} \quad (\text{Eq. 2 from Section 3.4})$$

Based on field CBR, NCDOT developed a CBR to PR correlation equation yielding a similar slope but offset as follows (Wu, 1987).

$$CBR = \frac{435}{(PR)^{1.08}} \quad (\text{Eq. 1 from Section 3.4})$$

The offset is understandable because it is known that lab CBRs are always smaller than field CBRs. Results from these two independent studies proved that the CBR to PR relationship is consistent.

The AASHTO 1993 design guide suggests that the CBR can be converted to the soil resilient modulus (M_R , in psi) using the following equation:

$$M_R = 1500 * CBR \quad (8)$$

NCDOT uses the following equation to convert the lab CBR to the soil support value (SSV):

$$SSV = 5.32 * \log (CBR) - 1.49 \quad (9)$$

Equations 2, 8, and 9 were used to convert the DCP penetration rate to the soil support value, which was used in the AASHTO design procedure for pavement thickness design.

6.2.2.2 Experimental Design and Analysis

The goal of this analysis was to establish a relationship between PR and sustainable stress. To cover a wider range of soil and traffic loading conditions, this study selected eight levels of PR in the range of 5 to 80 mm/blow (0.2 to 3.15 in/blow) and six levels of traffic loading in the range of 50 to 5,000 kESAL. The soil PRs are used as a measure of the strength of a uniform consolidated subgrade under the pavement.

The USACE Waterways Experiment Station equation (Equation 2) was used to convert PR to CBR. The AASHTO equation was used to calculate M_R . The NCDOT equation was used to calculate the SSV. These values were applied to the 1993 AASHTO design model to calculate the structure number (SN). The layer coefficients of the AC and the asphalt-treated base (ATB) were assigned values of 0.44 and 0.3 respectively to determine layer thickness. The pavement structural design results are summarized in Table 7.

To read the table, if the soil has the PR value on the left, then it should have the corresponding CBR, M_R , and SSV. Then, if one wants to build a an asphalt concrete road over that subgrade that will handle the indicated traffic load at the top on the right hand side, one needs to add asphalt concrete (AC) and possibly asphalt treated base (ATB) layers of the indicated minimum thicknesses.

Table 7. Pavement Structure Design Layer Thicknesses

(top section in English units, bottom in metric units)

Pavement Structure Design Layer Thicknesses																
				Traffic Loading (in kESAL)												
				50		100		500		1,000		2,000		5,000		
PR		CBR	M _R	SSV	AC	ATB	AC	ATB	AC	ATB	AC	ATB	AC	ATB	AC	ATB
mm/blow	in/blow		ksi		in	in	in	in	in	in	in	in	in	in	in	in
5	0.20	48.14	72215	7.46	2.8	0	3.2	0	4.3	0	4.8	0	5.4	0	2.5	5.5
10	0.39	22.15	33226	5.67	3.7	0	4.2	0	5.5	0	2.5	5.4	2.5	6.5	2.5	8.1
15	0.59	14.07	21099	4.62	4.3	0	4.9	0	2.5	5.7	2.5	6.8	2.5	8.1	5.5	5.6
20	0.79	10.19	15287	3.87	4.8	0	5.4	0	2.5	6.7	2.5	8	5.5	5	5.5	7
35	1.38	5.45	8168	2.43	2.5	5	2.5	6.1	5.5	4.7	5.5	6.1	5.5	7.7	5.5	9.9
50	1.97	3.65	5478	1.5	2.5	6.3	2.5	7.5	5.5	6.4	5.5	7.9	5.5	9.6	5.5	12
70	2.76	2.51	3758	0.63	2.5	7.6	5.5	4.5	5.5	8.1	5.5	9.7	5.5	11.5	5.5	14
80	3.15	2.16	3236	0.29	2.5	8.1	5.5	5.1	5.5	8.7	5.5	10	5.5	12.2	5.5	15

				Traffic Loading (in kESAL)												
				50		100		500		1,000		2,000		5,000		
PR		CBR	M _R	SSV	AC	ATB	AC	ATB	AC	ATB	AC	ATB	AC	ATB	AC	ATB
mm/blow	in/blow		MPa		mm	mm	mm	mm	mm	mm	mm	mm	mm	mm	mm	mm
5	0.20	48.14	497904.9	7.46	71	0	81	0	109	0	122	0	137	0	64	140
10	0.39	22.15	229085.2	5.67	94	0	107	0	140	0	64	137	64	165	64	206
15	0.59	14.07	145472.5	4.62	109	0	124	0	64	145	64	173	64	206	140	142
20	0.79	10.19	105400.2	3.87	122	0	137	0	64	170	64	203	140	127	140	178
35	1.38	5.45	56316.4	2.43	64	127	64	155	140	119	140	155	140	196	140	251
50	1.97	3.65	37769.5	1.5	64	160	64	191	140	163	140	201	140	244	140	302
70	2.76	2.51	25910.5	0.63	64	193	140	114	140	206	140	246	140	292	140	356
80	3.15	2.16	22311.4	0.29	64	206	140	130	140	221	140	264	140	310	140	376

The AASHTO Guide's suggested elastic modulus and Poisson's ratio for asphalt hot mix material are summarized in Table 8.

Table 8. Asphalt Material Properties

	Elastic Modulus	Poisson's Ratio
AC	400,000 psi (2757.9 MPa)	0.35
ATB	200,000 psi (1378.9 MPa)	0.35

6.2.3 Calculating Sustainable Stress Values

Over the years, many layer elastic models have been developed. In the early 1970s, Shell Oil Company developed BISAR, a layer elastic computer program that uses complex mathematical models to analyze stress and strain within the pavement structure and yields the most rigorous results (NHI, 1994). This study used BISAR to calculate sustainable stress values for single-layer soil and multiple-layer soil.

6.2.3.1 Calculating Stress Values for Single-Layer Soil

The pavement structure values shown in Table 7 were input into BISAR. The applied standard wheel load was a half axle dual wheels, 20 kN (4.5 kip) each with 550 kPa (80 psi) tire pressure. The soil layer was assumed to have uniform strength to infinite depth. Vertical stresses at the top of the subgrade under each wheel and at the center between two wheels were calculated. Vertical stresses 305, 610, and 915 mm (12, 24, and 36 in) below the subgrade under the wheels and at the center between the two wheels were also calculated. The maximum vertical stress on top of the subgrade is considered the sustainable stress for the soil with the given PR to carry the specific traffic loading. The resultant sustainable stresses are summarized in Table 9.

Table 9. Sustainable Stresses at Different PR and Traffic Loading

		Sustainable stresses											
		Daily Traffic Loading in kESAL											
PR		50		100		500		1000		2000		5000	
mm/blow	in/blow	psi	kPa	psi	kPa	psi	kPa	psi	kPa	psi	kPa	psi	kPa
5	0.20	49.3	339.9	43.8	302.0	32.6	224.8	28.9	199.3	25.2	173.7	18.1	124.8
10	0.39	28.6	197.2	24.8	171.0	17.9	123.4	13.4	92.4	11.3	77.9	8.99	62.0
15	0.59	19.9	137.2	16.9	116.5	10.4	71.7	8.72	60.1	7.23	49.8	6.43	44.3
20	0.79	15	103.4	12.9	88.9	7.53	51.9	6.28	43.3	5.86	40.4	4.66	32.1
35	1.38	7.29	50.3	5.98	41.2	4.38	30.2	3.66	25.2	3.03	20.9	2.4	16.5
50	1.97	4.62	31.9	3.85	26.5	2.8	19.3	2.33	16.1	1.94	13.4	1.54	10.6
70	2.76	3.06	21.1	2.92	20.1	1.82	12.5	1.52	10.5	1.26	8.7	1	6.9
80	3.15	2.56	17.7	2.42	16.7	1.52	10.5	1.26	8.7	1.06	7.3	0.83	5.7

This table can also be interpreted in a different way. The easiest way to explain this second concept is by example. Assume that a soil with PR equal to 10 mm/blow (0.39 in/blow) can carry 1 million ESAL without having excessive permanent deformation as long as the vertical stress on top of the subgrade is 13.4 psi (92.4 kPa) or less. From a different angle, if at some location in the subgrade soil under a pavement structure (say, 20 in (500 mm) below the top of the subgrade), the induced

vertical stress due to a surface axle load is 2.33 psi (16.1 kPa) and the expected loading is 1 million ESAL, then the required PR at that location must be less than 50 mm/blow (1.97 in/blow) for the soil to sustain the load without significant vertical permanent deformation. This is defined as the *maximum permitted PR* at that depth and under that ESAL. Figure 31 is a plot of sustainable vertical stress values on the subgrade surface at different traffic loading with different subgrade stiffness (PR equals 10, 20, and 50 mm/blow [0.39, 0.79, and 1.97 in/blow]).

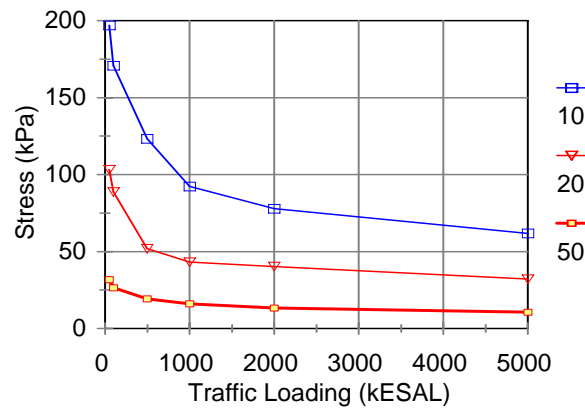


Figure 31. Sustainable Stress at Different ESAL (PR at 10, 20, and 50 mm/blow (0.39, 0.79, and 1.97 in/blow))

To establish the relationship of stress and PR at a given level of traffic loading, the statistical analysis package SPSS is used to find the best fit curve. It is found that the best fit curve is a power function, in the form of

$$PR = B_0 * S^{B_1}$$

Regression results are shown in Table 10.

Table 10. PR-Stress Regression Results

Daily traffic loading (kESAL)	B_0 (mm/blow)	B_0 (in/blow)	B_1	R^2
50	200.05	7.90	-0.90	0.990
100	184.92	7.29	-0.92	0.993
500	122.55	4.83	-0.90	0.997
1000	103.70	4.09	-0.90	0.998
2000	88.08	3.47	-0.88	0.998
5000	72.51	2.86	0.89	0.995

It is found that for all levels of traffic loading, correlation coefficients of B_1 are very close to -0.9. It is also found that B_0 changes as traffic level changes. The curve fit analysis for $kESAL$ and B_0 from Table 9 yielded the following power function,

$$B_0 = 507.7 * (kESAL)^{-0.23} \quad (R^2 = 0.996)$$

Hence,

$$PR = 507.7 * (kESAL)^{-0.23} * S^{-0.9} \quad (10)$$

Where S is stress in psi, or

$$PR = 89.32 * (kESAL)^{-0.23} * S^{-0.9}$$

Where S is stress in kPa.

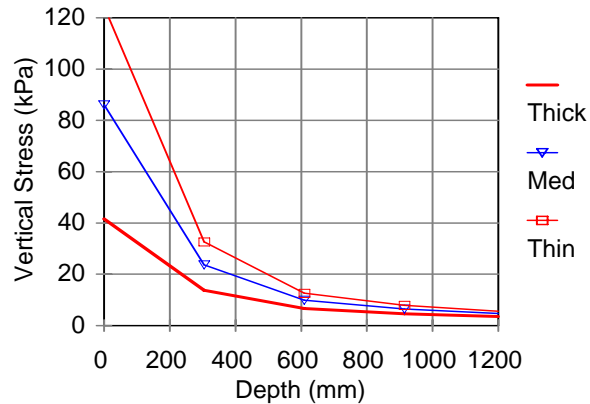
6.2.3.2 Calculating Stress Values for Multiple-Layer Soil

In the real world, there is no such thing as a uniform soil layer from the surface down to an infinite depth, so a subgrade with multiple layers having different strengths must be considered. To simulate real world conditions, three layers of soil with different permutations were applied to the BISAR model. Each of the top two layers was 300 mm (11.8 in) thick, and the third layer extended to infinite depth. The analysis used three levels of pavement structure: 2.5 in (63.5 mm) AC (thin), 2.5 in (63.5 mm) AC on 5 in (127 mm) ATB (mid), and 5.5 in (139.7 mm) AC on 6 in (152.4 mm) ATB (thick). The resilient modulus of the soil layers are 5,500 psi (37.9 kPa), 15,000 psi (103.4 MPa), and 30,000 psi (206.8 MPa) respectively. Table 11 shows the calculated stresses at different depths.

Table 11. Vertical Stresses At Different Depths

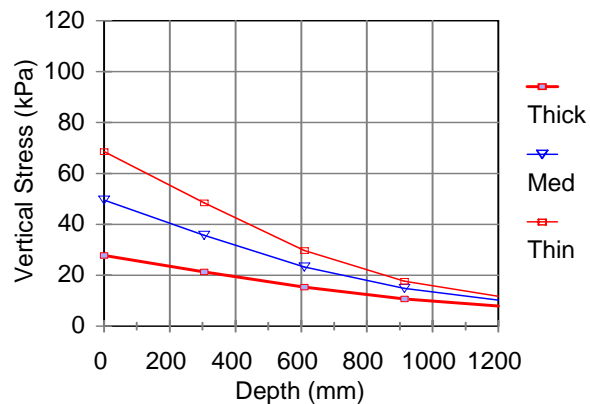
				Vertical Stresses (psi)				
Pavement	Soil Resilient Modulus (psi)			Stress Location (depth in inches)				
	Layer 1	Layer 2	Layer 3	0	12	24	36	48
Thick	30000	15000	5500	6.05	2.01	0.976	0.682	0.513
Thick	15000	30000	5500	5.18	2.53	1.08	0.767	0.574
Thick	30000	5500	15000	5.81	2.12	1.57	1.14	0.856
Thick	5500	30000	15000	4.07	2.98	1.9	1.36	0.998
Thick	15000	5500	30000	4.05	3.1	2.23	1.56	1.13
Thick	5500	15000	30000	4.75	2.67	2.07	1.5	1.12
Mid	30000	15000	5500	12.5	3.45	1.45	0.946	0.676
Mid	15000	30000	5500	10.1	4.56	1.62	1.07	0.757
Mid	30000	5500	15000	12.1	3.35	2.33	1.58	1.12
Mid	5500	30000	15000	7.33	5.17	2.9	1.9	1.3
Mid	15000	5500	30000	9.3	4.29	3.12	2.09	1.45
Mid	5500	15000	30000	7.2	5.2	3.39	2.16	1.45
Thin	30000	15000	5500	18.1	4.74	1.84	1.15	0.792
Thin	15000	30000	5500	14.4	6.41	2.04	1.28	0.879
Thin	30000	5500	15000	17.6	4.42	2.96	1.91	1.31
Thin	5500	30000	15000	10.2	7.09	3.65	2.26	1.49
Thin	15000	5500	30000	13.3	5.73	4	2.53	1.69
Thin	5500	15000	30000	9.97	7.04	4.32	2.58	1.66
				Vertical Stresses (kPa)				
Pavement	Soil Resilient Modulus (MPa)			Stress Location (depth in m)				
	Layer 1	Layer 2	Layer 3	0.00	0.30	0.61	0.91	1.22
Thick	207	103	38	41.71	13.86	6.73	4.70	3.54
Thick	103	207	38	35.71	17.44	7.45	5.29	3.96
Thick	207	38	103	40.06	14.62	10.82	7.86	5.90
Thick	38	207	103	28.06	20.55	13.10	9.38	6.88
Thick	103	38	207	27.92	21.37	15.38	10.76	7.79
Thick	38	103	207	32.75	18.41	14.27	10.34	7.72
Mid	207	103	38	86.18	23.79	10.00	6.52	4.66
Mid	103	207	38	69.64	31.44	11.17	7.38	5.22
Mid	207	38	103	83.43	23.10	16.06	10.89	7.72
Mid	38	207	103	50.54	35.65	19.99	13.10	8.96
Mid	103	38	207	64.12	29.58	21.51	14.41	10.00
Mid	38	103	207	49.64	35.85	23.37	14.89	10.00
Thin	207	103	38	124.80	32.68	12.69	7.93	5.46
Thin	103	207	38	99.28	44.20	14.07	8.83	6.06
Thin	207	38	103	121.35	30.47	20.41	13.17	9.03
Thin	38	207	103	70.33	48.88	25.17	15.58	10.27
Thin	103	38	207	91.70	39.51	27.58	17.44	11.65
Thin	38	103	207	68.74	48.54	29.79	17.79	11.45

Figure 32 is a plot of stress values at different depths for three pavement thicknesses when the soil strength increases as depth increases. Figure 33 is a plot of stress values at the same depths shown in Figure 32 but with soil strength decreasing as depth increases.



1 mm = 0.0394 in

Figure 32. Vertical Stress When Subgrade Strength Increases with Depth



1 mm = 0.0394 in

Figure 33. Vertical Stress When Subgrade Strength Decreases with Depth

6.2.3.3 Variable Pavement Strength, Single-Layer Soil

Again, BISAR was utilized to calculate vertical stresses at different depths in the subgrade. This time, the subgrade was assumed to be a uniform layer from surface to infinite depth. SPS1 designs, which included weak as well as strong pavement but with a uniform subgrade layer, were applied. Results of vertical stress at 0 (surface of the subgrade), 12 in (0.3 m), 24 in (0.6 m), 36 in (0.9 m), 48 in (1.2 m), and 60 in (1.5 m) depth are presented in Table 12.

Table 12. Vertical Stresses under SPS1 Designs

English Units											
SPS1 Section	Layer Thickness (in)				M _R (psi)	Depth (in)					
	AC	ATB	PATB	GB		0	12	24	36	48	60
						Vertical Stresses (psi)					
101	7			8	5000	2.73	1.66	1.14	0.83	0.64	0.5
					10000	3.99	2.25	1.45	1.02	0.75	0.57
					20000	5.62	2.96	1.8	1.21	0.86	0.64
					30000	6.71	3.42	2.02	1.32	0.92	0.68
102	4			12	5000	3.15	1.79	1.18	0.84	0.63	0.5
					10000	4.66	2.45	1.52	1.03	0.75	0.57
					20000	6.56	3.23	1.88	1.23	0.86	0.64
					30000	7.77	3.72	2.11	1.34	0.93	0.67
107	4		4	4	5000	4.52	2.48	1.58	1.09	0.8	0.6
					10000	6.49	3.28	1.95	1.28	0.91	0.67
					20000	8.88	4.18	2.34	1.47	1.01	0.73
					30000	10.4	4.74	2.57	1.58	1.06	0.76
108	7		4	8	5000	2.04	1.27	0.89	0.67	0.52	0.42
					10000	3.02	1.76	1.17	0.84	0.63	0.49
					20000	4.28	2.36	1.48	1.02	0.74	0.56
					30000	5.11	2.74	1.68	1.13	0.81	0.6
110	4	8	4		5000	1.96	1.36	0.98	0.74	0.58	0.46
					10000	2.92	1.85	1.26	0.91	0.69	0.54
					20000	4.22	2.47	1.58	1.1	0.8	0.61
					30000	5.15	2.89	1.79	1.21	0.87	0.65
112	4	12	4		5000	1.28	0.85	0.64	0.51	0.41	0.34
					10000	1.94	1.2	0.86	0.65	0.52	0.42
					20000	2.86	1.66	1.12	0.82	0.62	0.49
					30000	3.53	1.99	1.3	0.92	0.69	0.53
Max						10.4	4.74	2.57	1.58	1.06	0.76
Min						1.28	0.85	0.64	0.51	0.41	0.34

Table 12. Vertical Stresses under SPS1 Designs

(metric units)											
SPS1 Section	Layer Thickness (m)				M _R (MPa)	Depth (m)					
	AC	ATB	PATB	GB		0	0.30	0.61	0.91	1.22	1.52
Vertical Stresses (kPa)											
101	0.18			0.20	34.47	18.82	11.45	7.86	5.72	4.41	3.45
					68.95	27.51	15.51	10.00	7.03	5.17	3.93
					137.90	38.75	20.41	12.41	8.34	5.93	4.41
					206.84	46.26	23.58	13.93	9.10	6.34	4.69
102	0.10			0.30	34.47	21.72	12.34	8.14	5.79	4.34	3.45
					68.95	32.13	16.89	10.48	7.10	5.17	3.93
					137.90	45.23	22.27	12.96	8.48	5.93	4.41
					206.84	53.57	25.65	14.55	9.24	6.41	4.62
107	0.10		0.10	0.10	34.47	31.16	17.10	10.89	7.52	5.52	4.14
					68.95	44.75	22.61	13.44	8.83	6.27	4.62
					137.90	61.23	28.82	16.13	10.14	6.96	5.03
					206.84	71.71	32.68	17.72	10.89	7.31	5.24
108	0.18		0.10	0.20	34.47	14.07	8.76	6.14	4.62	3.59	2.90
					68.95	20.82	12.13	8.07	5.79	4.34	3.38
					137.90	29.51	16.27	10.20	7.03	5.10	3.86
					206.84	35.23	18.89	11.58	7.79	5.58	4.14
110	0.10	0.20	0.10		34.47	13.51	9.38	6.76	5.10	4.00	3.17
					68.95	20.13	12.76	8.69	6.27	4.76	3.72
					137.90	29.10	17.03	10.89	7.58	5.52	4.21
					206.84	35.51	19.93	12.34	8.34	6.00	4.48
112	0.10	0.30	0.10		34.47	8.83	5.86	4.41	3.52	2.83	2.34
					68.95	13.38	8.27	5.93	4.48	3.59	2.90
					137.90	19.72	11.45	7.72	5.65	4.27	3.38
					206.84	24.34	13.72	8.96	6.34	4.76	3.65
Max					71.71	32.68	17.72	10.89	7.31	5.24	
Min					8.83	5.86	4.41	3.52	2.83	2.34	

It was found that no matter what the pavement strength is over the range of subgrade modulus values in this study, the vertical stresses at 24 in (0.6 m) and 36 in (0.9 m) converged to ranges of 0.5 to 2.5 psi (3.4 to 17.2 kPa) and 0.5 to 1.5 psi (3.4 to 10.3 kPa) respectively. This result indicates that investigation of subgrade strength to a depth of 24 to 36 in (0.6 to 0.9 m) is sufficient.

From the law of stress distribution, we can restate that stress induced by surface loading decreases as depth increases. So soil layers whose strength increases as depth increases will not cause any concern to the pavement engineer. The situation of concern to the pavement engineer is when the soil layer underneath is weaker than the top. The weaker soil may still suffice to support the pavement underneath. In this case, we need to know how much weaker is still acceptable.

Figure 32 shows that when soil strength increases as depth increases, the top layer experiences higher stress. But, as Figure 33 indicates, when soil strength decreases as depth increases, the deeper layers experience higher stress.

To develop a general chart of required PR values, it was decided to investigate the stress required when soil strength decreases as depth increases. This approach provides a safety factor for the required soil strength by ensuring that the required soil strength covers the worst-case scenario. Table 13 summarizes the calculated stresses and the maximum allowable PR values at several different depths for three different asphalt pavement thicknesses handling different traffic loads. This table is intended to demonstrate the relationship between the depth and the required PR. It is not intended to be used for field applications.

Table 13. Soil Stresses and Maximum Allowable PRs for AC Pavements of Given Thicknesses Handling Selected Traffic Loads

Traffic load	5000 kESAL		1000 kESAL		50 kESAL	
	AC pavement 11.5 in		AC pavement 7.5 in		AC pavement 5 in	
Depth (in)	Stress (psi)	Maximum PR (in/blow)	Stress (psi)	Maximum PR (in/blow)	Stress (psi)	Maximum PR (in/blow)
0	4.05	0.8	7.2	0.691	9.97	1.026
12	3.1	1.018	5.2	0.926	7.04	1.404
24	2.23	1.369	3.39	1.36	4.32	2.178
36	1.56	1.889	2.16	2.041	2.58	3.464
48	1.13	2.525	1.45	2.921	1.66	5.151

Traffic load	5000 kESAL		1000 kESAL		50 kESAL	
	AC pavement 292 mm		AC pavement 190 mm		AC pavement 127 mm	
Depth (m)	Stress (kPa)	Maximum PR (mm/blow)	Stress (kPa)	Maximum PR (mm/blow)	Stress (kPa)	Maximum PR (mm/blow)
0	27.92	20.33	49.64	17.54	68.74	26.06
0.3	21.37	25.86	35.85	23.51	48.54	35.65
0.61	15.38	34.78	23.37	34.55	29.79	55.32
0.91	10.76	47.98	14.89	51.83	17.79	87.98
1.22	7.79	64.13	10	74.2	11.45	130.84

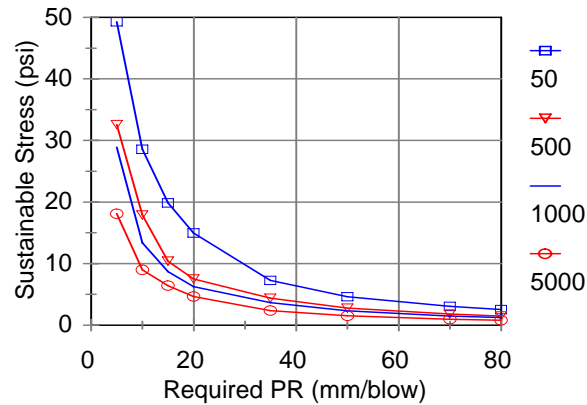
To determine the values shown in this table, the author started with the design kESAL values. From these were derived the design CBR, and then the required pavement thickness was computed. These are full-depth asphalt pavements without bases. The total AC thicknesses are 11.5, 7.5, and 5 inches (292.1, 190.5, and 127 mm) for traffic loads of 5000 kESAL, 1000 kESAL, and 50 kESAL respectively.

Based on kESAL, design CBR, and pavement thickness values, the soil stress values and required PR values were then calculated. The PR values were computed using Equation 10, so the PR is a function of both the stress and the traffic load, while the stress values do not depend on traffic volume.

The required PR values are therefore based on the designed pavement structure, which is thicker for higher traffic loading levels. Notice that the required subgrade stiffness is less when the

pavement is thicker, because a thicker layer of pavement is stiffer and thus transfers less of the stress to the subgrade.

Figure 34 is a plot of the sustainable stresses corresponding to required PR values for different traffic loading levels. This chart can be used to determine if the subgrade PR meets the design requirement.



1 mm = 0.0394 in

Figure 34. Sustainable Stress vs. Required PR under Different Traffic Loadings (in kESAL)

6.3 Application Example

Here is an example of how this concept can be applied to a simple pavement design consisting of a 50 mm (2 in) AC surface on cement-treated (CT) soil, following the Chestnut project. DCP test results showed that the in-situ thickness of the AC layer is 60 mm (2.4 in). The designed CT layer is 300 mm (11.8 in), but the in-situ CT thickness is 150 mm (5.9 in) and the average PR is 10 mm/blow (0.39 in/blow) ($M_R = 33,000$ psi [227.5 MPa]). Compare this to the average PR of natural soil, which is 18 mm/blow (0.71 in/blow) ($M_R = 17,000$ psi [117.2 MPa]). These data were input into BISAR. It was assumed that the modulus of the AC surface course was 3445 MPa (500,000 psi). The stresses under a standard axle (18 kip [80.1 kN], dual tires) at different layer interfaces were calculated.

It was assumed that the design life of the pavement is 10,000 ESAL loading. The vertical stresses on the surface of the CT, the surface of the natural soil, and at a point 300 mm (11.8 in) below the surface of the natural soil were converted to the required PRs using Equation 10 from Section 6.2.3.1. The results are summarized in Table 14.

Table 14. Summary of Stresses in Application Example					
Layer	Position Z (in)	Stress (psi)			Required PR (in/blow)
		Hx	Hy	Vz	
AC	2.36	-54.4	102	-18.7	
CT	2.36	-15	-5.09	-18.7	0.83
CT	8.27	2.91	9.21	-14.2	
Soil	8.27	-4.47	-1.34	-14.2	1.06
Soil	20.08			-6.14	2.28
Layer	Position Z (mm)	Stress (kPa)			Required PR (mm/blow)
		Hx	Hy	Vz	
AC	60	-375.07	703.27	-128.93	
CT	60	-103.42	-35.09	-128.93	21
CT	210	20.06	63.50	-97.91	
Soil	210	-30.82	-9.24	-97.91	27
Soil	510			-42.33	58

Figure 35 is the plot of the calculated required PR and the field test results. The required PR line is above the test results, indicating that the in-situ subgrade stiffness is sufficient for the design. Figure 36 shows a case in which the subgrade stiffness did not meet the required PR constraint.

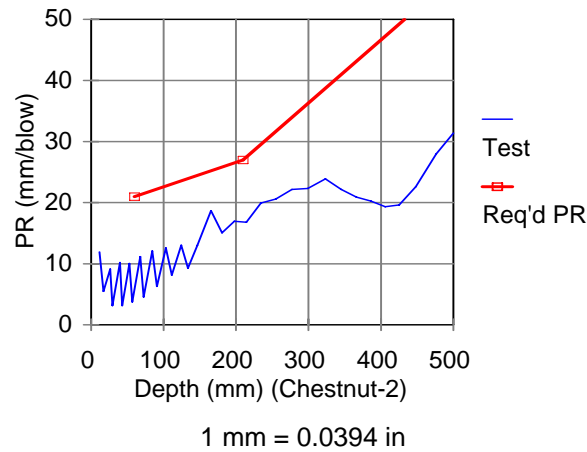
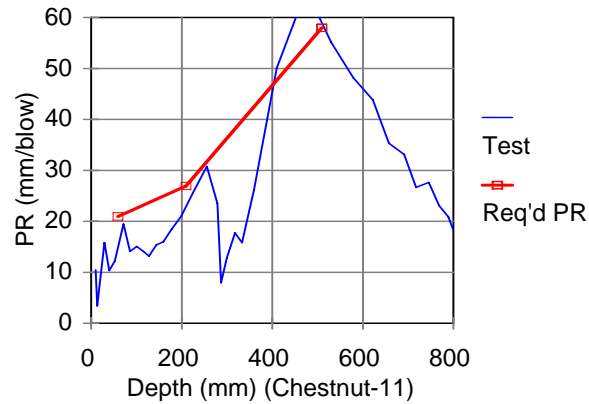


Figure 35. Required PR and Test Results



1 mm = 0.0394 in

Figure 36. A Questionable Subgrade Stiffness

BISAR results showed positive stress (tension) (see Table 14) at the bottom of the AC surface course and at the bottom of the CT layer. Verifying the fatigue lives of these two layers is necessary to ensure the pavement structure fulfills all design requirements. This issue is beyond the scope of this study.

7 Findings

The data collected and the analysis done in this research project yielded the following findings:

1. This study's DCP data showed that no matter what types of treatment were used, with 95 percent certainty one can expect the treated soil to have a PR less than or equal to 8 mm/blow (0.32 in/blow).
2. Test data showed that under the current Ohio specification and practice, construction of a 300 mm (11.8 in) homogeneously stabilized soil layer can be achieved.
3. The design depth of treated soil is 300 mm (11.8 in). Only 20 percent of the samples collected in this study showed a stiff layer reaching that depth. In other words, 80 percent of the samples showed that the treated layer did not achieve the design thickness.
4. The DCP soundings for a NJ OGGB and an Iowa OGGB are different. The average PR of the NJ base and Iowa base are 7 mm/blow (0.28 in/blow) and 14 mm/blow (0.55 in/blow) respectively. The coefficient of variation (COV) for the NJ base is 32 percent, as opposed to 43 percent for the Iowa base. The difference in these values shows that the NJ base is more uniform than the Iowa base.
5. In most cases, the top half (50 mm or 2 in) of the OGGB was not as stiff as the lower half (that is, the top half had a greater PR reading). It is possible that the unconfined open graded granular material shifted horizontally under the pressure of the cone.
6. The 95th percentile PR (stiffness) of the Ohio 304 base is 8 mm/blow (0.31 in/blow). The average PR for the Ohio 304 base is 5.35 mm/blow (0.2 in/blow).
7. The Ohio DOT construction specification requires special attention to construction of the subgrade layer, which is the top 300 mm (11.8 in) of the soil beneath the pavement structure. DCP test results indicated that although some of the samples had a stiffer layer within the 300 mm (11.8 in) subgrade layer, many samples indicated a subgrade layer weaker and/or less uniform than the foundation. These results indicated that despite the additional requirements in the construction specification, the goal of ensuring a stiffer soil layer beneath the pavement structure was not always achieved.
8. Theoretical PR acceptance criteria were developed. Results showed that the required PR has a good correlation with vertical stress and loading. The equation developed in this study can be applied during the project design stage to establish a subgrade stiffness requirement.
9. The DCP can penetrate through a thin layer of asphalt with little effort. Most of the PR values for the AC surface course were concentrated in the range of 2 to 7 mm/blow (0.07 to 0.28 in/blow). The average PR for the AC surface course is 5.2 mm/blow (0.2 in/blow).
10. A few AC surface course PR readings are far outside the normal range of AC surface course readings. These outlying data points coincide with a weak underlay of cement-treated soil. Weaker (less stiff) AC can be the result of poor compaction. Data showed that to provide a proper support for AC surface compaction, the layer immediately beneath the surface must be stiffer, with PR less than 12 mm/blow (0.47 in/blow).

8 Conclusions and Recommendations

DCP testing is a quick and dirty method for collecting in-situ subgrade soil stiffness data. Extensive sampling for subgrade evaluation can be accomplished in a reasonable time frame. DCP testing can be used to penetrate a thin AC surface course, a granular base, stabilized soil, and natural soil to evaluate the stiffness of these materials. An in-situ stiffness profile to an established depth can be obtained. This profile is a useful tool to evaluate the as-constructed stiffness of these layers.

Using the data from the ODOT projects, this study found that the 95th percentile PR for stabilized soil is 8 mm/blow (0.32 in/blow). Therefore, the acceptable PR for the stabilized soil layer shall be set at 8 mm/blow (0.32 in/blow).

DCP tests were performed on two types of OGGB. The PR readings in the top layer of the 100 mm (3.9 in) OGGB were usually higher than the PR readings in the lower layer. This finding raises two concerns: (1) the stability of OGGB is questionable, and (2) its ability to support the construction traffic without severe surface deformation is also questionable. This study also found that the NJ OGGB is stiffer (has a lower PR reading) and more uniform than the Iowa OGGB. As a result, it is recommended that the state use untreated OGGB with great care.

The 95th percentile PR of the Ohio 304 base is 8 mm/blow (0.32 in/blow). This value can be used initially to accept the Ohio 304 base.

At many test locations, the stabilized soil did not achieve its potential stiffness throughout its design depth. The DCP may be the only device available that can identify and verify this problem. Implementation of DCP testing in construction acceptance will help identify locations with such poor quality and understand the causes.

The study found that the quality of subgrade layer construction did not always fulfill the intention of providing a good platform beneath the pavement structure. Subgrade support is crucial for long-term pavement performance. To correct an inferior subgrade after road construction is very costly. It is in the best interest of the infrastructure owner to make certain that the pavement structure is placed on a sound subgrade. While other testing devices may be able to evaluate the composite strength of the soil, they cannot yield a soil layer profile in depth. The DCP can complete the evaluation of one test site in less than five minutes. At this pace, it is possible to collect enough in-situ data to realize the soil stiffness variation in all three dimensions. Implementing DCP testing for subgrade acceptance will greatly improve the chance that a quality subgrade will be constructed and hence help ensure pavement performance. It is recommended that Ohio develop a Project Special Provision based on the knowledge obtained from this study and then implement this provision in projects across the state to collect more data to improve the DCP-based acceptance procedure.

The conclusions of this study are based on 10 projects tested over a two-year period. The suggested standards are reasonably achievable under the current specification and practice. They may not be the optimal target values for these parameters. More DCP test data are needed to

formulate a good standard. ODOT should therefore develop a Project Special Provision based on this report and implement DCP testing on more construction projects. The data collected can be analyzed and utilized to modify and enhance the standard values this study recommends and eventually develop a standard specification.

The current Ohio DOT specification stipulates additional requirements for constructing the top 300 mm (11.8 in) of the soil to form a stronger platform to support the pavement structure. DCP test results indicated that, in many cases, the constructed subgrade layer did not meet this goal. Field study found that severe distress in a few localized weak areas can bring a project to total failure. To repair a failed subgrade is not only costly, but also greatly disturbing to the traveling public. It is therefore strongly recommended that field investigation be performed to identify the reasons for these poor quality results.

Study results strongly suggest that using a DCP to evaluate a thin AC layer is possible, and furthermore that a DCP-based low-volume road pavement design and acceptance procedure can be developed with further research. Development of such a procedure should greatly improve the quality of often-neglected low-volume road construction. It is recommended that more projects with thin AC on a gravel base, natural soil, or stabilized soil be identified and tested.

The acceptable PR for a thin AC surface course on a low-volume road shall be set at 7 mm/blow (0.28 in/blow). The subgrade shall be tested prior to the paving operation, making sure that the subgrade PR is less than 12 mm/blow (0.47 in/blow) to ensure the subsequent AC surface paving quality.

The cement-treated subgrade of the Chestnut project showed a much higher PR reading (indicating a weaker subgrade) than the rest of the treated-subgrade projects, which were subject to ODOT standards. Further investigation of the Chestnut project construction documentation is recommended to discover the reasons for this inferior result.

Data collected from the Chestnut project indicated that when the stabilized soil PR is greater than 12 mm/blow (0.47 in/blow), the stiffness of the AC surface layer increases proportionally. This finding implies that when the subgrade PR is greater than 12 mm/blow (0.47 in/blow), the demonstrated weakness may affect the quality of AC compaction. This is an issue that warrants further study.

9 Implementation Plan

Studies performed by other agencies indicated that DCP sounding values (penetration rate, PR) correlate well with CBR, resilient modulus, unconfined compression strength, and static plate load test values. These results prove that DCP is a viable alternative for measuring the stiffness of in-situ soil, unbound base material, and even a thin asphalt concrete (AC) surface course.

Based on this study, it is recommended that ODOT develop a project special provision based on this report and implement DCP testing for unbound base and subgrade acceptance, and possibly for accepting the whole low-volume road pavement system, from surface course down to subgrade soil. After a sufficient amount of data has been collected on a wide variety of projects, the collected data can eventually be used to develop a standard specification.

It is recommended that ODOT implement DCP testing for quality control in two phases, described as follows:

9.1 Phase 1

Develop a Project Special Provision to incorporate DCP acceptance criteria into construction contracts. Start collecting DCP data from a wide range of construction projects to verify the following recommended acceptance levels:

- For Ohio dense grade base, PR < 8 mm/blow (0.31 in/blow)
- For cement, lime, and lime/cement stabilized soil, PR < 8 mm/blow (0.31 in/blow)
- For subgrade construction, a uniform stiffness (indicated by uniform PR readings) for the top 300 mm (11.8 in) of soil
- For a thin AC layer (e.g., on a low volume road), PR < 7 mm/blow (0.28 in/blow).

9.2 Phase 2

Establish acceptance levels for different soil types and/or regions and modify the acceptance standards based on data collected during Phase 1. Revise and migrate the Project Special Provision to the ODOT Construction Specification as a standard specification.

10 References

- AASHTO. *Guide for Design of Pavement Structures*. AASHTO, Washington, DC, 1986, Appendix J.
- Abu-Farsakh, M. Y., Alshibli, K., Nazzal, M. D., and Seyman, E. *Assessment of In-situ Testing Technology for Construction Control of Base Course and Embankments*, LTRC Project No. 02-1GT, Louisiana Department of Transportation and Development, May, 2004.
- ASTM. *Standard Test Method for Use of the Dynamic Cone Penetrometer in Shallow Pavement Applications*. Publication number D6951-03, ASTM, Washington, DC, 2003.
- Chen, D. H., Wu, W., He, R., Bilyeu, J., and Arrelano, M. *Evaluation of In-Situ Resilient Modulus Testing Techniques*. Geotechnical Special Publication No. 89, ASCE, 1999.
- Chen, D. H., Lin, D. F., Liau, P. H., and Bilyeu, J. "A Correlation Between Dynamic Cone Penetrometer Values and Pavement Layer Moduli," *Geotechnical Testing Journal*, Vol. 28, No. 1. ASTM International, West Conshohocken, PA, 2005.
- Chen, J., Hossain, M., and LaTorella, T. M. "Use of Falling Weight Deflectometer and Dynamic Cone Penetrometer in Pavement Evaluation," *Transportation Research Record 1655, Pavement Management Systems and Other Pavement Design Issues*. TRB, Washington, DC, 1999.
- Coonse, J. "Estimating California Bearing Ratio of Cohesive Piedmont Residual Soil Using the Scala Dynamic Cone Penetrometer." Master's Thesis(MSCE), North Carolina State University, Raleigh, N.C., 1999.
- Crovetti, J. A., and Schabelski, J. P. *Comprehensive Subgrade Deflection Acceptance Criteria*. WI/SPR 02-01, Wisconsin DOT, 2001.
- Ese, D., Myre, J., Noss, P., and Vaernes, E. "The Use of Dynamic Cone Penetrometer (DCP) for Road Strengthening Design in Norway," *Proceedings. The Fourth International Conference on the Bearing Capacity of Roads and Airfields*, 1994.
- Harison, J. A. "In Situ CBR Determination by DCP Testing Using a Laboratory- Based Correlation." *Australian Road Research*. 19(4), December, 1989.
- Kleyn, E. G. *The Use of the Dynamic Cone Penetrometer (DCP)*. Transvaal Roads Department, South Africa, July, 1975.
- Kleyn, E. G., Maree, J. H., and Savage, P. F. "The Application of a Portable Pavement Dynamic Cone Penetrometer to Determine in situ Bearing Properties of Road Pavement Layers and Subgrades in South Africa." *The European Symposium on Penetration Testing*, Amsterdam, Netherlands, May, 1982.

Kleyn, E. G., and Savage P. F. "The Application of the Pavement DCP to determine the Bearing Properties and Performance of Road Pavements." The International Symposium on Bearing Capacity of Roads and Airfields, Trondheim, Norway, June, 1982.

Kleyn, E. G., and van Heerden, M. J. J. "Using DCP Sounding to Optimize Pavement Rehabilitation." Annual Transportation Convention, Johannesburg, South Africa, July, 1983.

Kremer, C., and Dai, S. Improvement and Validation of MN/DOT Specification for Aggregate Base, Minnesota Department of Transportation, Maplewood, MN, 2004.

Livneh, Moshe, and Ishai, Ilan. "Pavement and Material Evaluation by a Dynamic Cone Penetrometer," Proceedings, Sixth International Conference Structural Design of Asphalt Pavements. Volume I, Ann Arbor, Michigan, USA, July 13-17, 1987, pp 665 to 676.

Livneh, M. "The Use of Dynamic Cone Penetrometer in Determining the Strength of Existing Pavements and Subgrades," Proceedings. 9th Southeast Asian Geotechnical Conference, Bangkok, 1987.

Livneh, M., Ishai, I., and Livneh, N. A. "Automated DCP Device Versus Manual DCP Device." Road and Transport Research. Vol. 1, No. 4, 1992.

NHI. Pavement Deflection Analysis. Participant Workbook, FHWA-HI-94-021, FHWA, 1994

Ohio DOT. The 2002 Construction and Material Specifications. Office of Construction Administration, Ohio DOT, Columbus, OH, 2002.

Smith, R. B., and Pratt, D. N. "A Field Study of In Situ California Bearing Ratio and Dynamic Cone Penetrometer Testing for Subgrade Investigations," Australian Road Research. 13(4) pp. 285-294. Australian Road Research Board, 1983.

De Villiers, P. J. Dynamic Cone Penetrometer Correlation with Unconfined Compressive Strength. University of Pretoria, Pretoria, South Africa, 1980

van Vuuren, D. J. "Rapid Determination of CBR with the Portable Dynamic Cone Penetrometer," The Rhodesian Engineer, September, 1969.

Webster, S. L., Grau, R. H., and Williams, T. P. "Description and Application of Dual Mass Dynamic Cone Penetrometer." Instruction Rep. GL-92-3, U.S. Army Engineer Research and Development Center, Waterways Experiment Station, Vicksburg, Miss., 1992.

Webster, S. L., Brown, R. W., and Porter, J. R. Force Projection Site Evaluation Using the Electronic Cone Penetrometer (ECP) and the Dynamic Cone Penetrometer (DCP). Technical Report GL-94-17, U.S. Army Engineer Research and Development Center, Waterways Experiment Station, Vicksburg, MS, 1994.

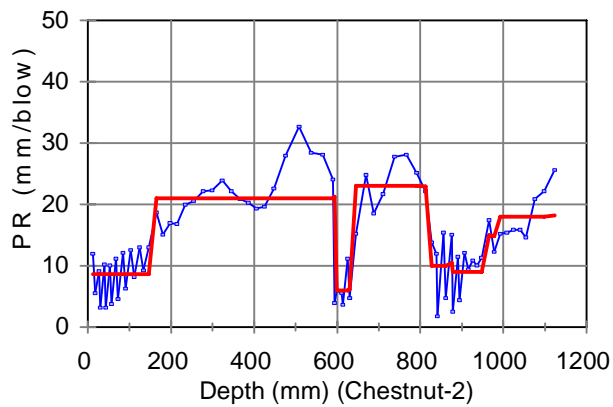
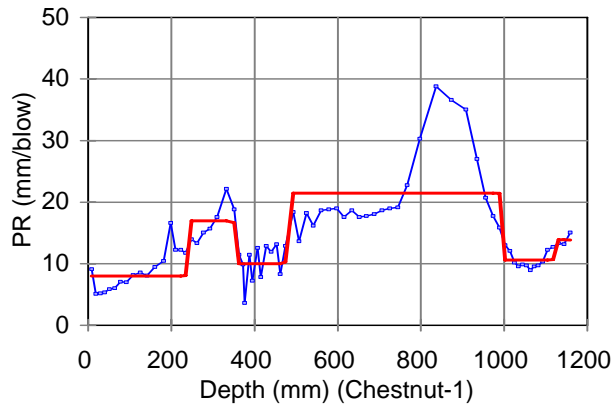
Wu, S. "DCP Field Application." Internally circulated report, North Carolina Department of Transportation, 1987.

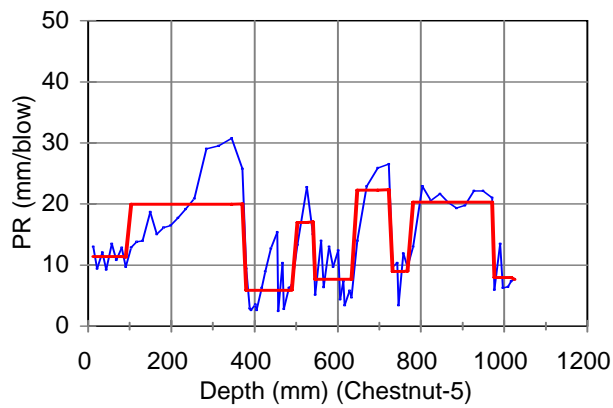
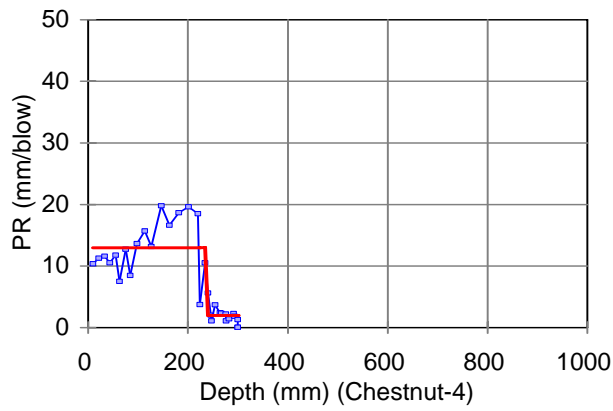
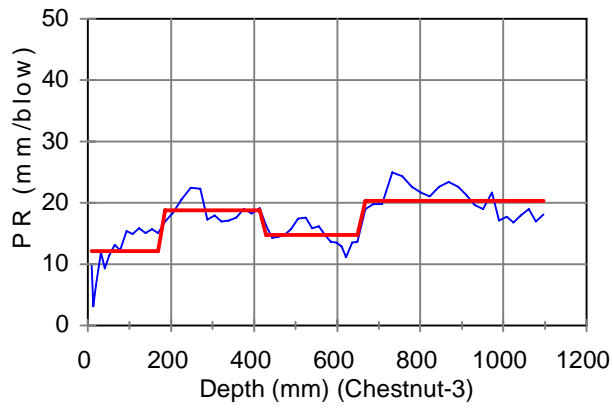
Appendix: Plots of Penetration Rate Data Collected for this Study

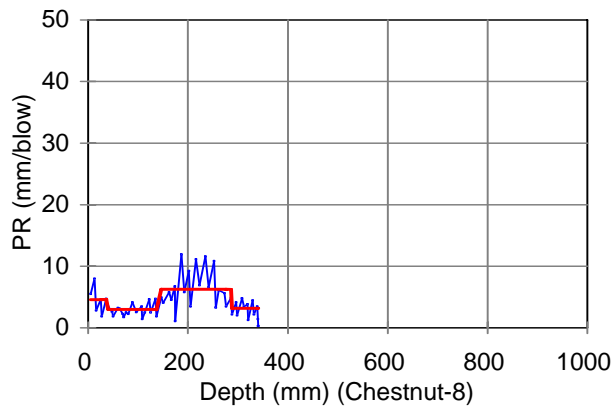
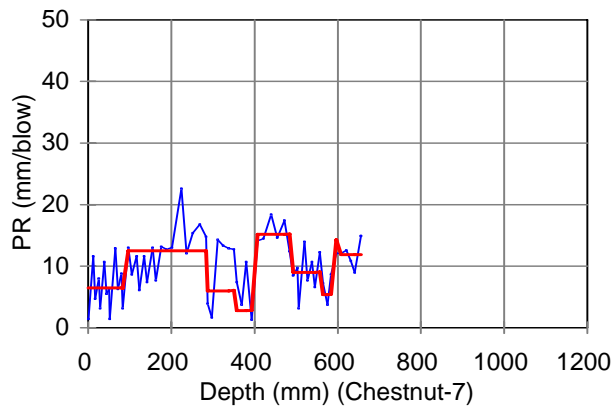
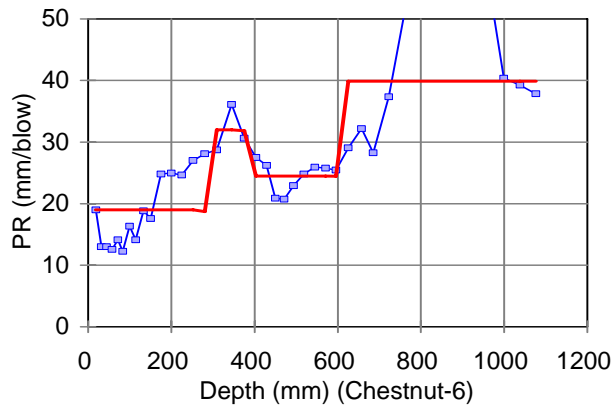
This appendix contains PR plots of all data collected for this study. Vertical axes for all plots have the same scale to facilitate comparison.

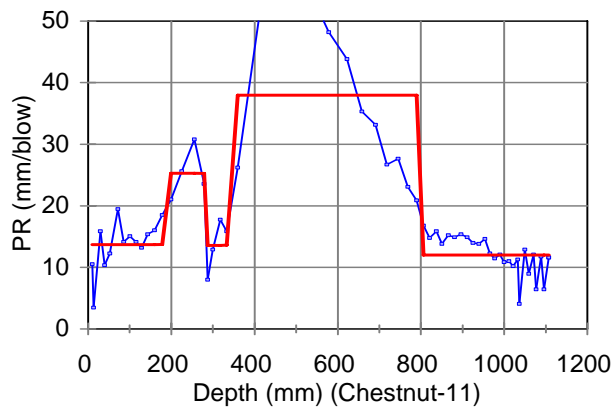
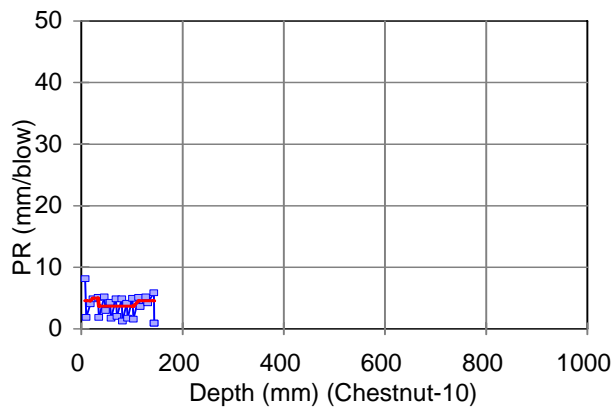
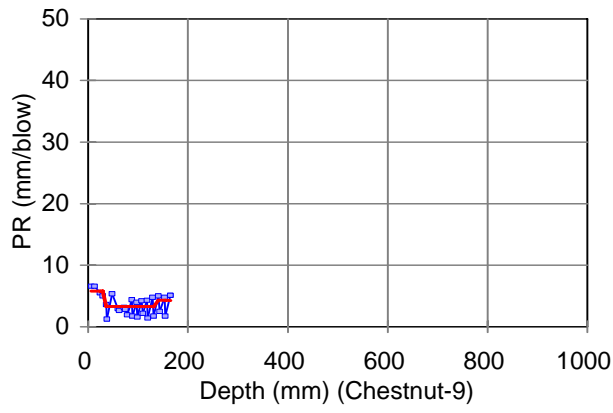
Note: 25.4 mm = 1 in, 304.8 mm = 1 ft

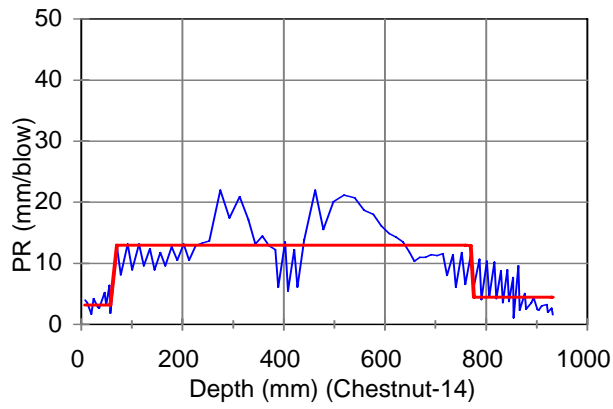
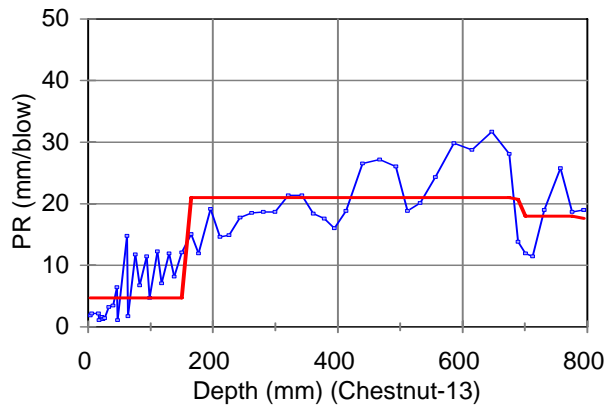
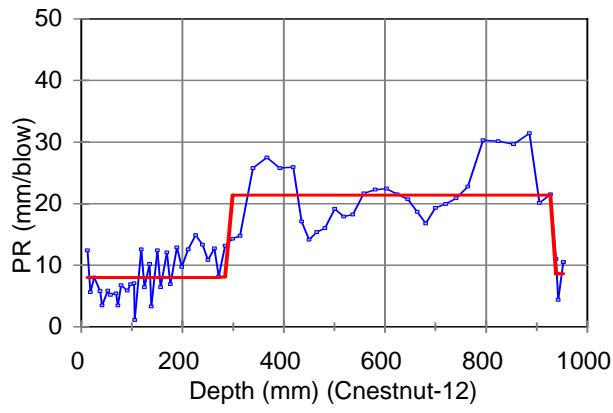
Chestnut 1 to 23: 50mm AC, 300mm CT

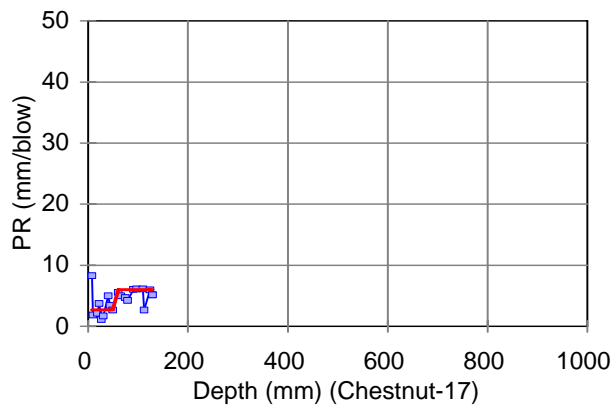
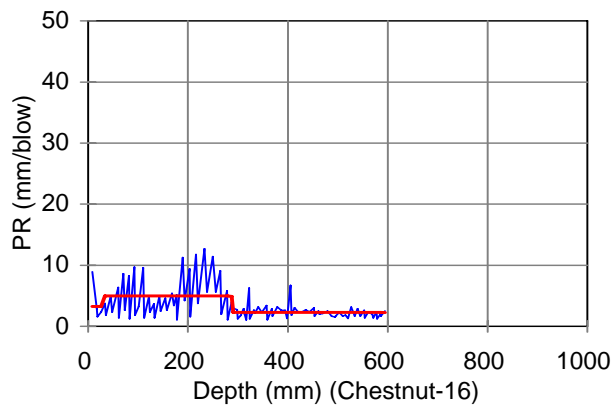
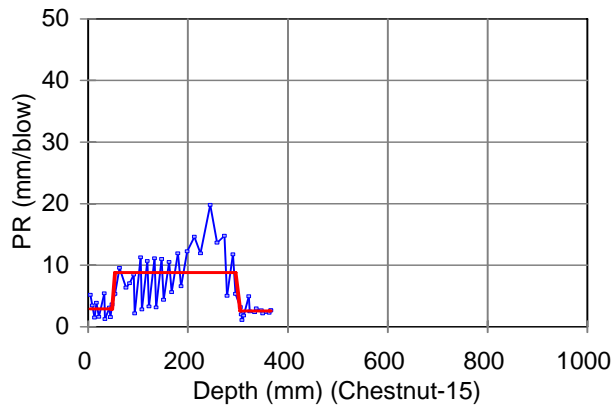


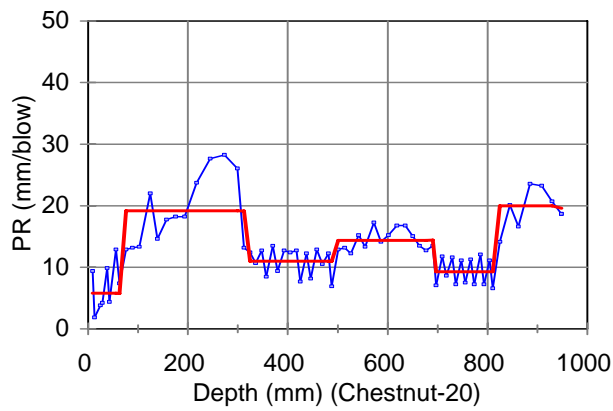
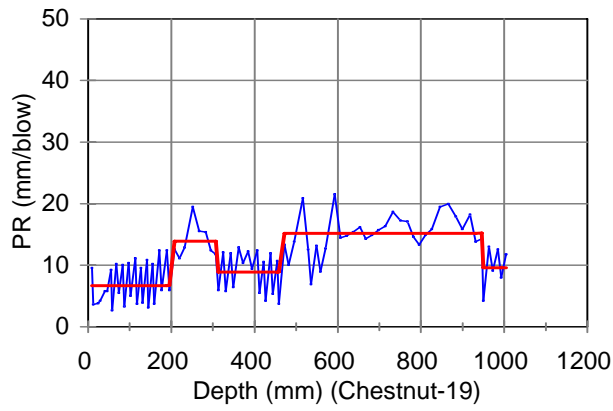
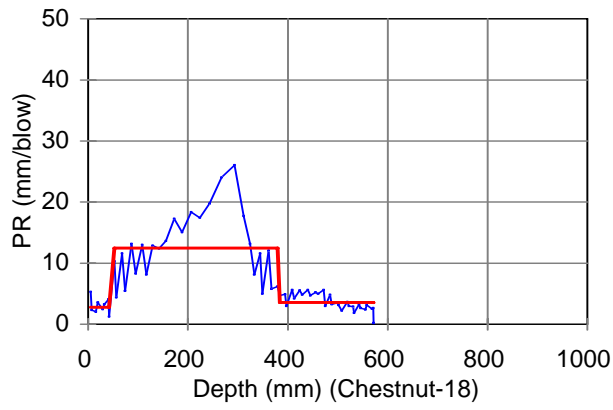


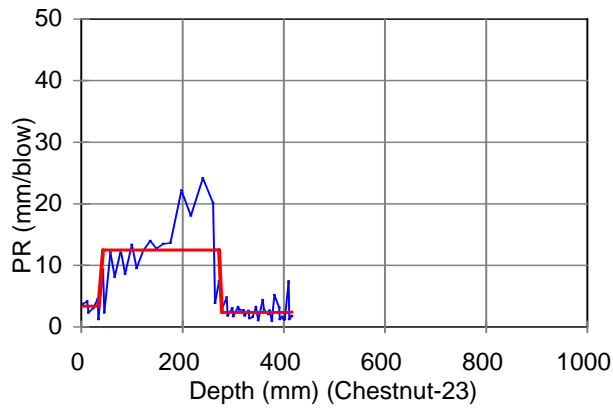
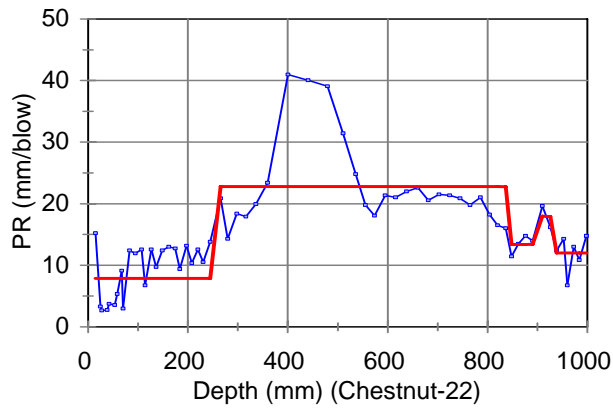
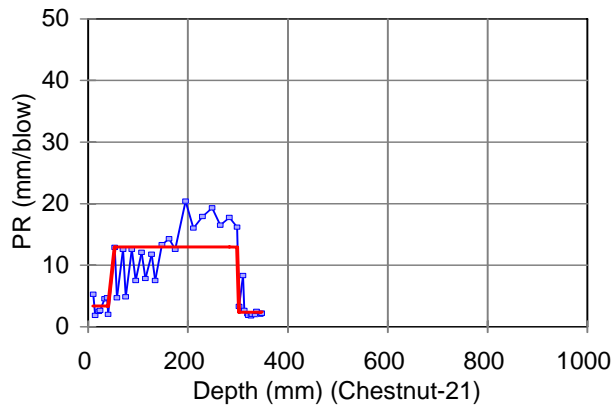






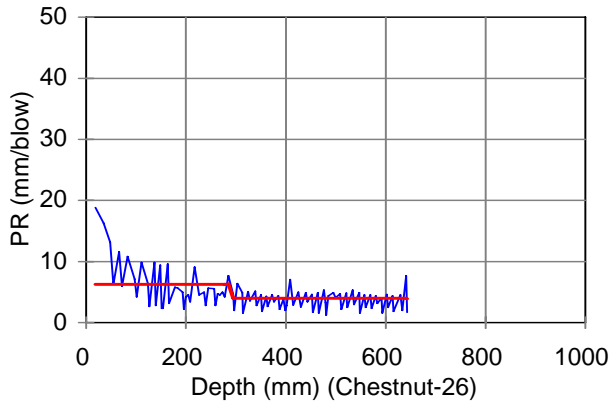
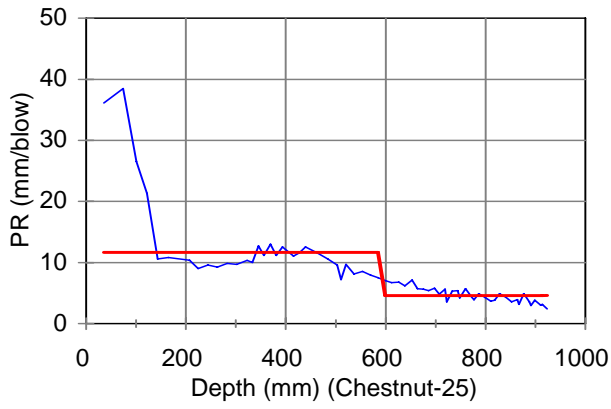
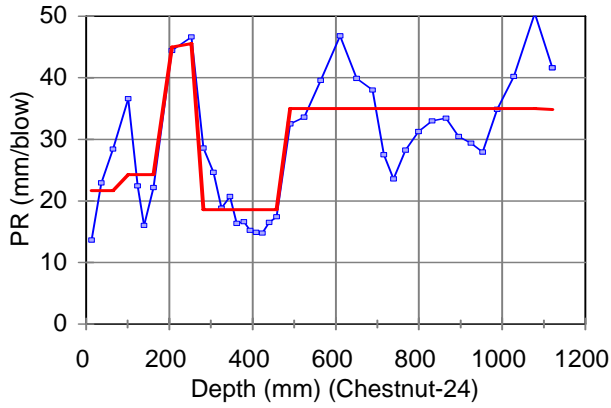




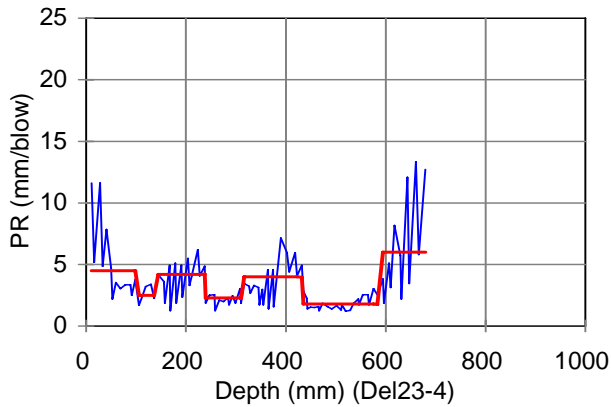
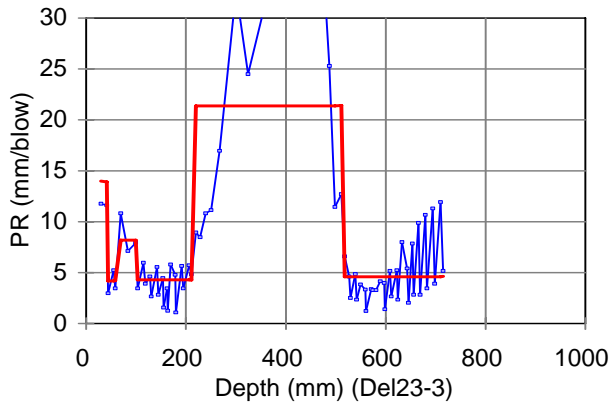
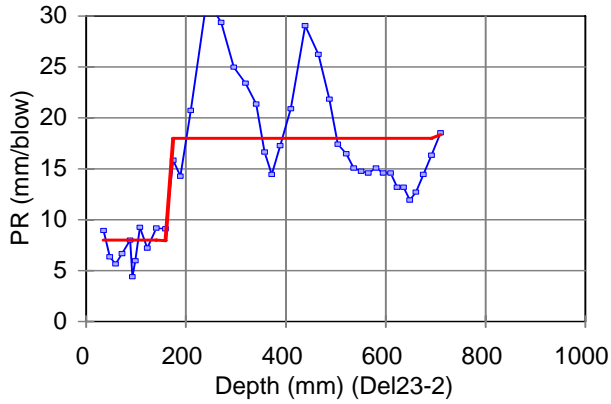


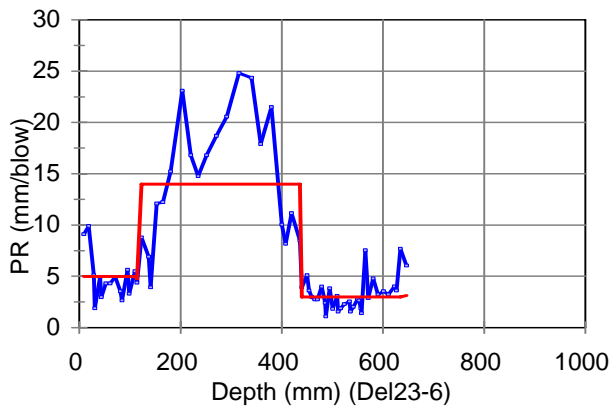
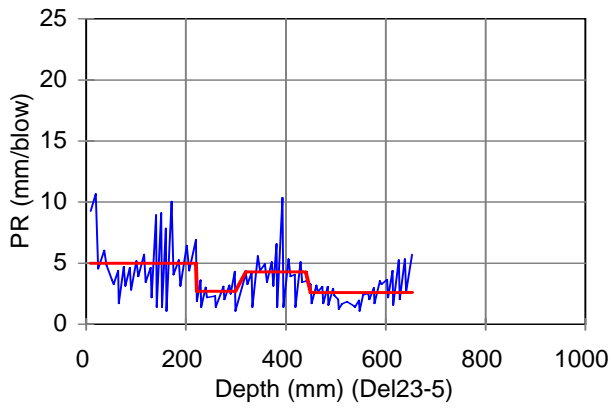
Chestnut 24 to 26:

50mm AC on Untreated Soil

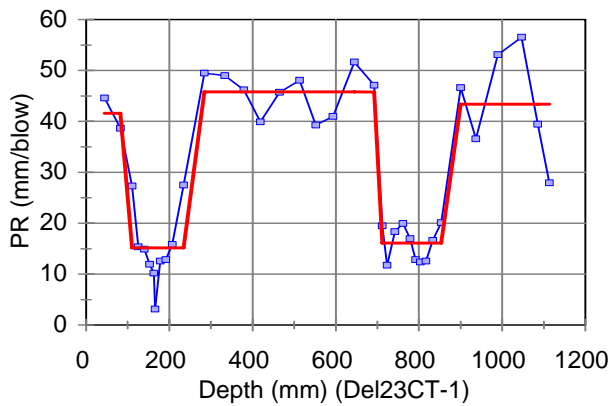


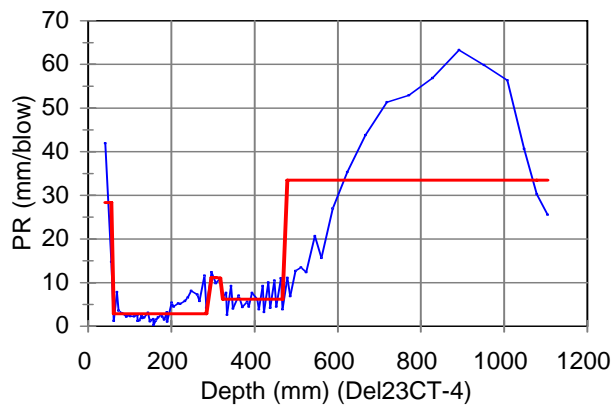
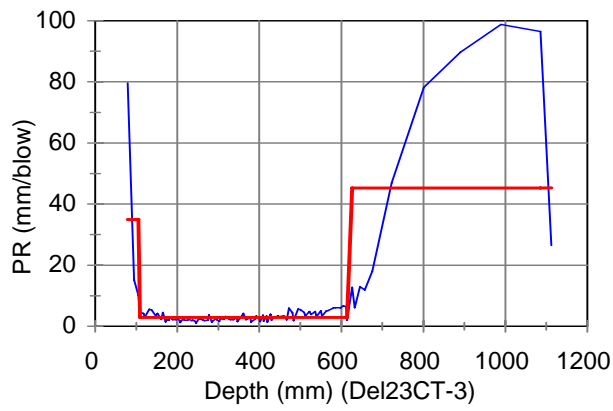
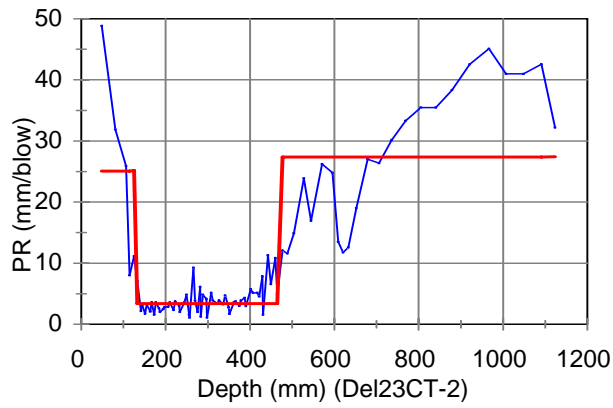
Del23: 2 to 6: 300mm Cement Treated Soil

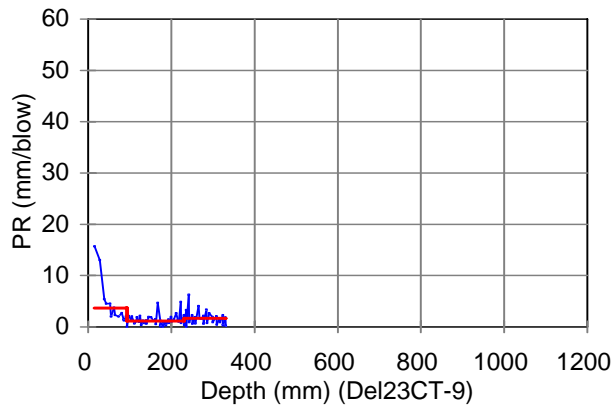
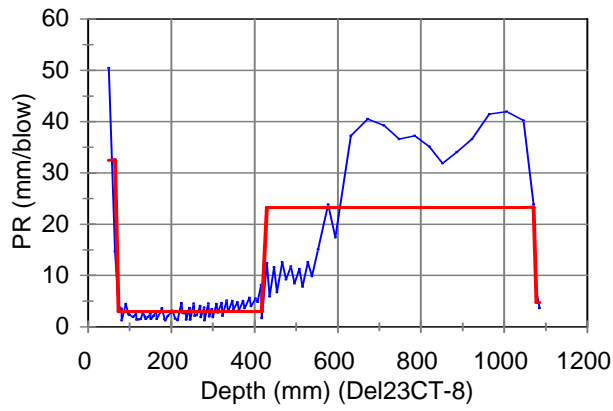
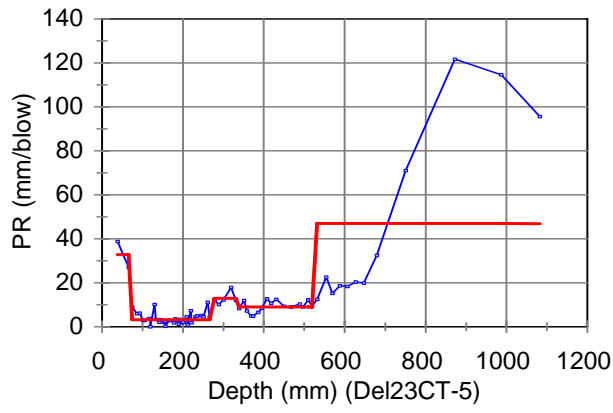


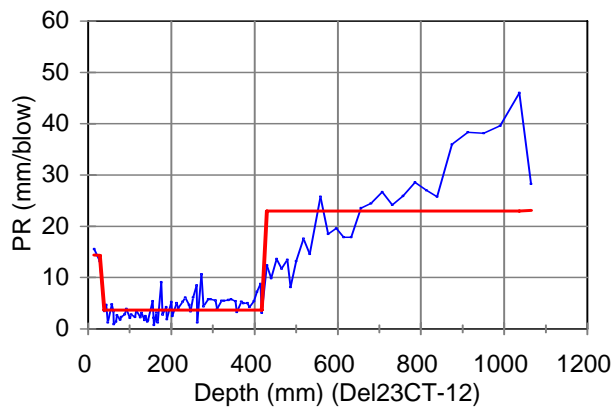
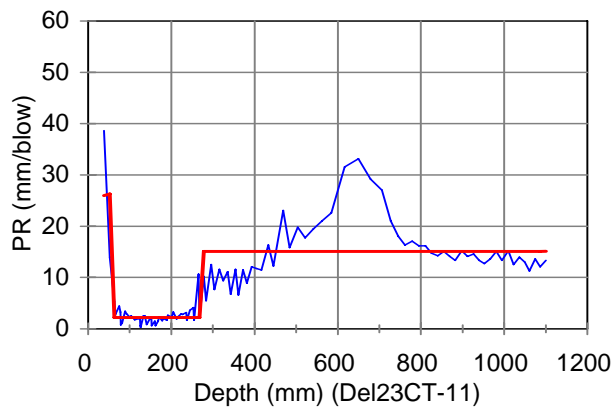
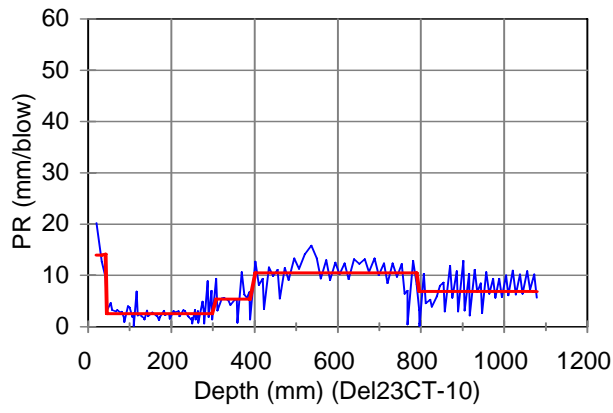


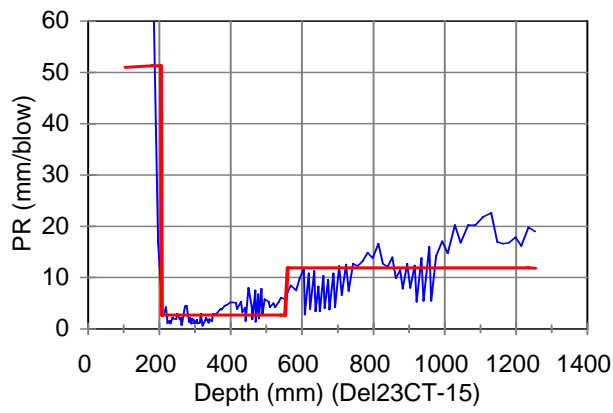
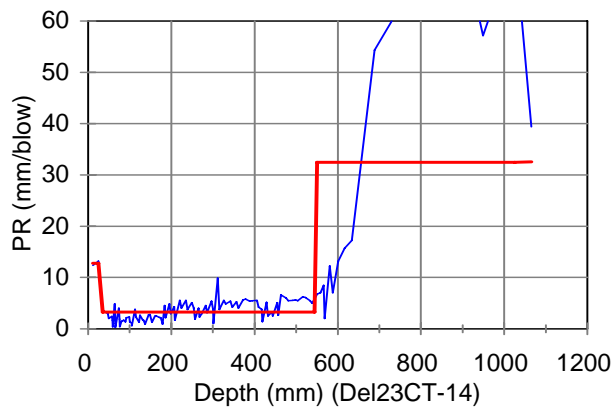
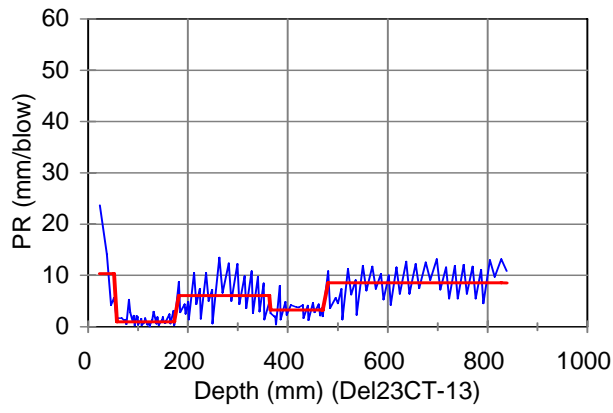
Del23CT: 1 to 33: Tested Through Core Hole, 300mm Cement Treated Soil

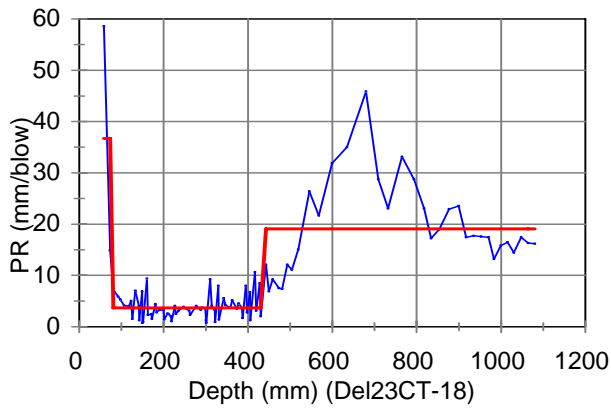
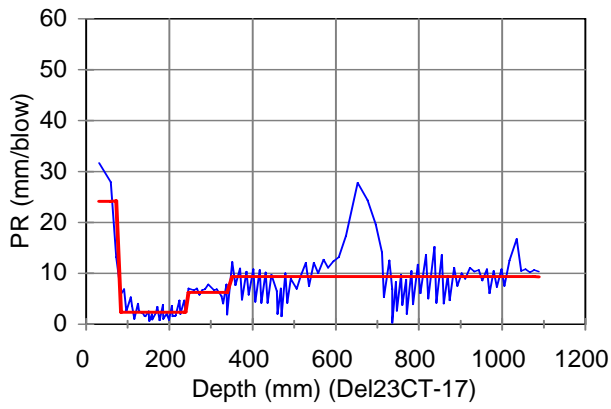
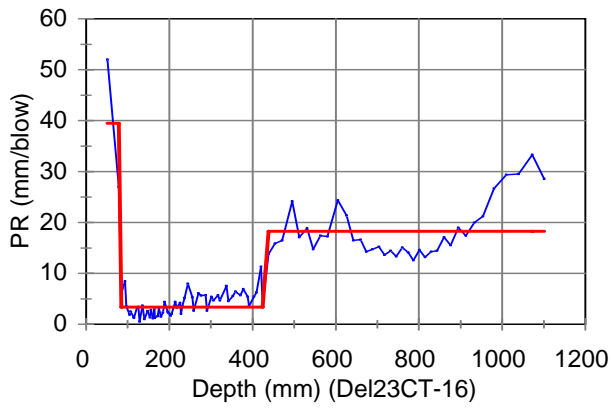


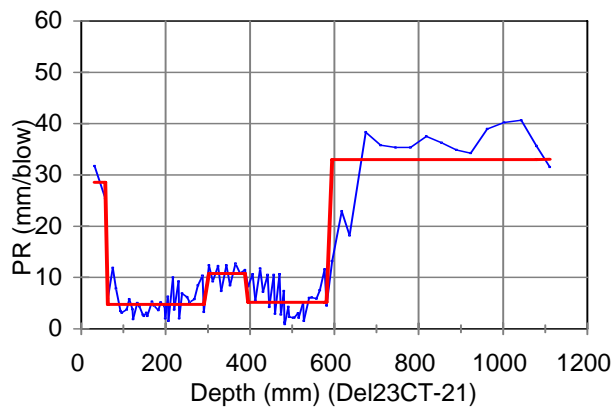
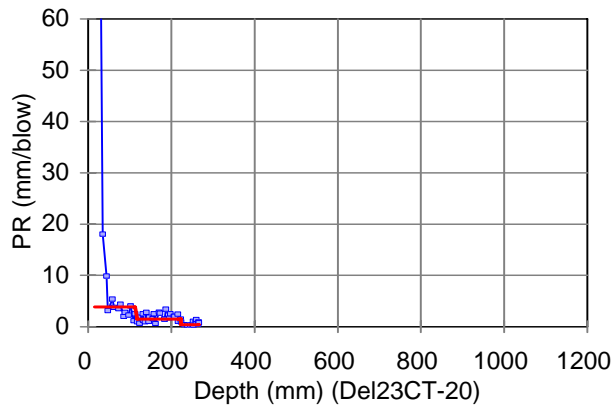
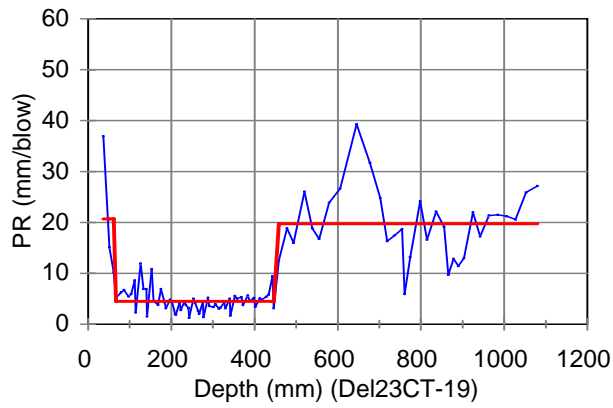


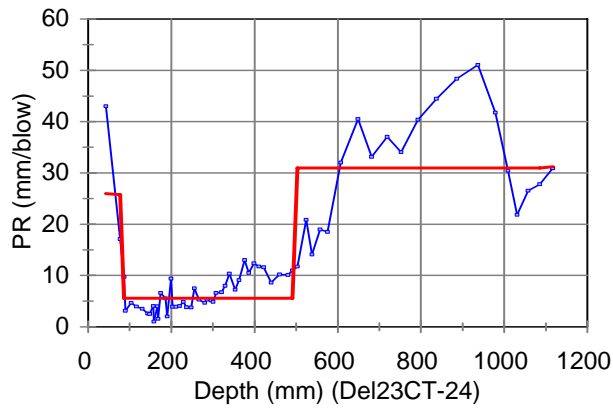
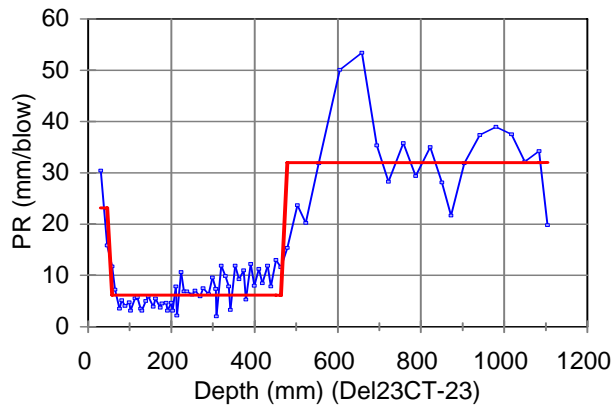
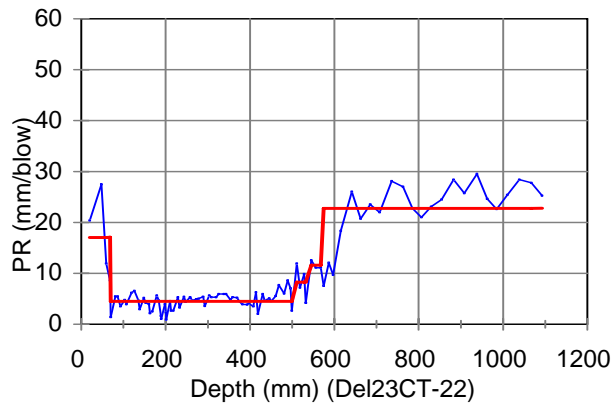


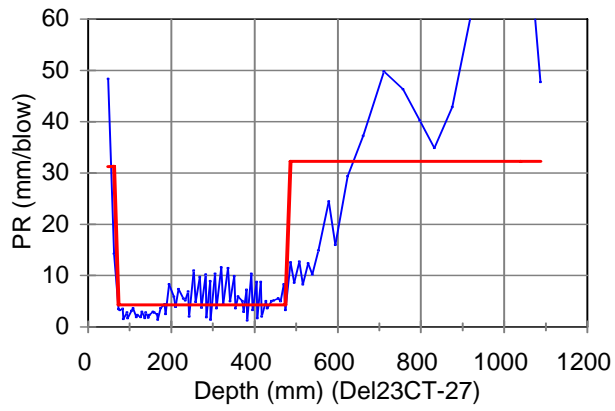
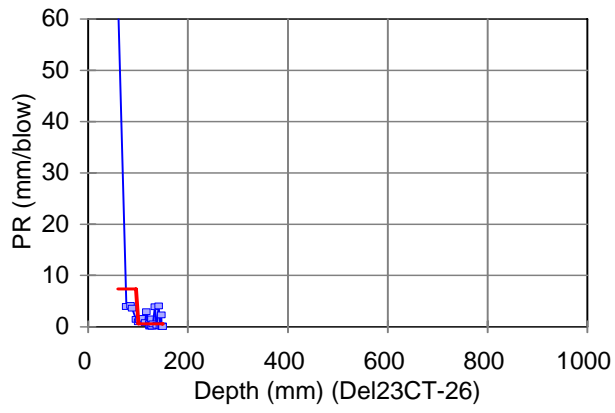
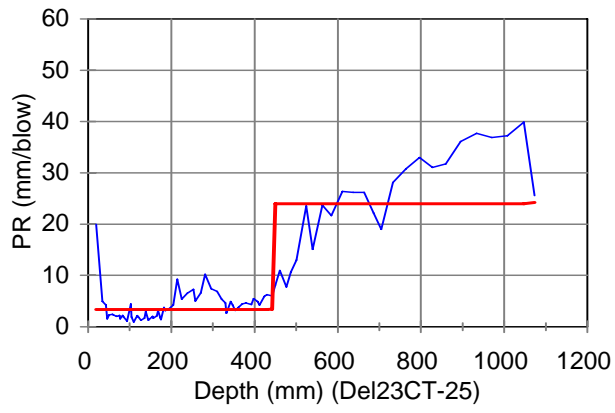


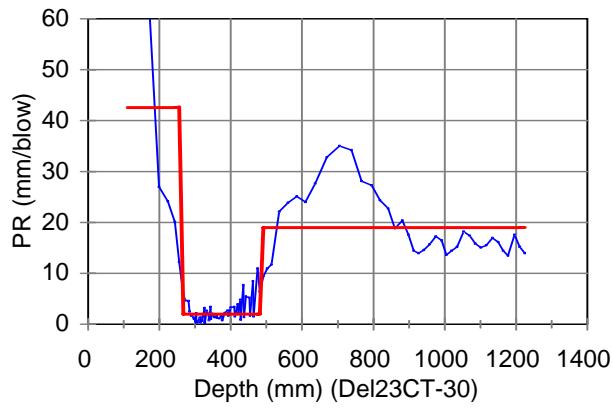
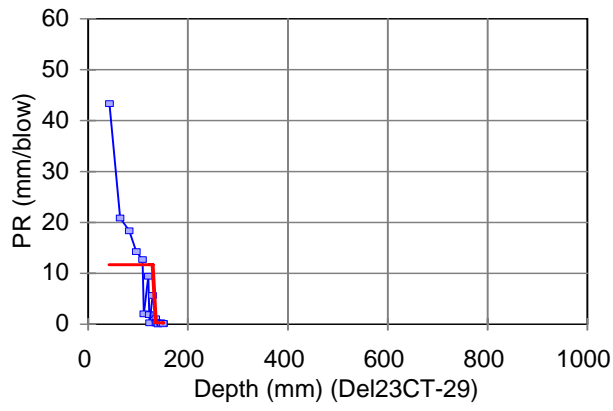
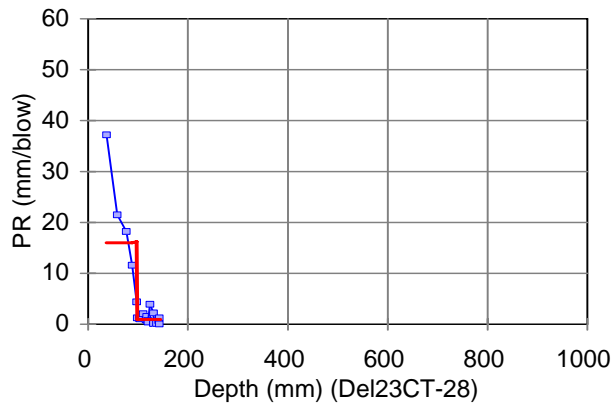


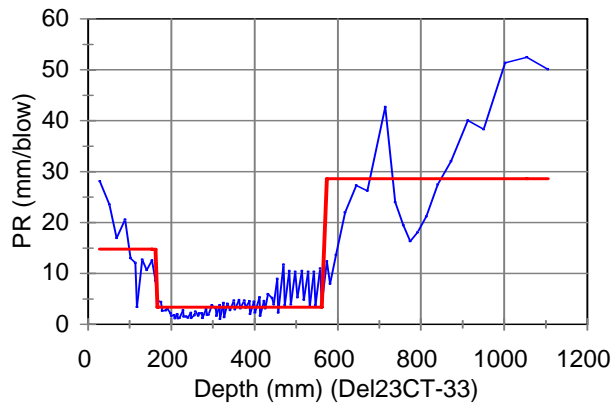
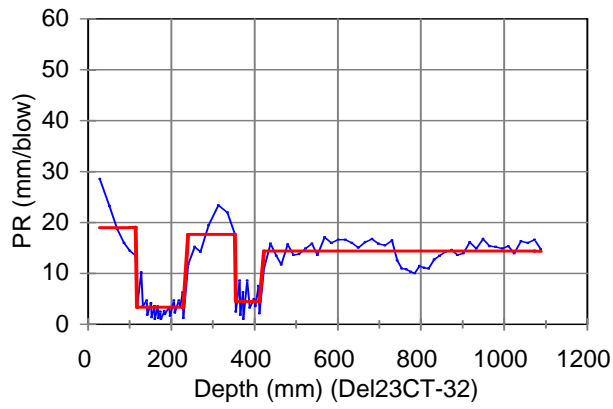
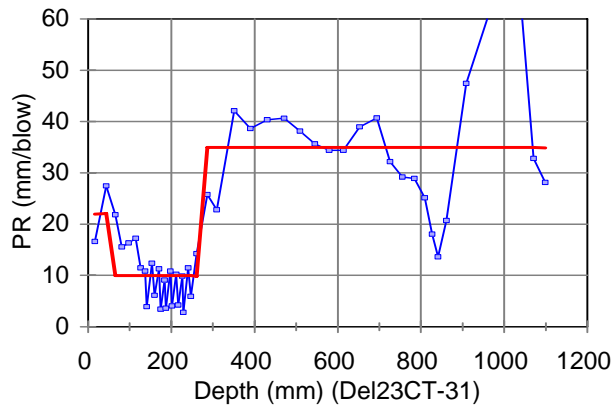




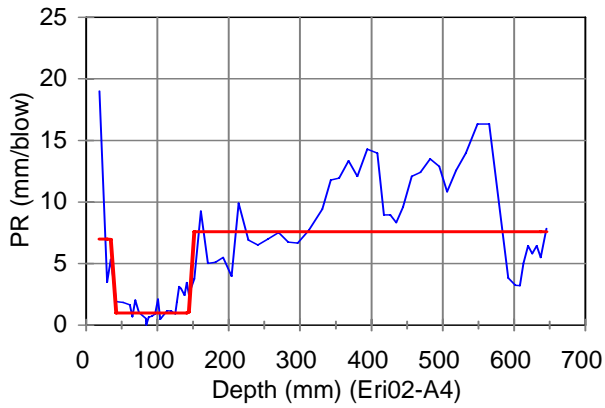
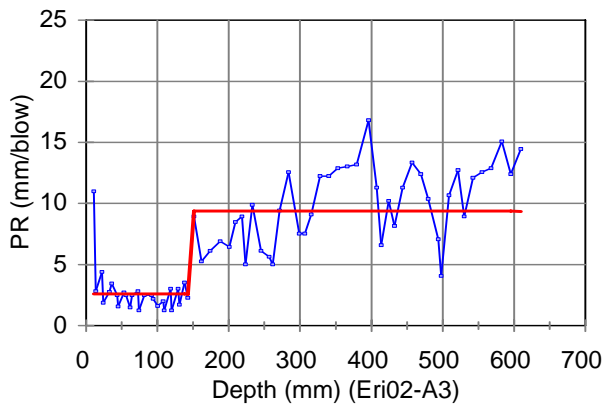
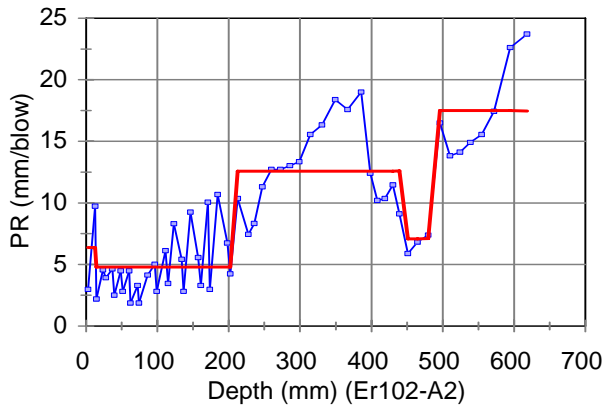


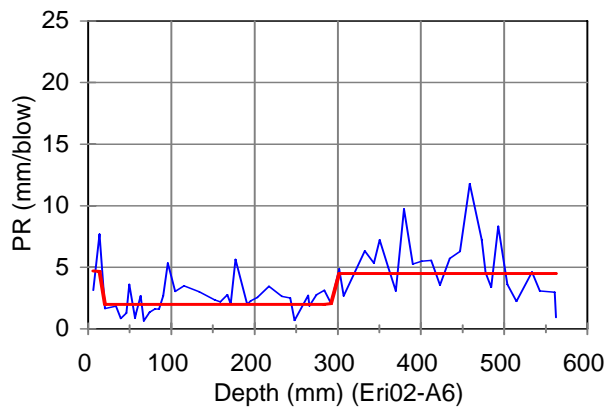
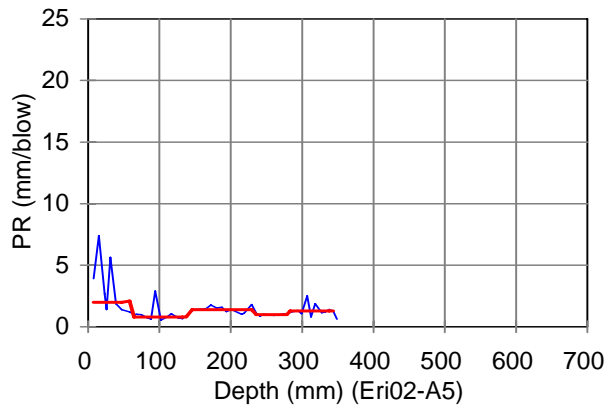




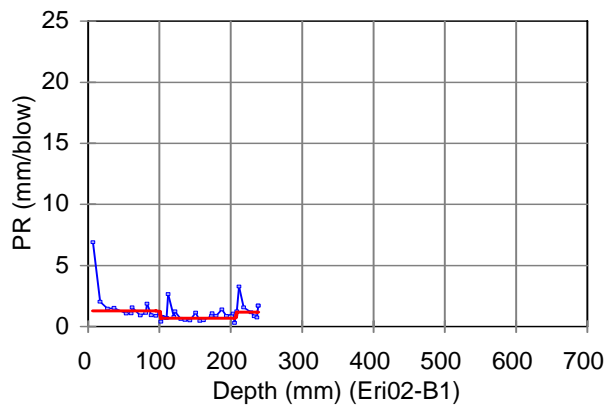


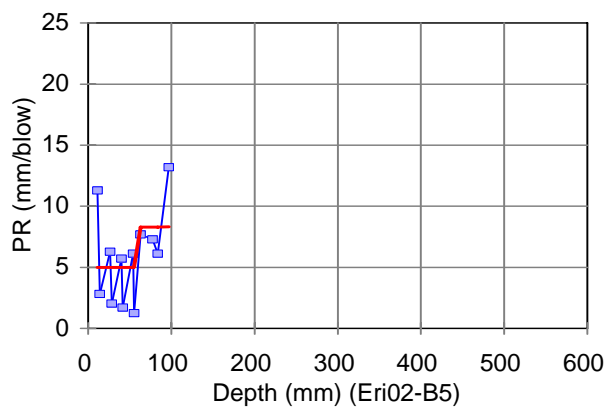
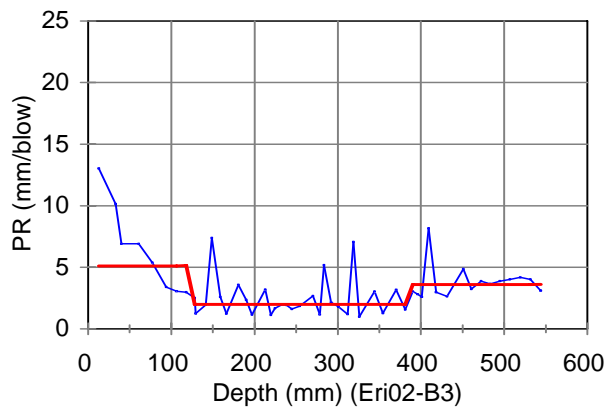
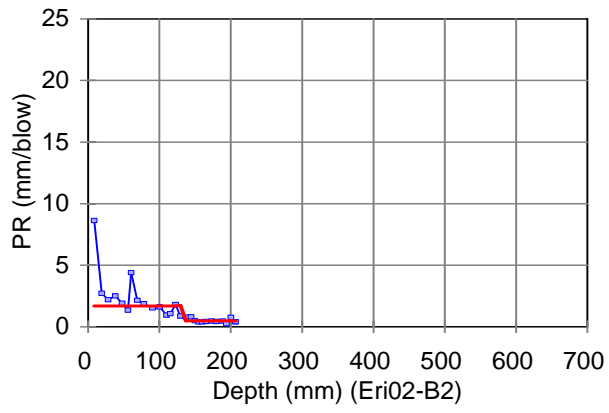
Eri02: A2 to A6: Tested Through Core, 300mm Cement Treated Soil

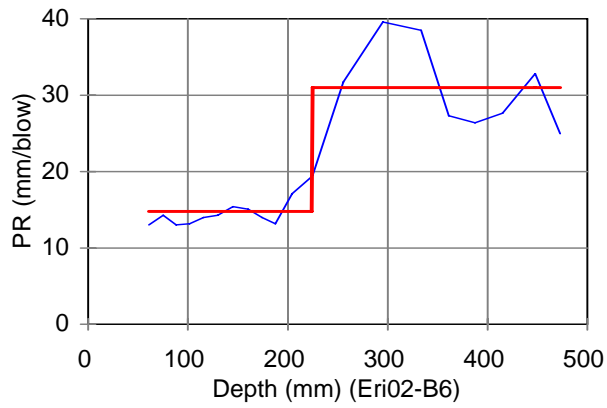




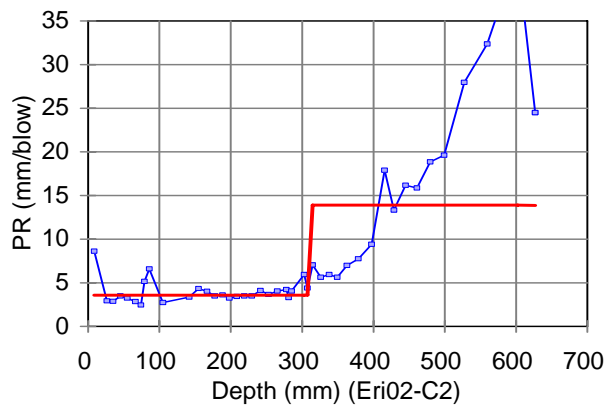
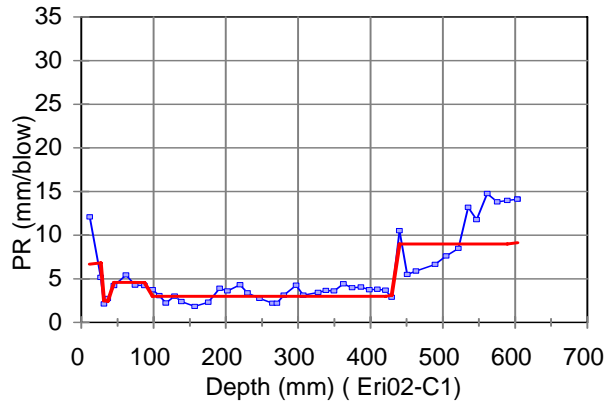
Eri02: B1 to B6: Test Through Core, Untreated Soil

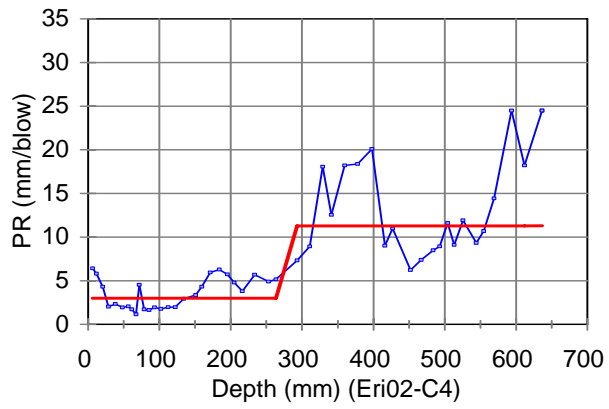
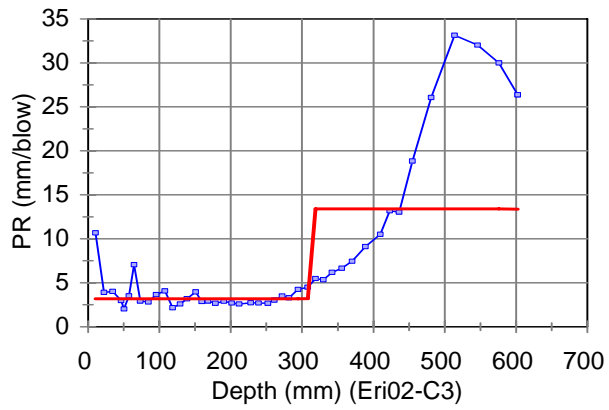




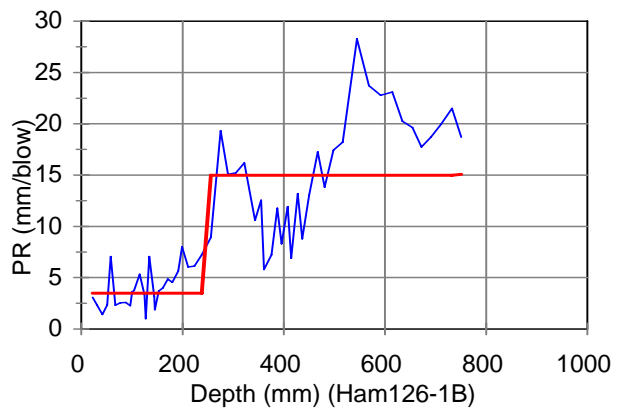


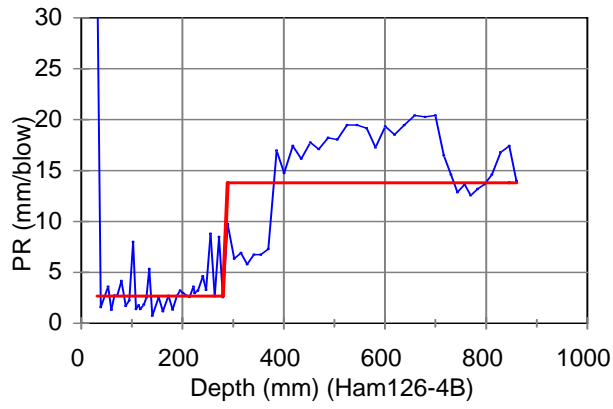
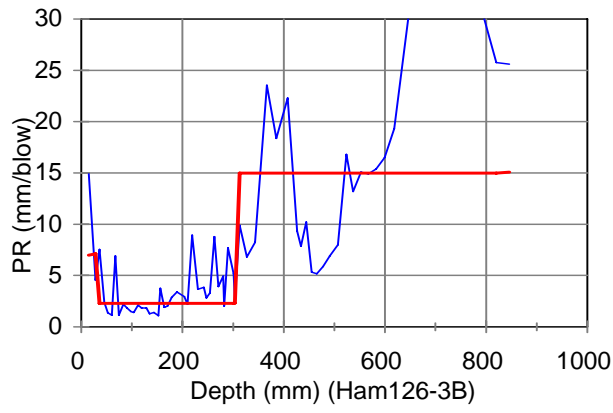
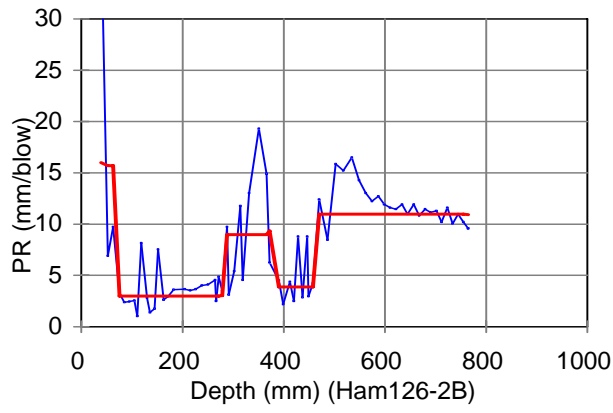
Eri02: C1 to C6: Tested Through Core, 300mm Lime-cement Treated Soil

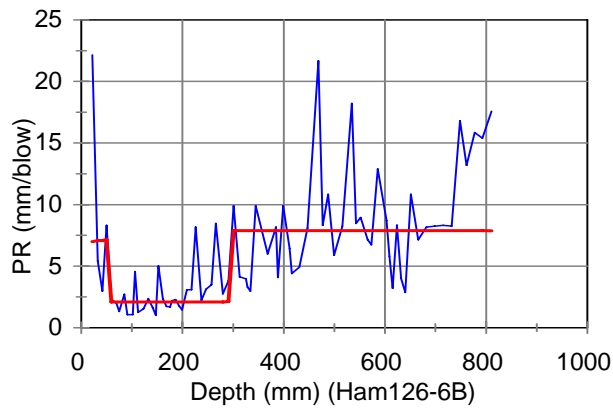
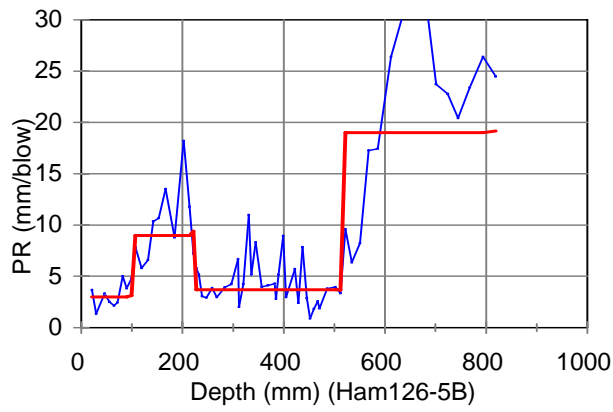
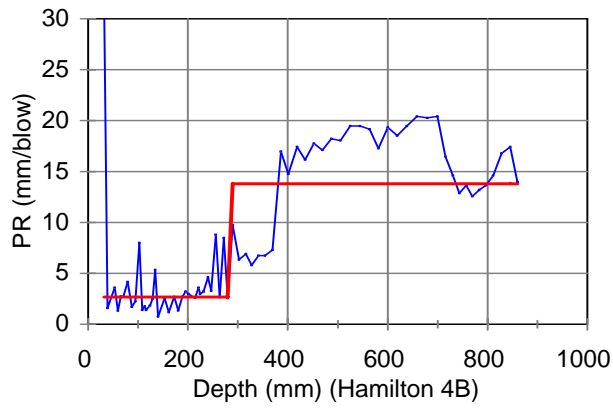




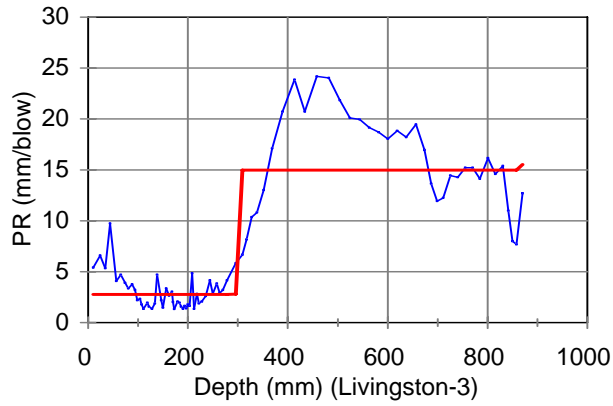
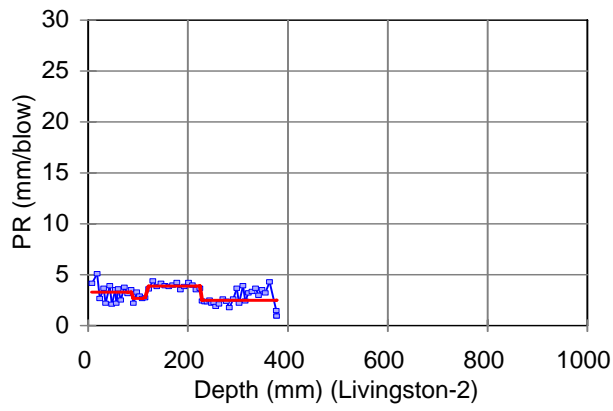
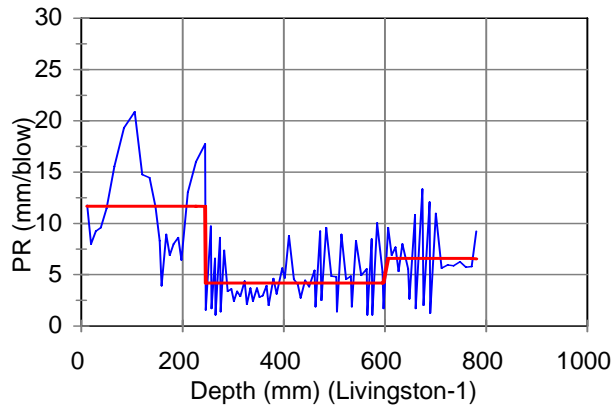
Ham126: 1b to 6b: Test Through Core, Untreated Soil

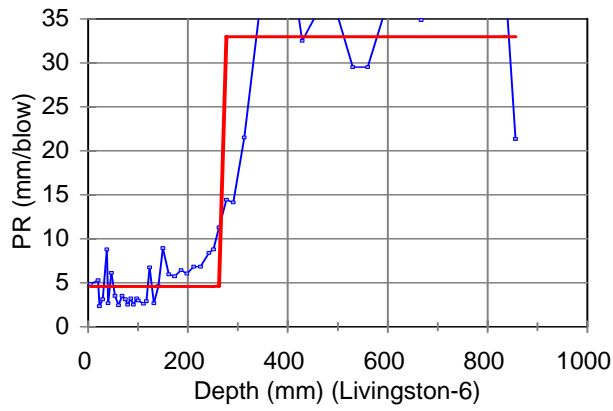
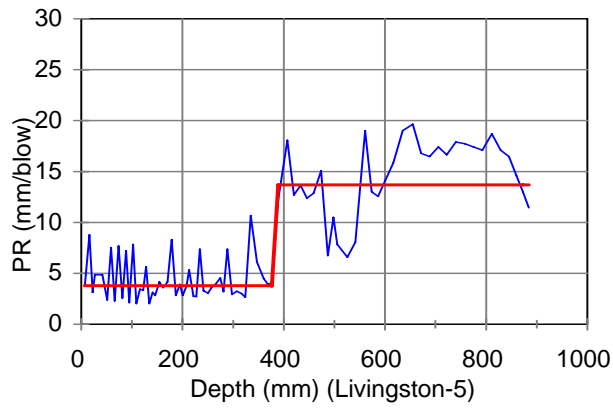
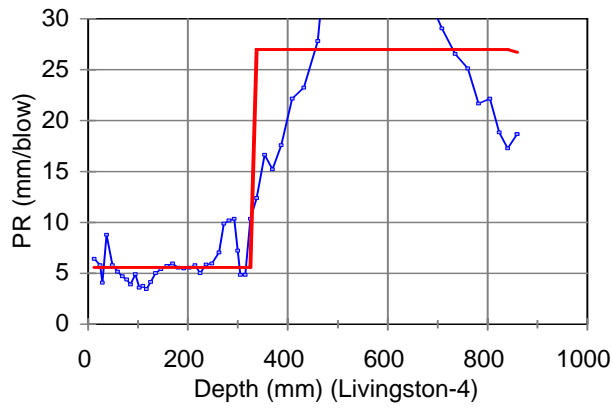




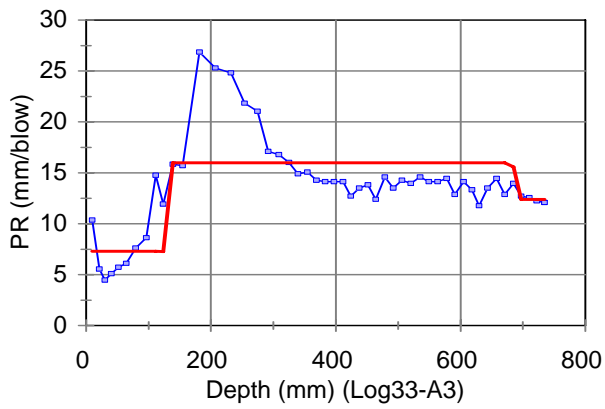
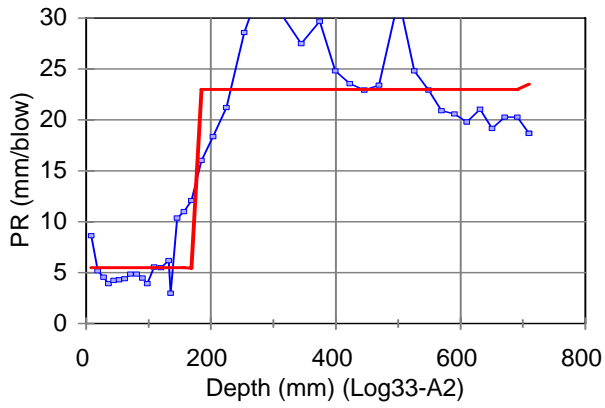
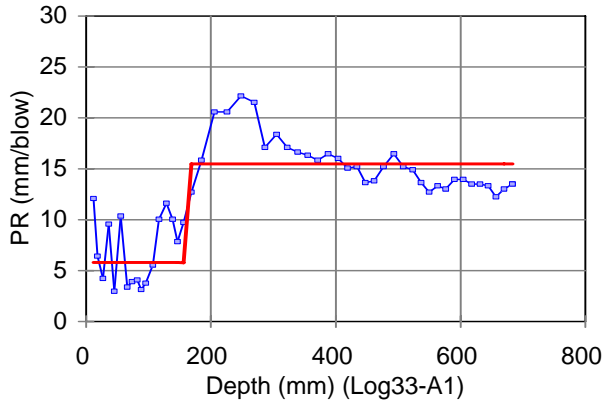


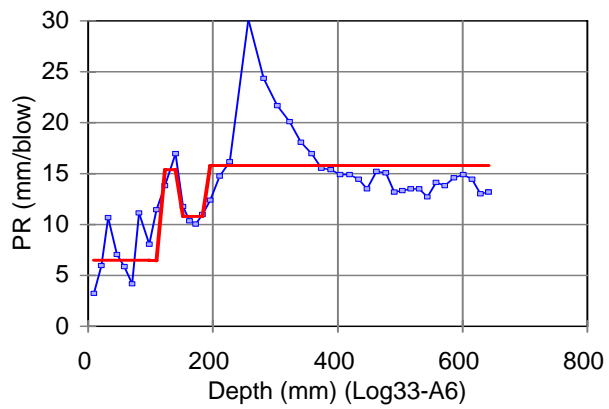
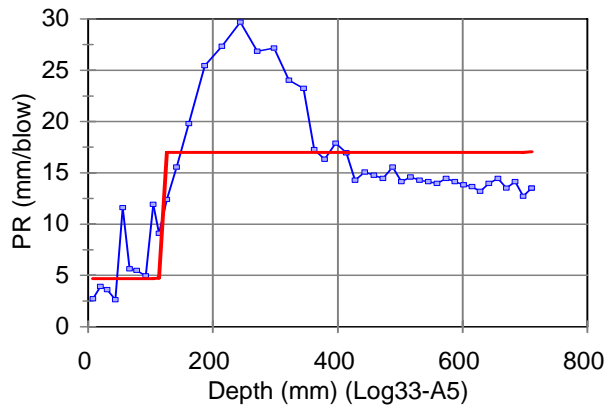
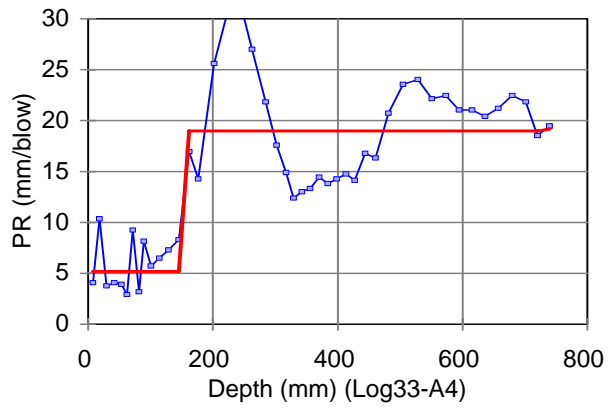
Livingston: 1 to 6: 300mm Lime Treated Soil



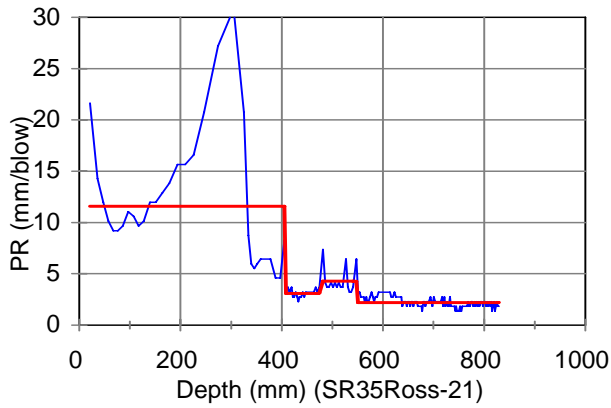
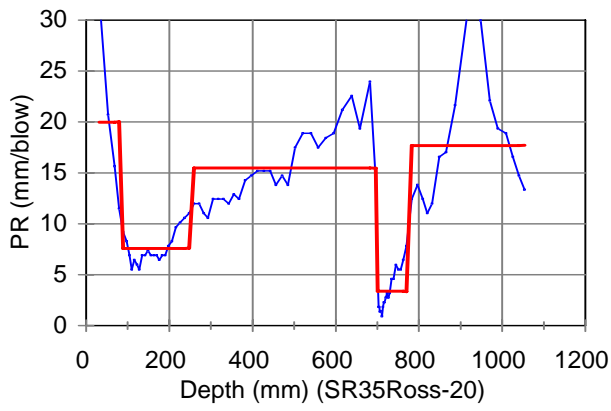
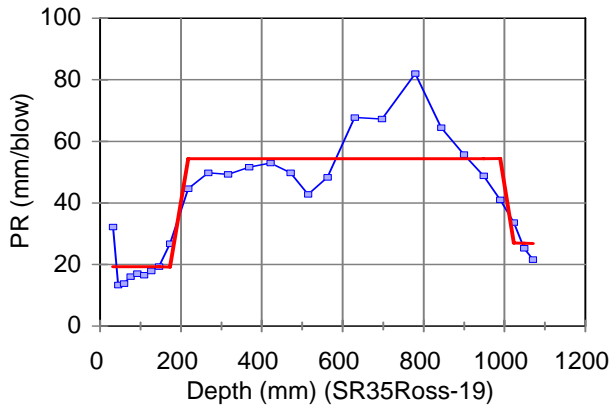


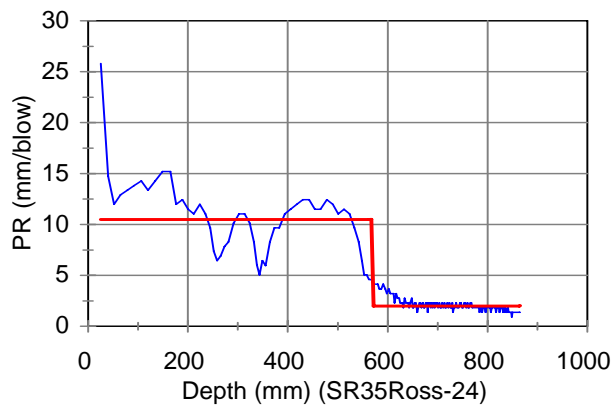
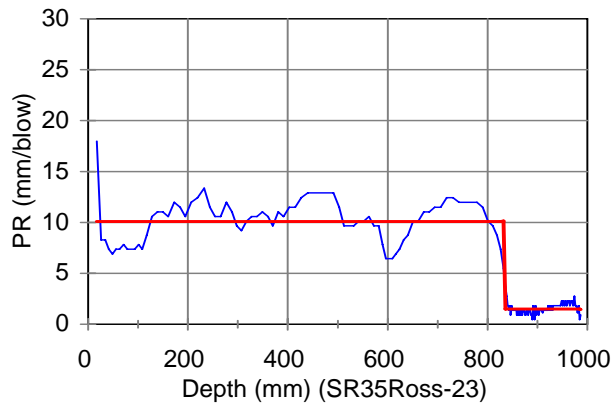
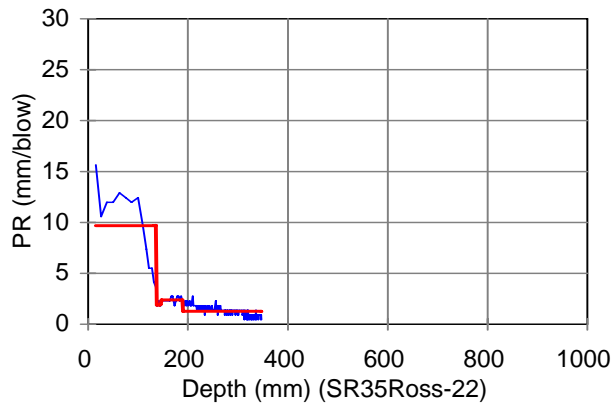
Logan 33: A1 to A6: Tested Through Core, 300mm Cement Treated Soil

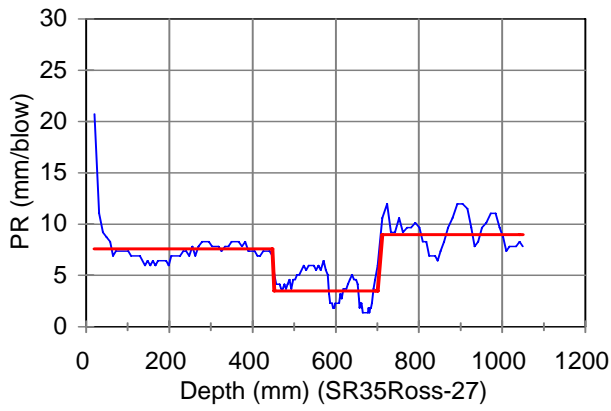
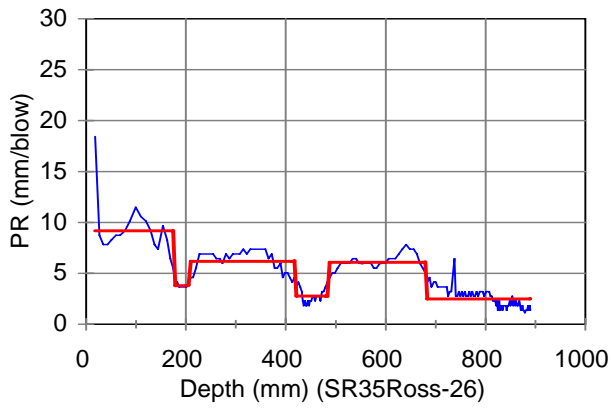
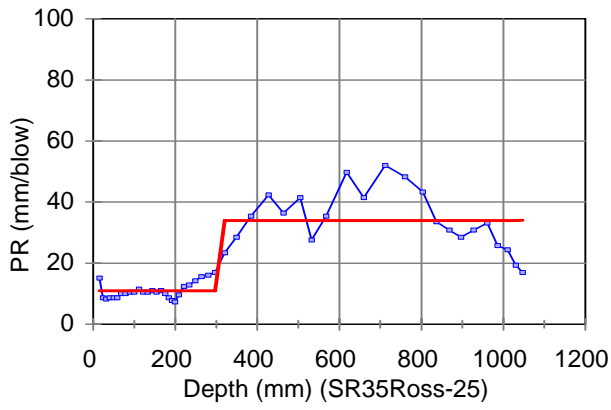


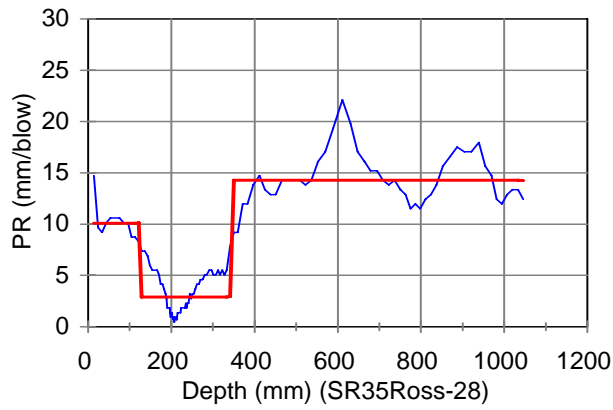


US35 Ross: 19 to 28: Untreated Soil

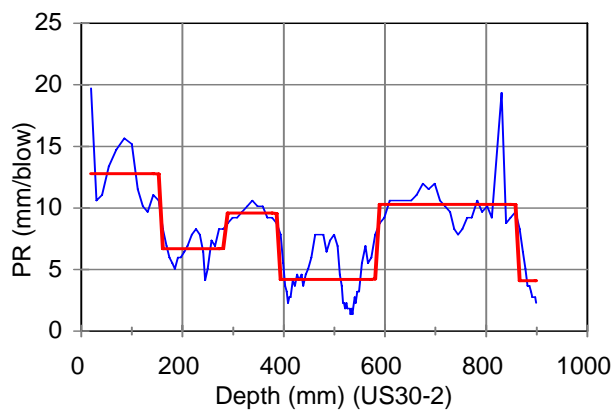
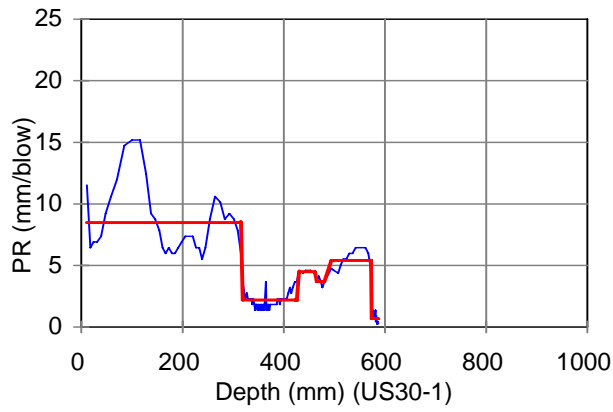


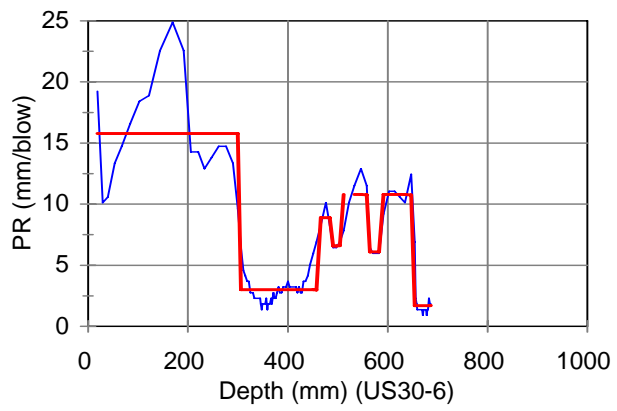
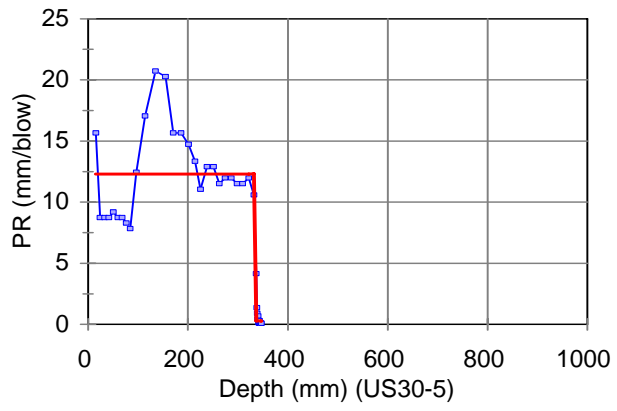
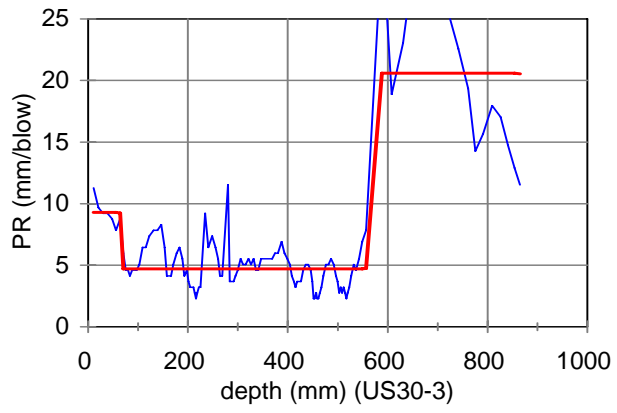


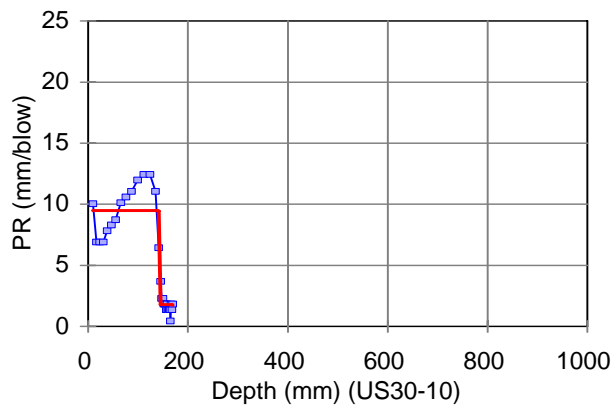
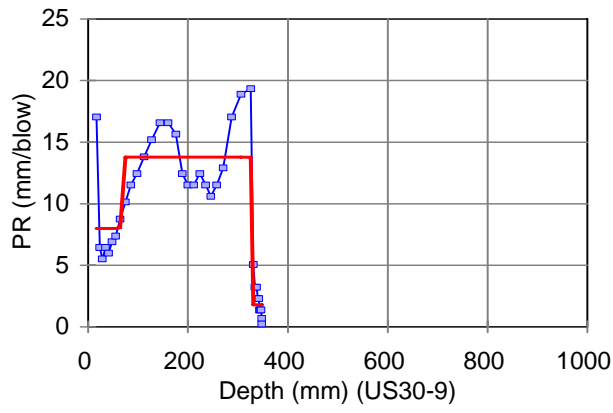
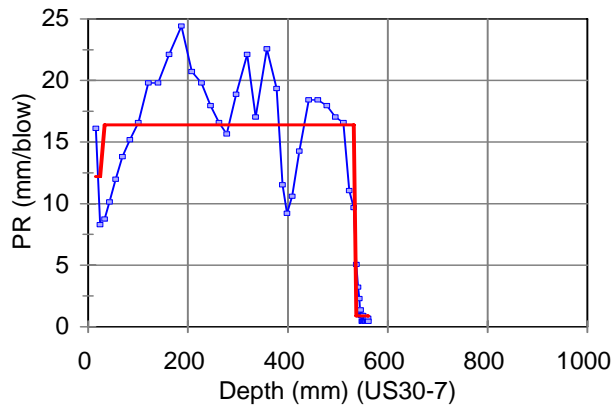


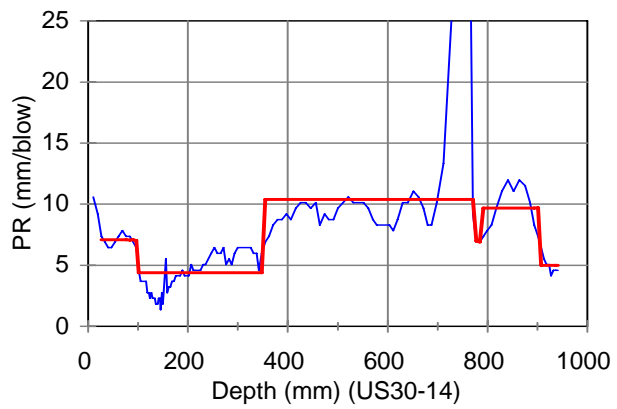
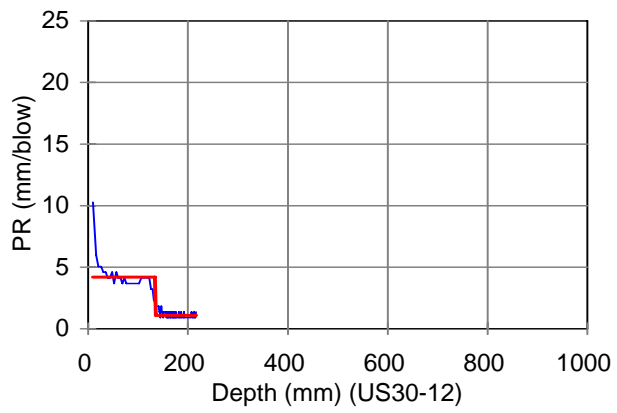
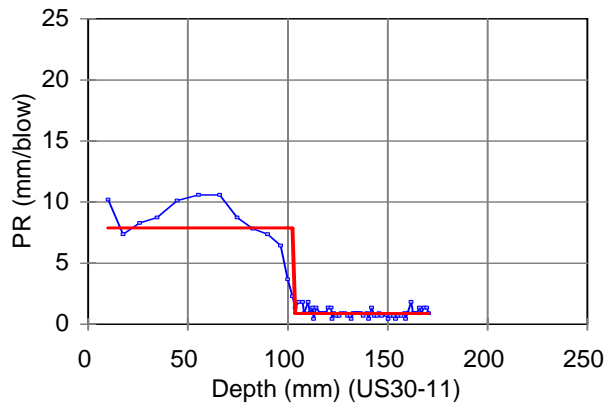


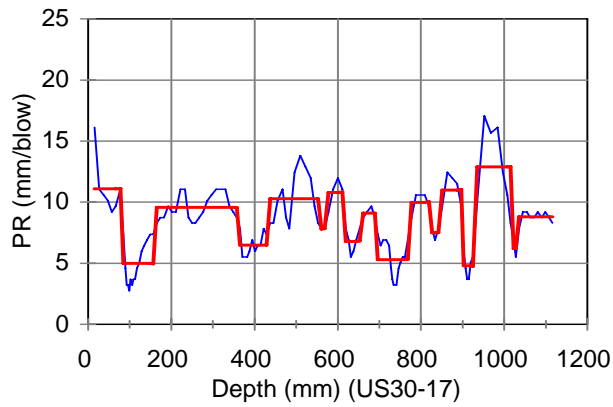
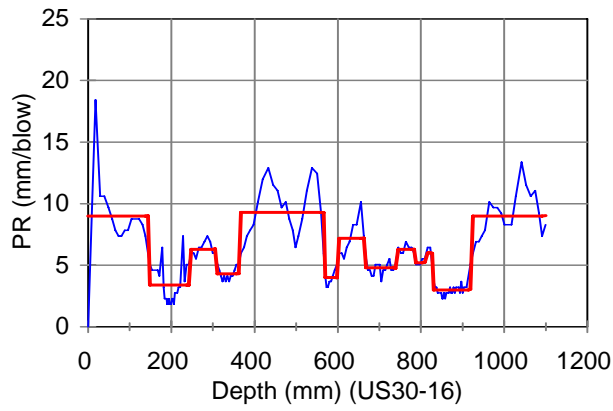
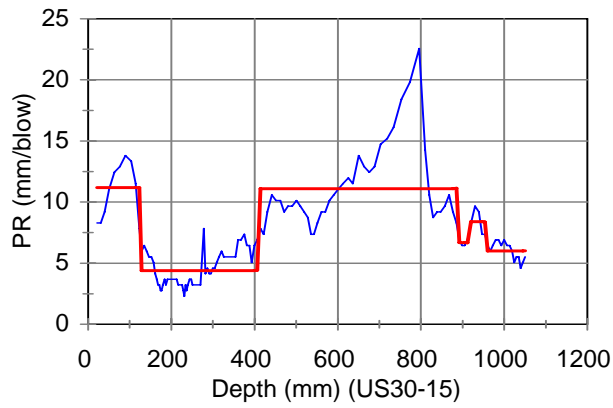
US30: 1 to 20: Untreated Soil

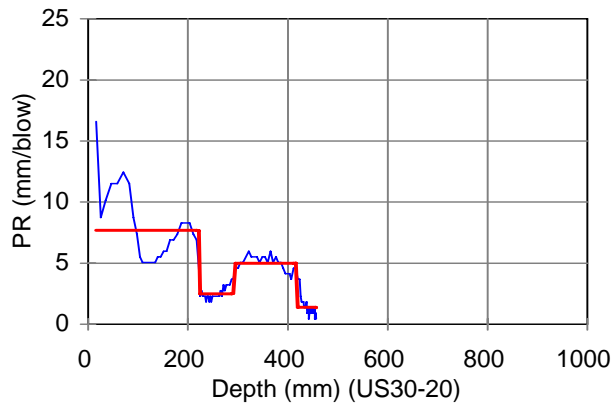
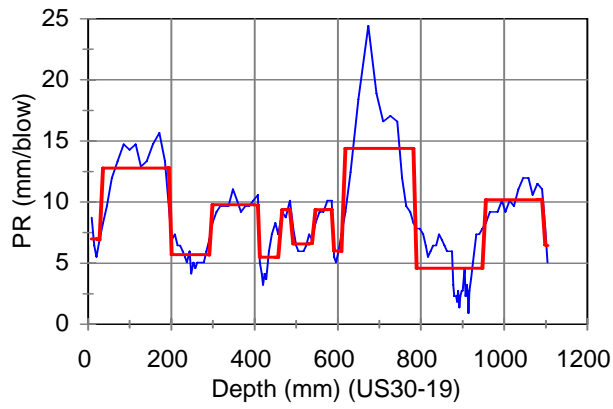
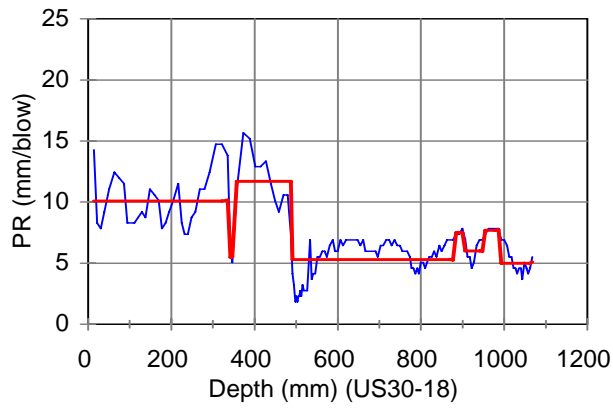


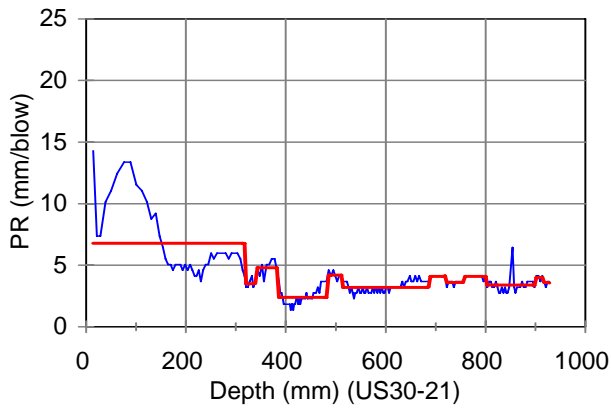




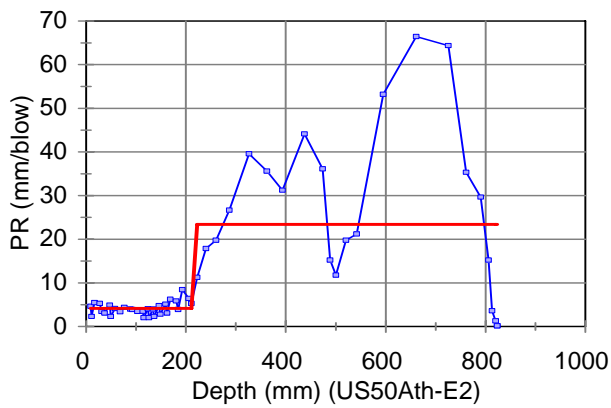
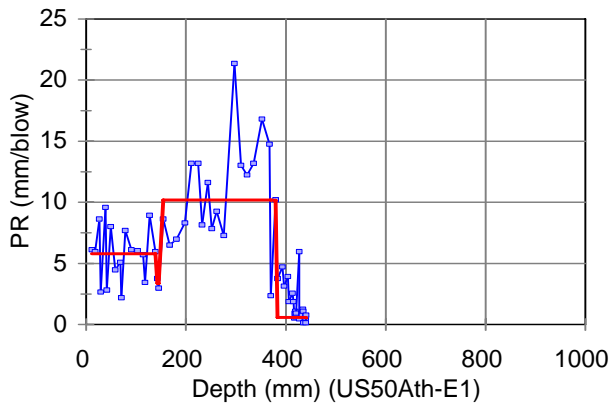


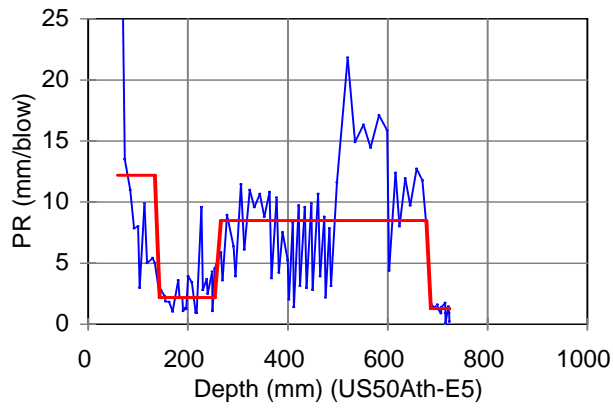
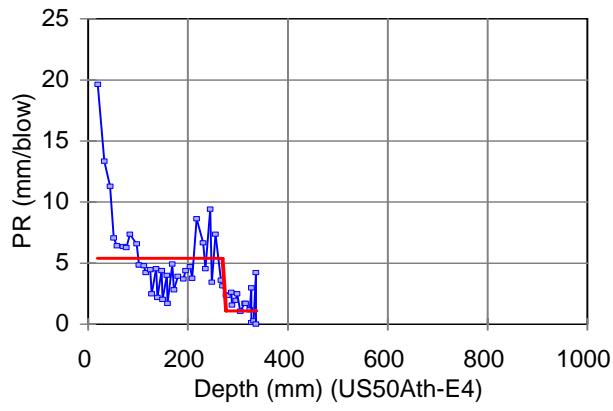
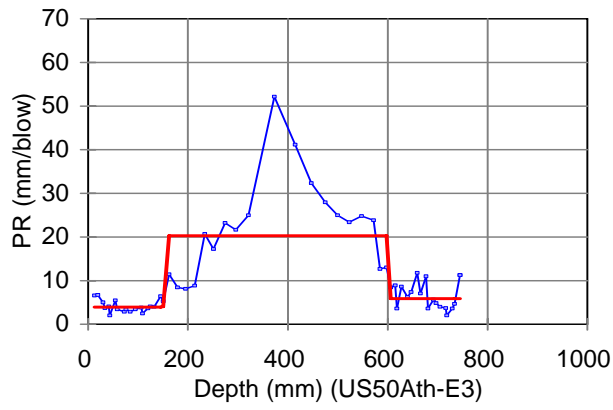


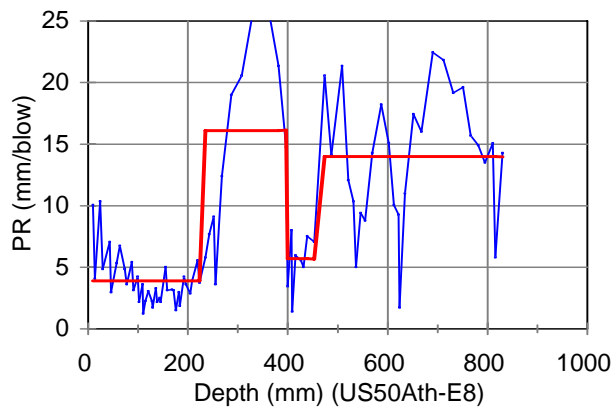
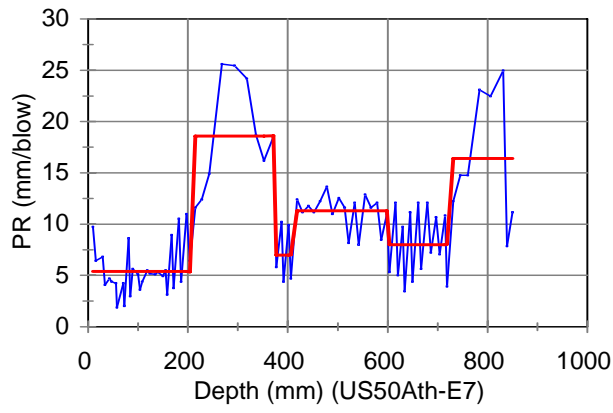
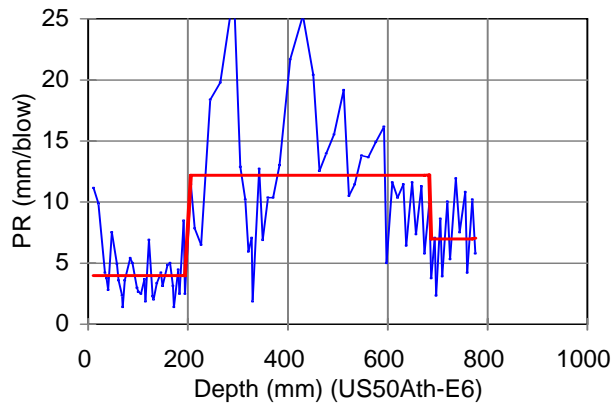


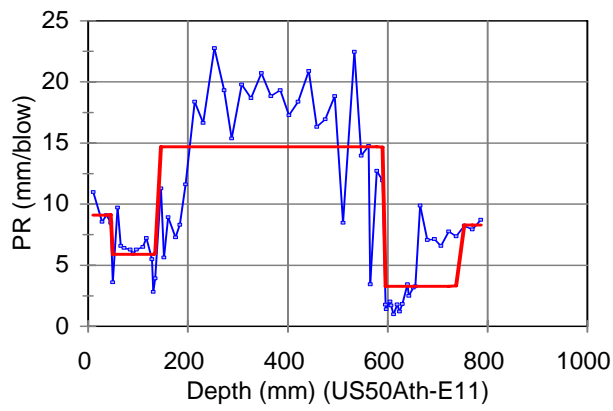
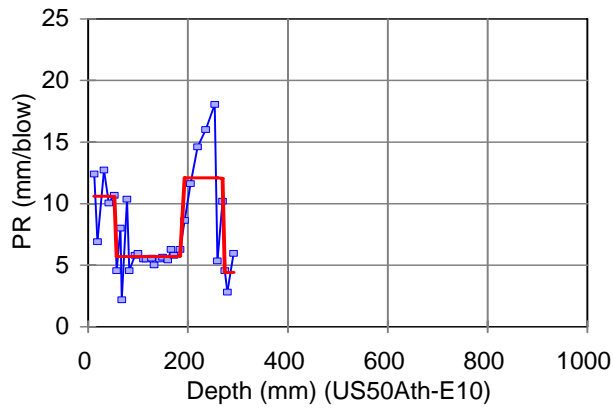
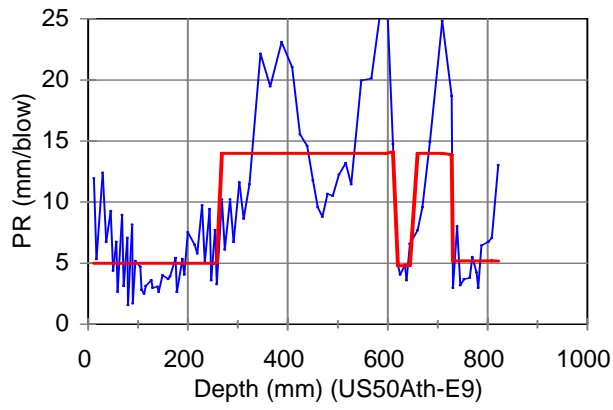


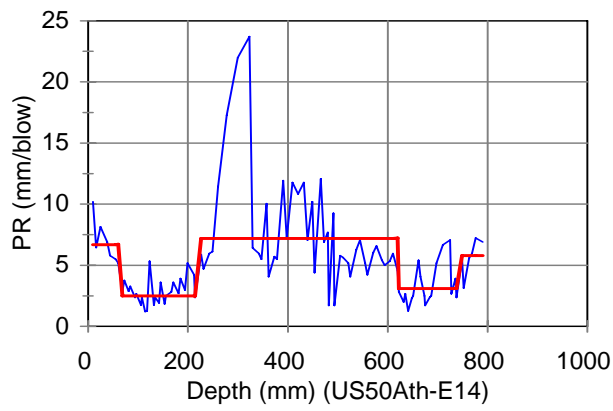
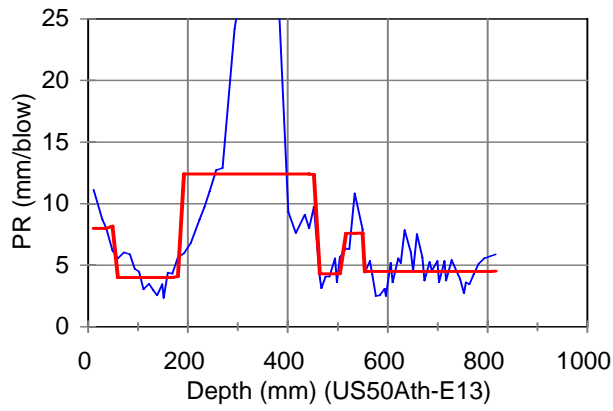
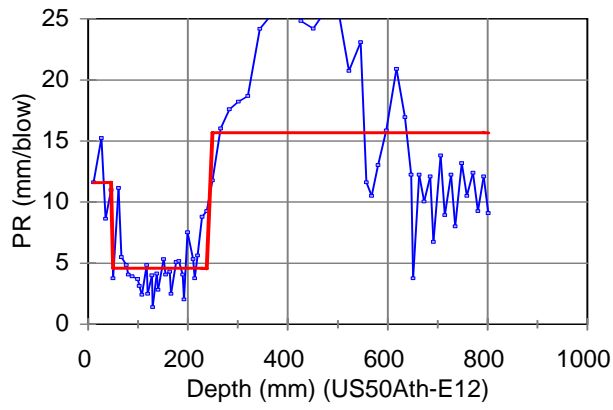
US50Ath East Bound: E1 to E17: 100mm NJ Base on 150mm Ohio304

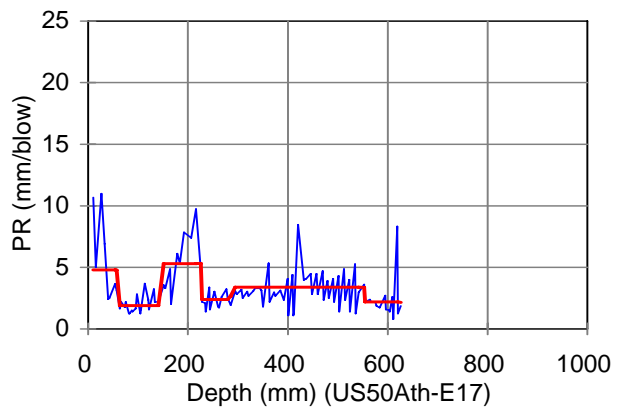
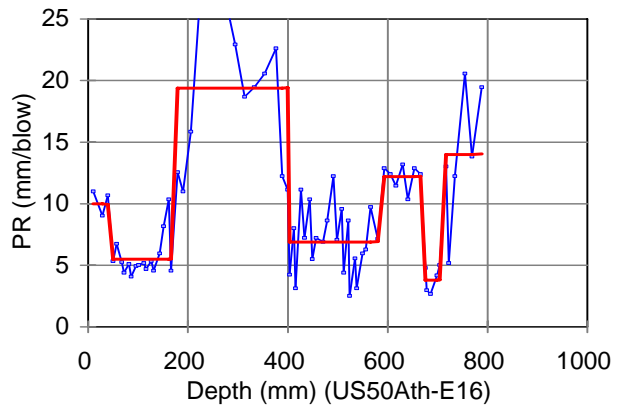
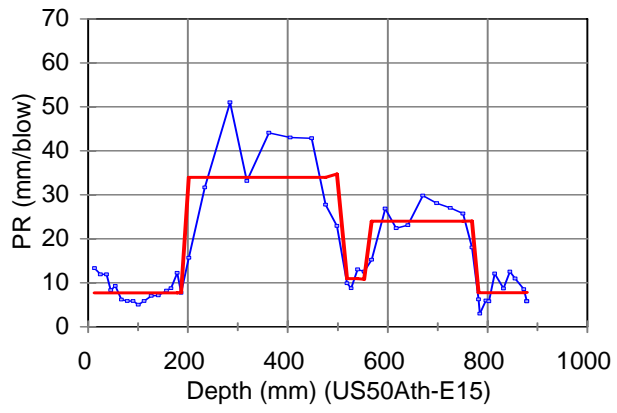




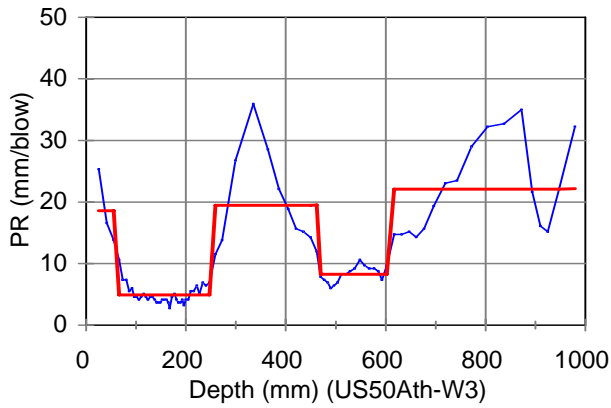
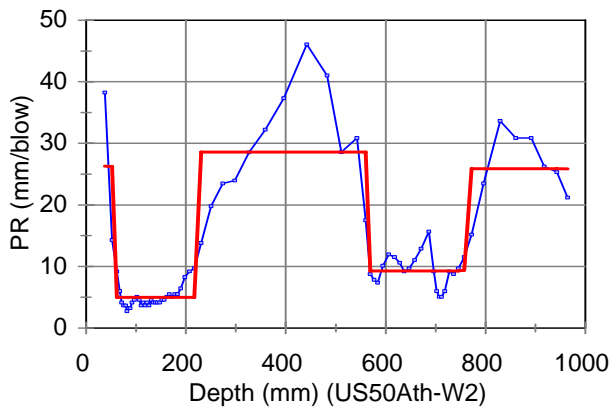
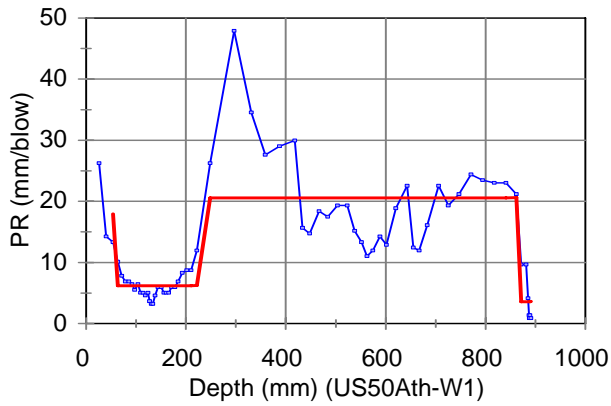


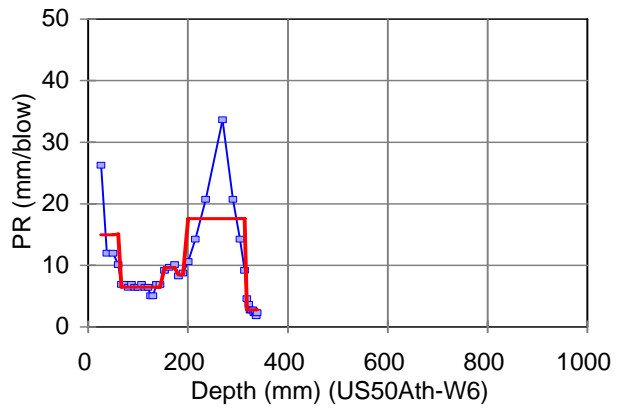
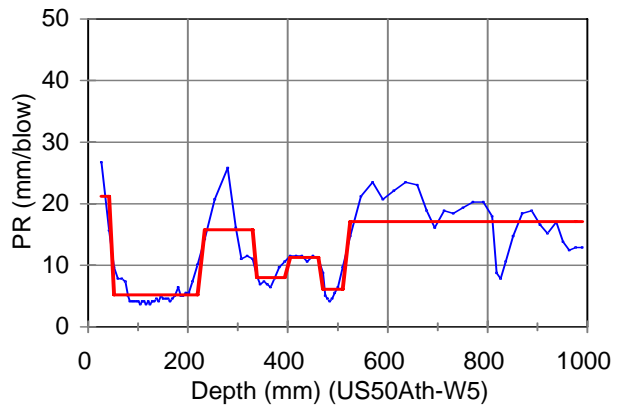
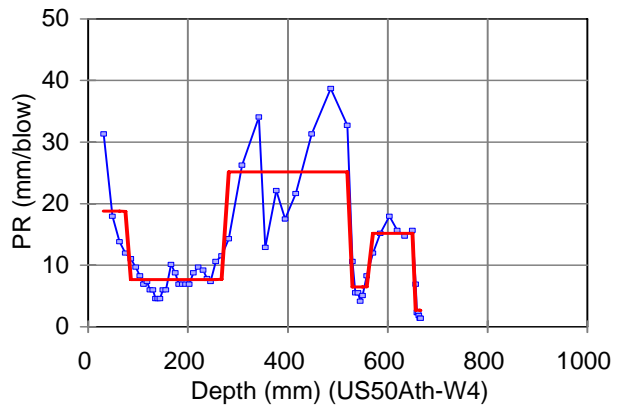


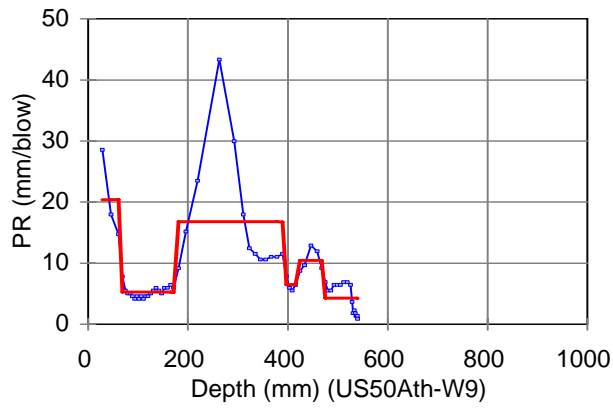
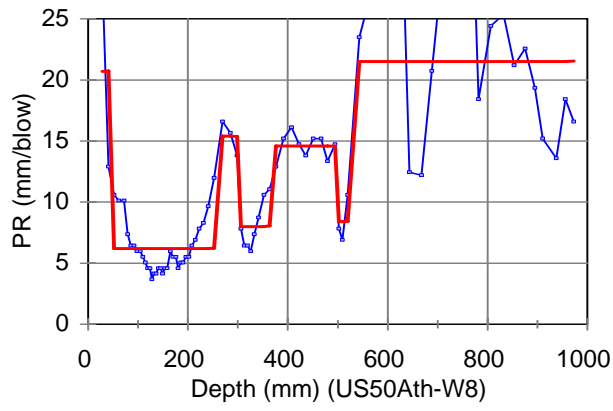
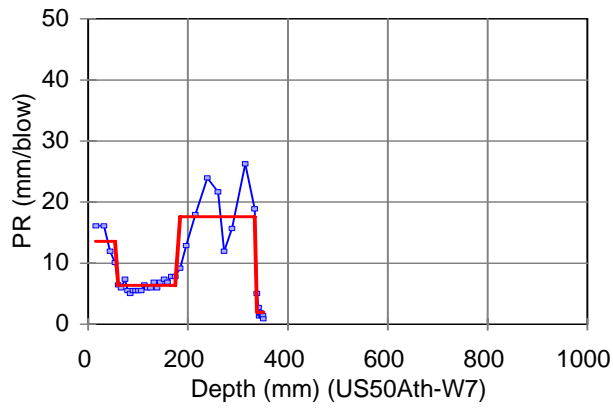


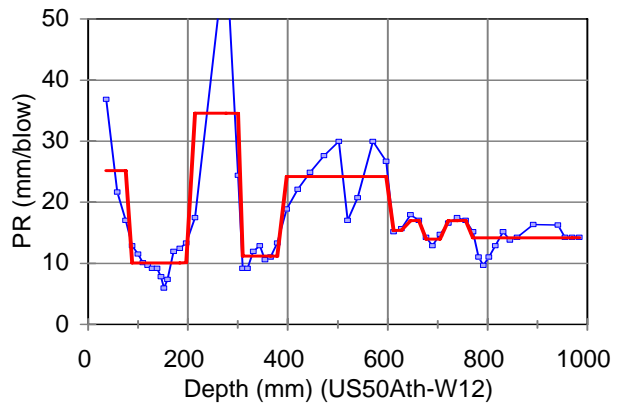
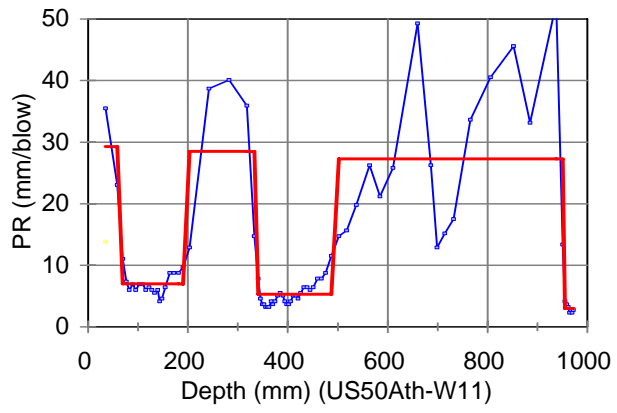
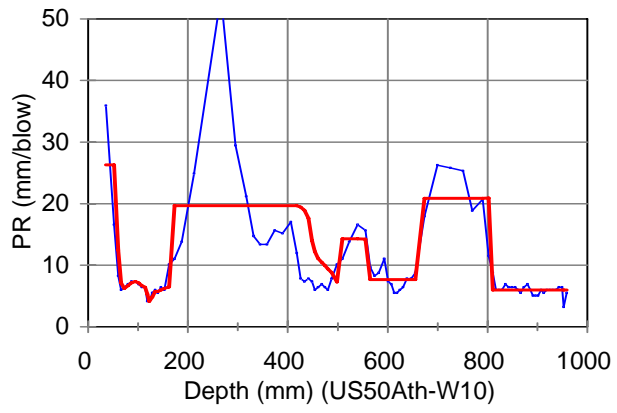


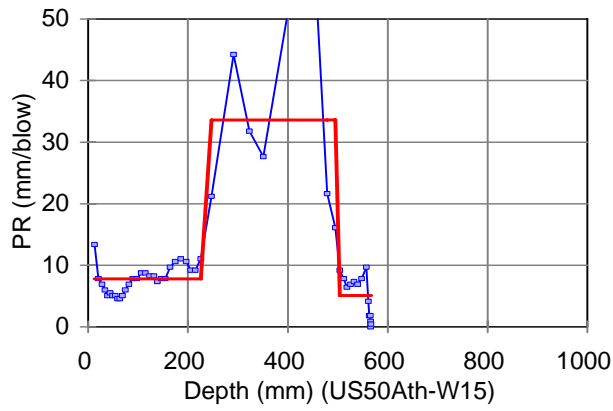
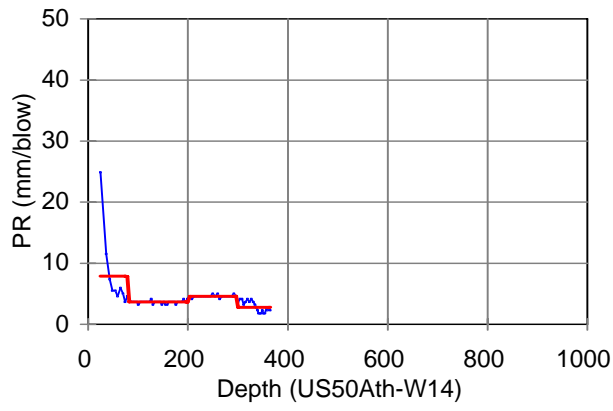
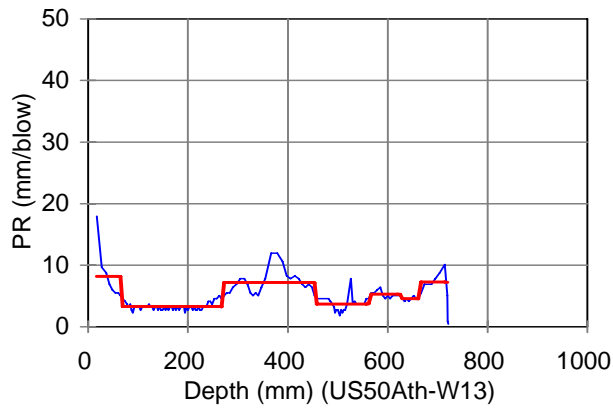
US50Ath West Bound: W1 to W17: 100mm Iowa Base on 150mm Ohio304

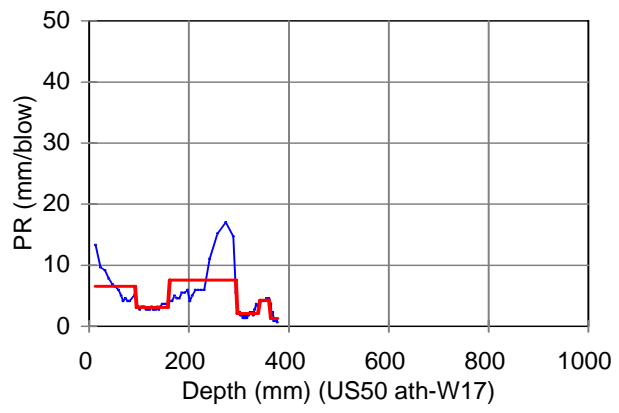
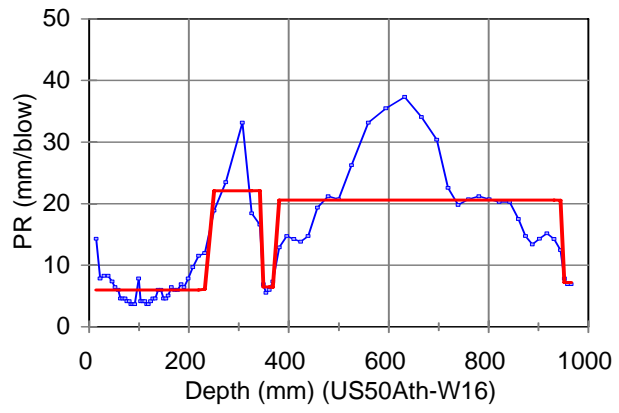














ORITE • 141 Stocker Center • Athens, Ohio 45701-2979 • 740-593-2476
Fax: 740-593-0625 • orite@bobcat.ent.ohiou.edu • <http://webce.ent.ohiou.edu/orite/>